U.S. Department of Transportation
National Highway Traffic Safety Administration

NHTSA

DOT HS 813 332 March 2024

Crash Compatibility for Occupantless Delivery Vehicles

This page intentionally left blank.

Suggested APA Format Citation:

Kan, S., Reichert, R., & Park, C. K. (2024, March). *Crash compatibility for occupantless delivery vehicles* (Report No. DOT HS 813 332). National Highway Traffic Safety Administration.

This page intentionally left blank.

Technical Report Documentation Page

<table>
<tr><td>1. Report No.
DOT HS 813 332</td><td>2. Government Accession No.</td><td colspan="2">3. Recipient's Catalog No.</td></tr>
<tr><td colspan="2" rowspan="2">4. Title and Subtitle
Crash Compatibility for Occupantless Delivery Vehicles</td><td colspan="2">5. Report Date
March 2024</td></tr>
<tr><td colspan="2">6. Performing Organization Code</td></tr>
<tr><td colspan="2">7. Authors
Steve Kan, Rudolf Reichert, and C. K. Park, Center for Collision Safety and Analysis, George Mason University</td><td colspan="2">8. Performing Organization Report No.</td></tr>
<tr><td colspan="2" rowspan="2">9. Performing Organization Name
Center for Collision Safety and Analysis
George Mason University
4087 University Drive, Fairfax, VA 22030</td><td colspan="2">10. Work Unit No. (TRAIS)</td></tr>
<tr><td colspan="2">11. Contract or Grant No.
TOR #: 693JJ920R000059</td></tr>
<tr><td colspan="2" rowspan="2">12. Sponsoring Agency Name and Address
National Highway Traffic Safety Administration
1200 New Jersey Avenue SE.
Washington, DC 20590</td><td colspan="2">13. Type of Report and Period Covered
Final Report, September 15, 2020 - December 29, 2021</td></tr>
<tr><td colspan="2">14. Sponsoring Agency Code</td></tr>
<tr><td colspan="4">15. Supplementary Notes
Ian Hall was the contracting officer representative.</td></tr>
<tr><td colspan="4">16. Abstract
Crash compatibility plays an important role in minimizing the risk of injury during a vehicle-to-vehicle crash event. Optimizing vehicle mass, geometry, and structural stiffness characteristics with respect to compatibility have improved both self-protection and partner protection for traditional vehicles. Automated Driving System technologies and battery-powered electric vehicles are advancing fast, and designs with different crash characteristics and potentially higher mass will continue to evolve. Occupantless delivery vehicles (ODVs), also referred to as unmanned delivery systems and uncrewed delivery systems, are expected to differ from vehicles designed to have human occupants onboard, and occupant presence and safety regulation may not be applied the same or at all. For example, an ODV designed only for delivery purposes may not require occupant self-protection, allowing designs to focus on compatibility and partner protection. NHTSA contracted the Center for Collision Safety and Analysis at the George Mason University to explore the effect ODV compatibility variations have on occupant and structural responses when striking an occupied light passenger vehicle. Full-frontal, frontal oblique, and perpendicular side impact crash configurations were determined as relevant ODV-to-LPV crash scenarios. Impact scenarios are like the existing New Car Assessment Program full-frontal, NCAP moving deformable barrier side, and NHTSA's research frontal oblique impact crash test configurations. Simulations were conducted for both the ODV-to-vehicle and barrier-to-vehicle reference impact scenarios.</td></tr>
<tr><td colspan="2">17. Key Words
Automated Driving System, ADS, battery-powered electric vehicle, BEV, occupantless delivery vehicle, ODV, NCAP</td><td colspan="2">18. Distribution Statement
This document is available to the public from the DOT, BTS, National Transportation Library, Repository & Open Science Access Portal, https://rosap.ntl.bts.gov.</td></tr>
<tr><td>19. Security Classif. (of this report)
Unclassified</td><td>20. Security Classif. (of this page)
Unclassified</td><td>21. No. of Pages
119</td><td>22. Price</td></tr>
</table>

Form DOT F 1700.7 (8-72) Reproduction of completed page authorized

This page intentionally left blank.

Table of Contents

List of Figures

This page intentionally left blank.

List of Tables

This page intentionally left blank.

List of Acronyms and Abbreviations

AAM	Alliance of Automobile Manufacturers
AIAM	Association of International Automobile Manufacturers
ADS	Automated Driving System
ADAS	advanced driver assistant systems
AHoF400	average height of force when vehicle deformation is 400mm
ATD	anthropomorphic test device
AV	automated vehicle
BEV	battery-powered electric vehicle
CARMA	Collision Avoidance and Resolution Multiple Access
CCODV	Crash Compatibility in Occupantless Delivery Vehicles
CISS	Crash Investigation Sampling System
EuroNCAP	European New Car Assessment Program
FE	finite element
FMVSS	Federal Motor Vehicle Safety Standard
IARV	injury assessment research values
IIHS	Insurance Institute for Highway Safety
Kw	work stiffness (not kilowatt)
KW400 or Kw400	stiffness related crush energy absorbed by a vehicle in the first 400 mm of crush
LPV	light passenger vehicle
MDB	moving deformable barrier
MPDB	mobile progressive deformable barrier
NCAP	New Car Assessment Program
NGSIM	next generation simulation
ODD	operational design domain
ODV	occupantless delivery vehicles
OL 316	name of the California DMV form for reporting a crash with an automated vehicle
OLC	occupant load criterion
OMDB	offset moving deformable barrier
ORB	override rigid barrier
PEAS	primary energy-absorbing structure
PDOF	principal direction of force

SEAS	secondary energy-absorbing structure
UADS	unoccupied automated driving system
UDS	uncrewed delivery system

Executive Summary

Crash compatibility is important in minimizing risk of injury during a vehicle-to-vehicle crash. Optimizing vehicle mass, geometry, and structural stiffness with respect to compatibility have improved both self-protection and partner-protection for traditional vehicles. Automated Driving System technologies and battery-powered electric vehicles are advancing fast, and designs with different crash characteristics and potentially higher mass will continue to evolve. Occupantless delivery vehicles, also known as uncrewed delivery systems, unmanned delivery systems, and unoccupied automated driving systems, are expected to differ from occupied vehicles and regulations related to occupant presence and safety are not applicable. For example, an ODV used only for delivery purposes may not require occupant self-protection, allowing designs to focus on compatibility and partner protection. NHTSA contracted the Center for Collision Safety and Analysis at the George Mason University to explore the effect of ODV compatibility variations have on occupant and structural responses when striking occupied light passenger vehicles.

The following approach was adopted.

1. Evaluate crash data and existing crash test configurations to determine relevant ODV-to-LPV impact scenarios.
2. Develop variations with different compatibility characteristics for four ODV categories.
3. Select FE models of occupied LPVs representing the sedan and SUV vehicle classes.
4. Establish ODV compatibility and LPV evaluation metrics.
5. Conduct a thorough simulation study to quantify the occupant and vehicle responses.

Full-frontal, frontal oblique, and perpendicular side impact crash configurations were determined as relevant ODV-to-LPV crash scenarios. Impact scenarios are like the existing New Car Assessment Program full-frontal, NCAP moving deformable barrier side, and NHTSA's research frontal oblique impact crash test configurations. Simulations were conducted for both the ODV-to-vehicle and barrier-to-vehicle reference impact scenarios.

Compatibility for ODV variations was quantified using occupant load criterion and crush work stiffness (KW400), which were developed by changing the material strength and thickness of relevant parts, as well as vehicle mass for select cases. Their effect on occupied sedan and SUV vehicles was evaluated based on vehicle and occupant response criteria.

Based on more than 120 ODV-to-LPV simulations, it was found that

1. In full-frontal and frontal oblique impact configurations for all ODV categories, better ODV compatibility correlated with lower LPV crash pulses, lower occupant compartment intrusions, and lower occupant injury metric values.
2. In side impact configurations, better ODV compatibility correlated with less LPV vehicle damage and lower occupant injury risk for three of the four ODV categories. The large and tall ODV that had a more compatible lower frontal structure and a relatively stiff upper frontal structure produced higher roof deformation in the LPV crash partner and high head injury risk.

Existing compatibility metrics from traditional vehicles are suitable for quantifying and optimizing ODV compatibility. Results indicate that ODV mass, design, and structural stiffness can have a substantial effect in collisions with an occupied crash partner vehicle.

1. Introduction

Background

The National Highway Traffic Safety Administration is responsible for devising strategies to reduce injuries and save lives in motor vehicle crashes. Because industry and research organizations are developing new types of vehicles that do not rely on human drivers, the automotive environment is changing. These emerging ADS have the potential to significantly reduce fatalities and injuries. Most ADS crashworthiness research has focused on protecting vehicle occupants, but a subset of new ADS vehicles is aimed at transporting cargo instead of people.

The ODV studied in this project will be used for delivery purposes and can vary in size, weight, storage capacity, and function. The specific mix of vehicle types and crash scenarios will vary depending on the operational design domain (ODD) for each vehicle. ODVs do not need to protect internal occupants, but they also need to interact with other road vehicles and will likely be designed to protect their cargo. Vehicle crash compatibility methods will be used in this study to evaluate ODV crash interaction with other occupied vehicles.

Research organizations have studied vehicle-to-vehicle crash compatibility for years (IIHS, AAM, & AIAM, 2006). Voluntary compatibility agreements require that the vehicle's primary energy-absorbing structure overlaps at least 50 percent with the zone defined by the United States Code of Federal Regulations (CFR) 49 Part 581, bumper standard (49 CFR, 1997), which establishes requirements for the impact resistance of vehicles in low-speed front and rear collisions. If this is not met, then the vehicle must have a secondary energy-absorbing structure (AAM, 2003). In addition, the SEAS must withstand at least 100 kN within 400 mm of structural crush. In 2009 the IIHS, AAM, and the AIAM reported a 19-percent reduction in passenger car driver deaths in vehicles designed to meet the compatibility requirements (Enhanced Vehicle-to-Vehicle Crash Compatibility Technical Working Group, 2009).

European New Car Assessment Program developed a mobile progressive deformable barrier test that incorporates a compatibility assessment (Ellway, 2019; European New Car Assessment Programme, 2019). The test consists of a 50 km/h 50-percent offset impact with a progressive stiffness MPDB profile. The compatibility assessment is part of the overall EuroNCAP score based on the variation in the MPDB's deformation, the OLC, and the extent of the MPDB deformation.

Scope

The purpose of this research was to study how variations in an ODV vehicle design can affect the occupants of a crash partner vehicle, across a range of expected ODDs.

Objective

The objective of this research was to use finite element simulations to study how the front-end structural compatibility and energy absorption of various ODV vehicles affect occupants in an LPV crash partner, across a range of ODD categories.

The selected crash scenarios in this study were grouped by vehicle type and ODD category, and separate requirements were considered for each ODD, where appropriate. Specifically, the following sub-tasks were carried-out during this study.

- Review and identify real-world crashes involving the front-end of various types of delivery vehicles and an LPV crash partner. The crashes must be relevant to ODV and grouped as per the expected ODDs.
- Identify existing crash test configurations and evaluate the relevance to expected ODV vehicle crashes. Develop new ODV-to-vehicle crash test configurations if existing crash test configurations are not sufficiently relevant.
- Select and develop two LPV crash partner FE models.
- Select and develop appropriate ODV FE models to represent a range of potential ODV vehicle types.
- Develop and execute a FE simulation plan focusing on crash scenarios between the front-end of a ODV and an occupied crash partner, including proposed performance criteria.

2. Identification of Real-World Crash Scenarios

Approach

We have reviewed and identified potential crashes involving the front-end of a ODV and an LPV crash partner. The crashes were grouped to represent at least four ODV ODDs, ranging from small local delivery vehicle to interstate heavy truck. At least two real-world crash scenarios per expected ODV ODD were identified.

The first step in identifying crash scenarios relevant to ODV was to conduct a thorough literature search[1] to understand potential changes in crash configurations due to the introduction of advance driver assistant systems and ADS.

The second step was to study an existing Department of Motor Vehicle database that specifically documented crashes with highly automated vehicles. Since data based on crashes involving fully automated vehicles and ODS were limited, the existing NHTSA databases were used as well.

Hence, the third step included an extensive crash data analysis for model year 2007 to 2017 vehicles. To understand the difference in crash types and configurations due to the introduction of such systems, crashes were grouped by vehicles that were equipped with ADAS and not equipped with ADAS.

Literature Search

Previous research suggests that collisions at intersections and left turns can have more dominant roles and may require special considerations (Östling et al., 2019). Additional relevant literature (Abraham et al., 2017; Benmimoun et al., 2013; Jenness et al., 2008; Liers et al., 2019; Östling et al., 2019; NHTSA, 2017; Pereira, 2015; Trübswetter, 2015) is documented in the reference section at the end of this report. There are a limited number of research papers that specifically studied the effect of ODV vehicles on impact configurations.

Related research includes the Federal Highway Administration’s CARMA program, which utilizes cooperative driving automation and communication that allows automated vehicles to interact and cooperate with infrastructure such as stop lights and other vehicles (FHWA, 2022).

The Wyoming Department of Transportation Connected Vehicle Pilot Project (Wyoming DOT, 2018) is another useful data source for determining potential future ADS impact scenarios. It currently collects data related to connected vehicles such as intersection movement assist and the “do not pass” application. Data is being monitored and may unveil future real-world crash configurations prone to connected ADS vehicles.

The “Next Generation Simulation Vehicle Trajectories and Supporting Data” project (FHWA, 2016) collects detailed vehicle trajectory data on select highways in Los Angeles and Atlanta. Monitoring the available data sets can become another source for understanding impact scenarios of next-generation vehicles.

DMV Data Analysis

State DMV databases are a valuable source of real-world crash scenarios and were evaluated for this study. Specifically, the California DMV (“OL316”) uses a report form called OL 316,

[1] The 26 citations from the literature search are denoted in the reference section preceded by asterisks.

Report of Traffic Crash Involving an Autonomous Vehicle,[2] to collect reports of traffic collisions involving AVs based on documented crashes and information from 13 AV companies. A total of 144 traffic crashes involving AVs have been reported from 2014 to 2019. The Center for Collision Safety and Analysis team has reviewed and categorized all cases, as shown in Figure 1 and Table 1. Manufacturers reporting crashes included Apple, Aurora, GM Cruise, Google, Waymo, Zoox, and others. About a third (34%) of impacts were rear-end (38 of 144) and side-swipe (11 of 144) collisions.

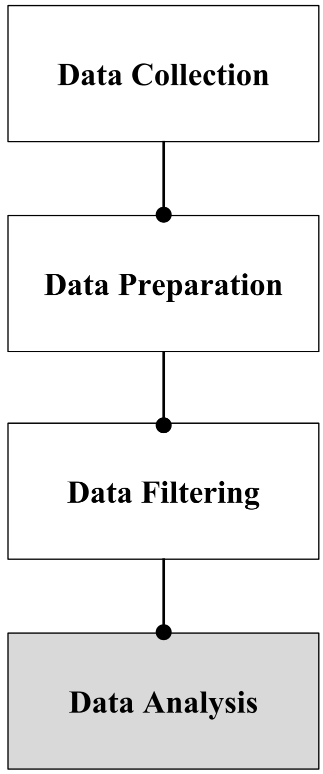

Figure 1. California DMV ADS crash database process

Table 1. California DMV ADS crash database results overview

Accident Years (2014-2019)

Manufacturers	Types of Collision							
Driving Modes	**broadside**	**head-on**	**hit object**	**other**	**rear-end**	**side swipe**	**(blank)**	**grand total**
Apple Inc.					**1**		**1**	**2**
autonomous mode					1			1
conventional mode							1	1
Aurora Innovation Inc					**3**			
conventional mode					3			

[2] www.documentcloud.org/documents/4063115-California-DMV-s-OL-316-form-Report-of-Traffic.html

Manufacturers	Types of Collision							
Driving Modes	**broadside**	**head-on**	**hit object**	**other**	**rear-end**	**side swipe**	**(blank)**	**grand total**
Delphi Automotive System, LLC							**1**	**1**
conventional mode							1	1
Drive.ai, Inc.							**1**	**1**
conventional mode							1	1
GMCruise	**2**	**1**	**1**	**2**	**8**	**7**	**50**	**71**
autonomous mode				1	7	4	35	47
conventional mode	2	1	1	1	1	3	15	24
Google Auto LLC							**24**	**24**
autonomous mode							17	17
conventional mode							7	7
Jingchi Corp					**1**			**1**
autonomous mode					1			1
Lyft, Inc.		**1**			**1**			**2**
conventional mode		1			1			2
Nissan North American INC							**1**	**1**
conventional mode							1	1
Toyota Research Institute, Inc.			**1**					**1**
conventional mode			1					1
UATC, LLC					**2**		**1**	**3**
conventional mode					2		1	3
Waymo LLC	**1**		**1**		**18**	**3**	**4**	**27**
autonomous mode	1				15		3	19
conventional mode			1		3	3	1	8
Zoox, Inc					**4**	**1**	**2**	**7**
autonomous mode					1		1	2
conventional mode					3	1	1	5
grand total	**3**	**2**	**3**	**2**	**38**	**11**	**85**	**144**

When focusing on cases in which the vehicles were operated only in autonomous mode, a similar trend was observed. The majority of documented cases were rear-end collisions where the case vehicle's rear-end was struck by a crash partner, as shown in Table 2.

Table 2. California DMV ADS crashes in autonomous mode

Accident Years (2014-2019)

Manufacturers	Types of Collision					
Driving Modes	**broadside**	**other**	**rear-end**	**side swipe**	**(blank)**	**grand total**
Apple Inc.			**1**			**1**
autonomous mode			1			1
GMCruise		**1**	**7**	**4**	**35**	**47**
autonomous mode		1	7	4	35	47
Google Auto LLC					**17**	**17**
autonomous mode					17	17
Jingchi Corp			**1**			**1**
autonomous mode			1			1
Waymo LLC	**1**		**15**		**3**	**19**
autonomous mode	1		15		3	19
Zoox, Inc			**1**		**1**	**2**
autonomous mode			1		1	2
grand total	**1**	**1**	**25**	**4**	**56**	**87**

Table 3 shows the movement of the autonomous and involved traditional crash partner vehicle. Note that the most often occurring impact scenario engaged a stopped AV and a traditional vehicle proceeding straight.

Table 3. California DMV ADS crash database – impact configurations

Movement of AV	Movement of Involved veh 1 in AV collisions							
	making left turn	**making right turn**	**passing other vehicle**	**proceeding straight**	**slowing/ stopping**	**(blank)**	**grand total**	**%**
making left turn				1			1	4%
making right turn				2			2	8%
proceeding straight	1			1			2	8%

Movement of AV	**Movement of Involved veh 1 in AV collisions**							
	making left turn	**making right turn**	**passing other vehicle**	**proceeding straight**	**slowing/ stopping**	**(blank)**	**grand total**	**%**
proceeding straight / slowing / stopping				1			1	4%
stopped		4	1	**10**	3	1	19	76%
grand total	1	4	1	15	3	1	**25**	
%	4%	16%	4%	60%	12%	4%		

A detailed description of identified impact scenarios is shown in Table 4. Most documented crashes occurred at speeds below 5 mph, where vehicle damage was minor and there were no injuries.

Table 4. California DMV ADS crash database – impact characteristics and speeds

															Impact Speed		
Accident Year	**Manufacturer**	**Make Vehicle**	**Vehicle Model**	**# of Vehicles Involved**	**Types of Collision AV**	**Movement Preceding Collision Accident AV**	**Details of AV Movement**	**Movement Preceding Collision Involved Veh1**	**AV Driving Mode**	**Time of Collision (am/pm)**	**Geometric**	**Weather**	**Lighting**	**Surface**	**Impact Speed Appx.**	**Damage**	**Injury**
2019	Waymo	Chrysler	Pacifica	2	rear-end	stopped in traffic	stopped at an exit ramp	proceeding straight	autonomous mode	a.m.	no unusual condition	clear	daylight	dry	4 mph	minor/ rear bumper	no
2018	Waymo	Chrysler	Pacifica	2	rear-end	stopped	stopped at an intersection with a red light	proceeding straight	autonomous mode	p.m.	no unusual condition	clear	daylight	dry	3 mph	minor/ rear bumper	no
2018	Waymo	Chrysler	Pacifica	2	rear-end	stopped	stopped at an intersection	proceeding straight	autonomous mode	p.m.	no unusual condition	clear	daylight	dry	low	minor	no
2018	Waymo	Chrysler	Pacifica	2	rear-end	stopped	stopped to turn right at a traveling line	proceeding straight	autonomous mode	a.m.	no unusual condition	clear	daylight	dry	2 mph	minor	no
2018	Waymo	Chrysler	Pacifica	2	rear-end	stopped	stopped at a traveling line	proceeding straight	autonomous mode	p.m.	no unusual condition	clear	daylight	dry	5 mph	minor	no
2018	Waymo	Chrysler	Pacifica	2	rear-end	stopped	stopped at an exit ramp with a stop sign	proceeding straight	autonomous mode	a.m.	no unusual condition	clear	daylight	dry	1 mph	minor/ front bumper	no
2018	Waymo	Chrysler	Pacifica	2	rear-end	stopped/ merging	stopped at an exit ramp	proceeding straight	autonomous mode	p.m.	no unusual condition	clear	daylight	dry	2 mph	minor/ rear bumper	no
2018	Zoox	Toyota	Highlander	2	rear-end	stopped	stopped at an intersection with a stop sign	proceeding straight	autonomous mode	p.m.	no unusual condition	clear	dark-street-light	dry	5-10 mph	minor	no

In summary, we found that the California DMV database provides detailed documentation of crashes that involved automated vehicles from different manufacturers. Collisions that occurred were mainly rear-end collisions at low speeds and with minimal vehicle damage. Hence, additional real-world data analysis was needed to determine appropriate impact configurations for the Crash Compatibility in Occupantless Delivery Vehicles research.

NHTSA's Crash Data Collection Programs

NHTSA's crash data collection programs, shown in Figure 2, are a rich source of real-world crash scenarios. Currently, the programs provide information mostly involving traditional vehicles. After the introduction of ADAS technologies, additional impact characteristics were specified and documented. This is especially true for the Crash Investigation Sampling System database with distinct documentation of ADAS options.

Highlight of CISS

1. Sample design
    - CDS PSU 24 sites to CISS 32 sites in 2018
    - Injury coding
2. Weighting procedure
3. Estimation method
4. Flexibility with other data system
    - CDS/CRSS/FARS
5. Modernization
    - EDR/CDR tool
    - Crash avoidance (AVOID table)

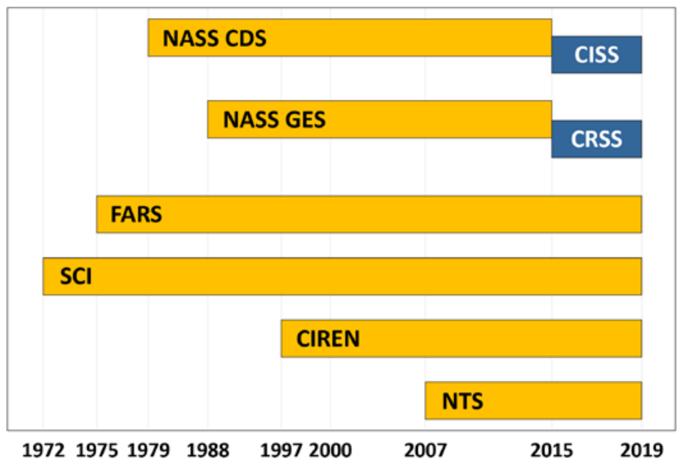

Figure 2. NHTSA's crash data collection programs

We are aware that using NHTSA-CDS and CISS databases can only provide initial indications on how existing ADAS influence impact scenarios in SAE level 2 and level 3 vehicles.

Having a limited amount of crash data for fully automated occupied and unoccupied vehicles, the existing databases were used and two data sets were developed based on more than 9,000 cases: (1) crashes that involved vehicles without ADAS equipment; and (2) crashes that involved vehicles with ADAS equipment. This gave an indication of how these and similar systems, which are anticipated to be used in ODV vehicles, will affect impact configurations in the future.

Figure 3 shows a comparison of impact types for vehicles with and without ADAS systems. The overall distribution is similar, i.e., the most frequent impact type is frontal with 65 percent and 71 percent for not-ADAS-equipped and ADAS-equipped vehicles. Similarly, the second most frequent impact type was side impact, representing 30 percent and 25 percent. Rear impact was the least frequent impact configuration, with 5 percent and 4 percent of all impacts for not-ADAS-equipped and ADAS-equipped vehicles.

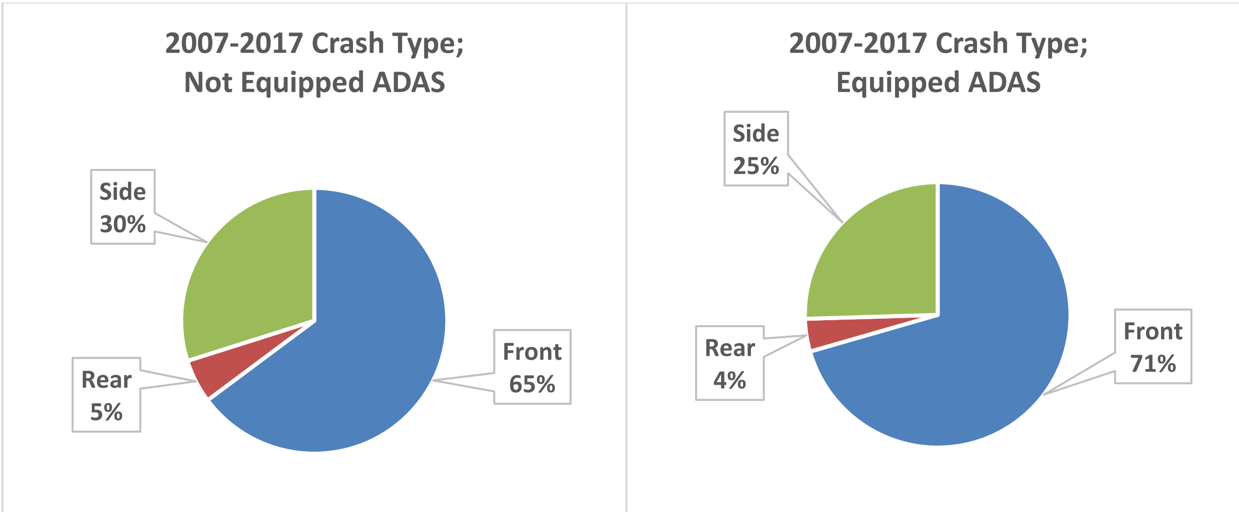

Figure 3. Crash types involving not-ADAS-equipped versus ADAS-equipped vehicles

Figure 4 shows the comparison for crashes involving not-ADAS-equipped versus ADAS-equipped vehicles for 2007 to 2017. A similar overall trend can be observed for most years.

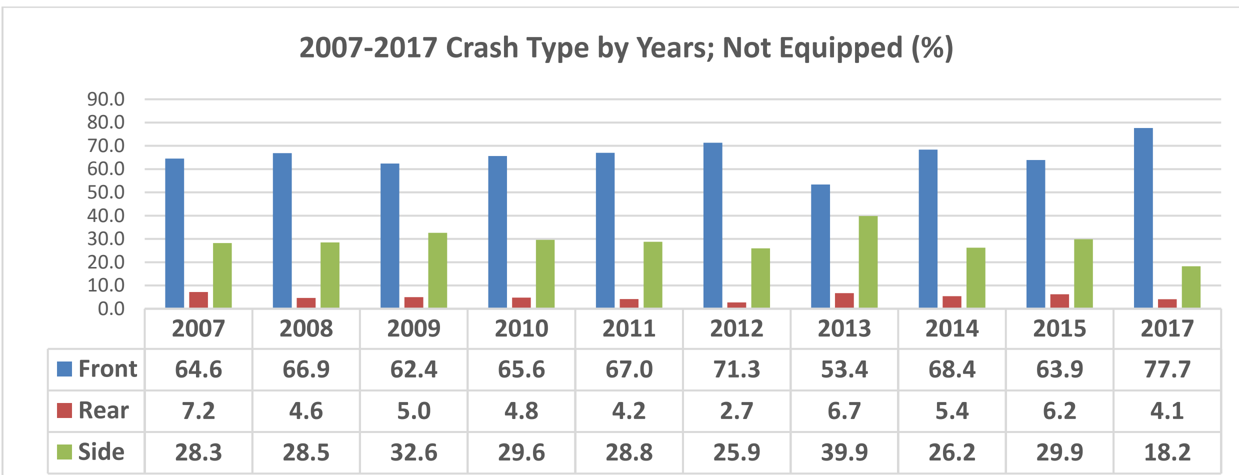

	2007	2008	2009	2010	2011	2012	2013	2014	2015	2017
Front	64.6	66.9	62.4	65.6	67.0	71.3	53.4	68.4	63.9	77.7
Rear	7.2	4.6	5.0	4.8	4.2	2.7	6.7	5.4	6.2	4.1
Side	28.3	28.5	32.6	29.6	28.8	25.9	39.9	26.2	29.9	18.2

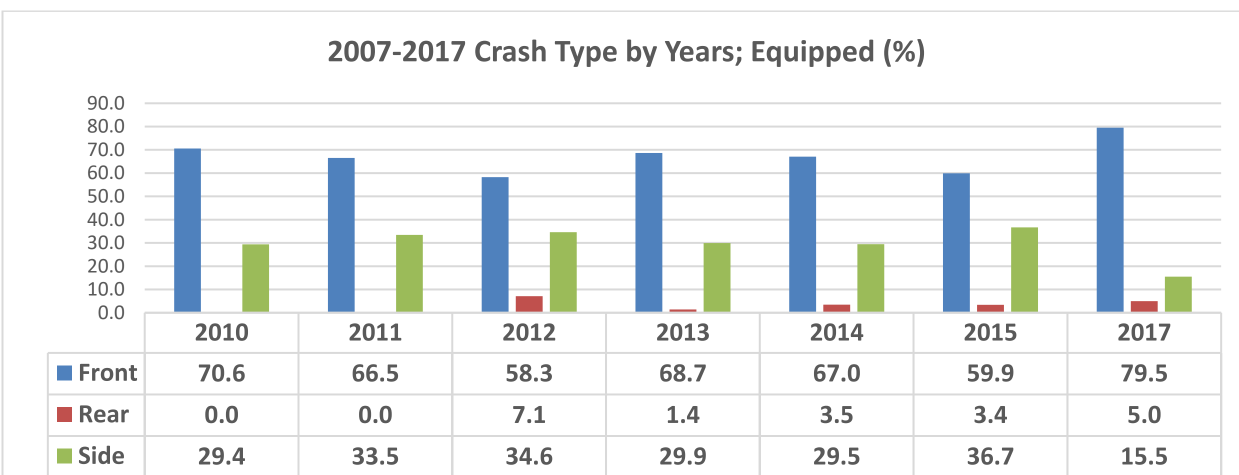

	2010	2011	2012	2013	2014	2015	2017
Front	70.6	66.5	58.3	68.7	67.0	59.9	79.5
Rear	0.0	0.0	7.1	1.4	3.5	3.4	5.0
Side	29.4	33.5	34.6	29.9	29.5	36.7	15.5

Figure 4. Crash types involving not-ADAS versus ADAS-equipped vehicles by year

For the frontal impact type, most crashes (44.6%) showed damage across the full vehicle front, as shown in Figure 5 (a). Crashes with left and center vehicle front damage were the second highest percentage (14.3%). The principal direction of force distribution is shown in Figure 5 (b), demonstrating that most crashes occurred at a 0° full-frontal direction, with a high percentage also for frontal oblique angles of +/- 10°. For the full-frontal and frontal oblique scenarios, 42 km/h and 36 km/h, were found to be representative relative impact velocities.

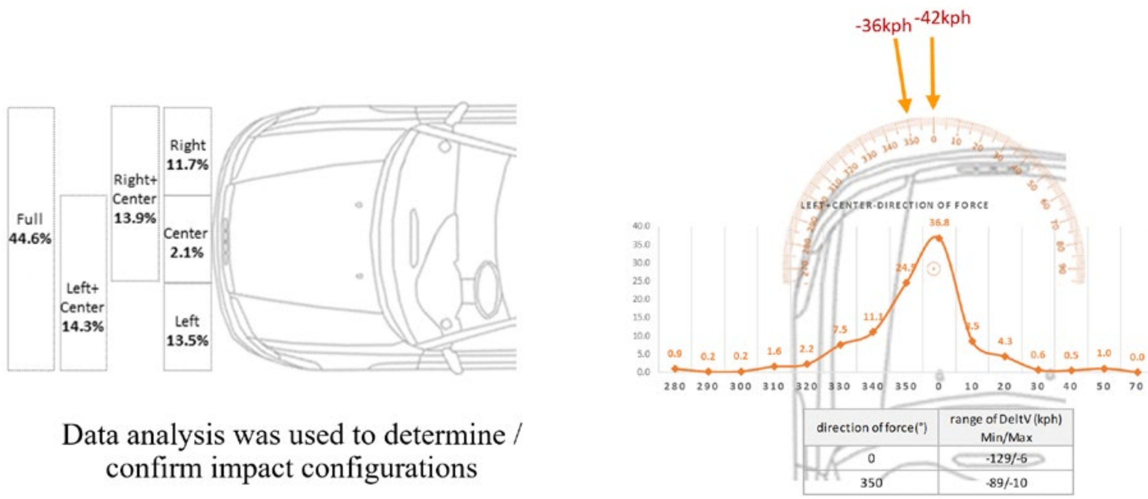

Figure 5. Frontal impact (a) overlap distribution; (b) PDOF

Figure 6 (a) shows the comparison of full-frontal versus partial frontal impacts for sedan vehicles. Not-ADAS-equipped vehicles are denoted by blue bars, and ADAS-equipped sedans are shown in orange. Full-frontal impacts represent most cases. Figure 6 (b) shows the comparison for SUV-type vehicles. Again, frontal impacts with full damage distribution represented most cases. In contrast to sedans, SUVs had a trend of reduced percentage of full-frontal damage distribution and a consequently higher percentage for the different partial overlap/partial damage distribution configurations for ADAS-equipped vehicles. Overall, full-frontal cases represent the most frequent real-world impact scenario for both sedan and SUV vehicles.

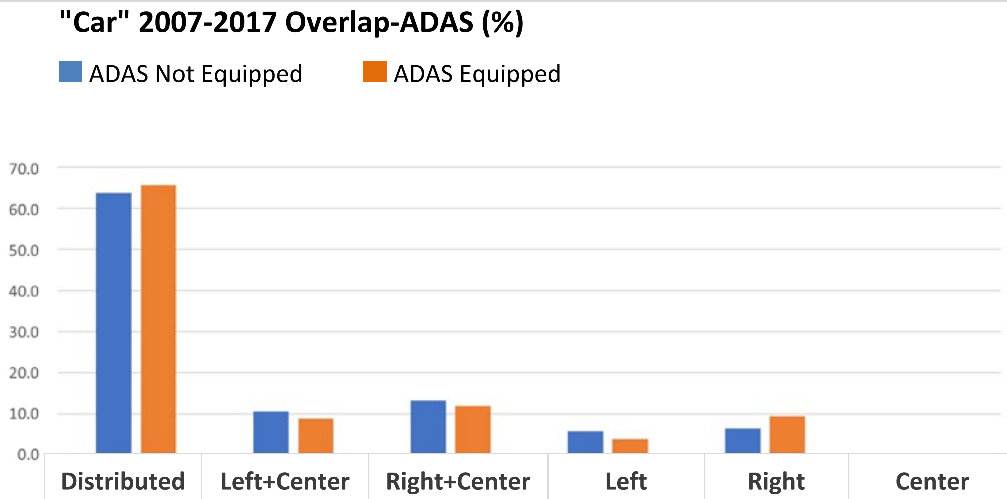

	Full	Moderate		Small		
	Distributed	Left+Center	Right+Center	Left	Right	Center
ADAS Not Equipped	63.6	10.6	13.3	5.8	6.5	0.2
ADAS Equipped	65.6	8.9	12.0	3.9	9.5	0.1

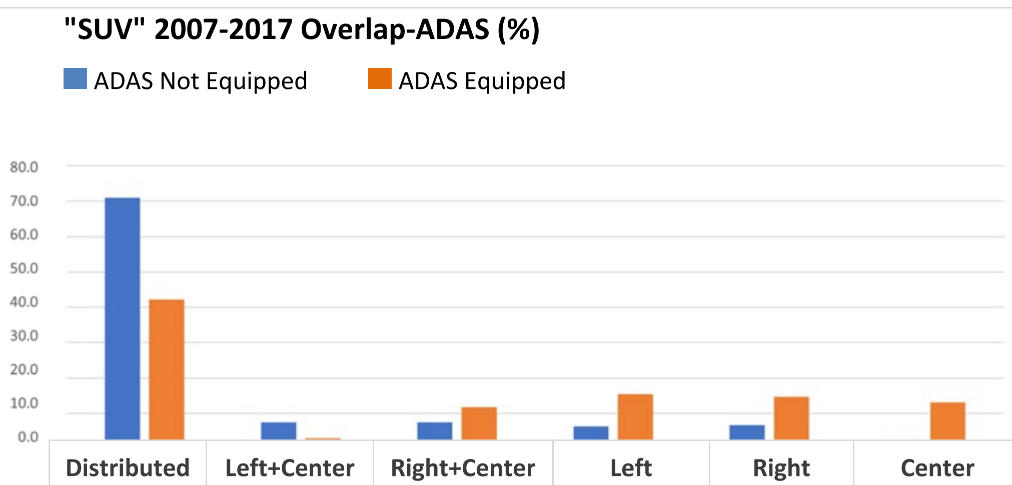

	Full	Moderate		Small		
	Distributed	Left+Center	Right+Center	Left	Right	Center
ADAS Not Equipped	71.0	7.4	7.4	6.3	6.7	1.2
ADAS Equipped	42.1	2.9	11.8	15.5	14.7	13.1

Figure 6. Not-ADAS-equipped versus ADAS-equipped vehicle frontal damage (a) sedans; (b) SUVs

For side impact configurations, crashes with damage at the forwardmost third of the vehicle side represented the highest percentage of cases (29%), followed by the center of the vehicle (10%), as shown in Figure 7 (a). A 280° PDOF direction with a 22 km/h delta V was found to be the most frequent scenario, as shown in Figure 7 (b).

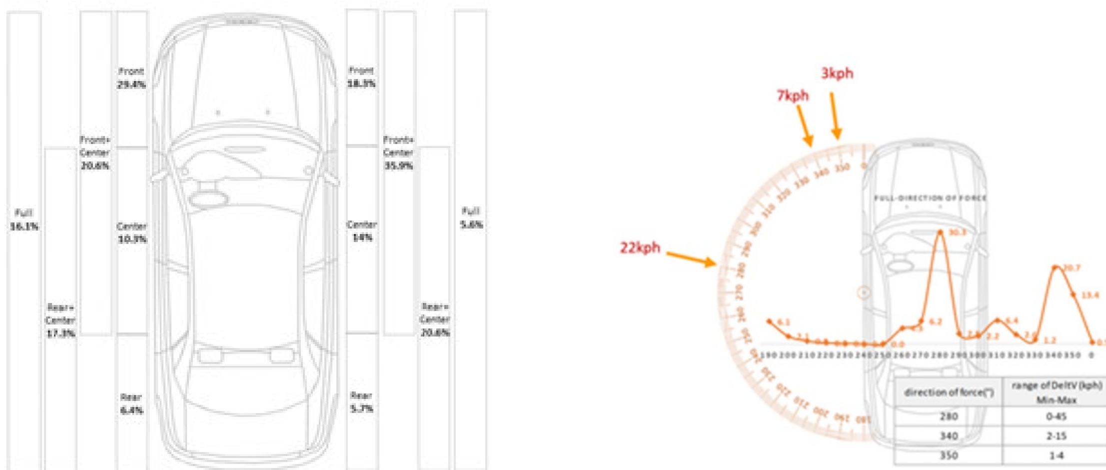

Figure 7. Side impact (a) damage distribution; (b) PDOF

Real-world Crash Scenarios

Having a limited amount of data for occupied vehicles and ODV in fully automated drive mode, existing NHTSA databases with a high number of cases were used to evaluate the effect of ADAS equipment on crash configurations. It was found that frontal cases with vehicle damage at the full width of the vehicle represented the most frequent scenario, with a trend to more moderate overlap cases for SUV vehicles. For the CCODV research, a full-frontal impact scenario with 100-percent overlap and a partial overlap oblique frontal impact were considered the most representative configurations.

For side impact configurations, impacts at a perpendicular (270°) or close to perpendicular (280°) PDOF impact direction were found to be the most representative scenarios. Although many crashes occur with the bullet vehicle striking the forwardmost third of the target vehicle side, it was decided to conduct the compatibility study research such that the different ODV vehicle categories impact the center of the target vehicles at a perpendicular angle. This agrees with existing consumer information rating test programs and regulatory side impact requirements.

ODV Delivery Vehicle Groups and ODDs

Four ODV vehicle groups and respective ODDs were determined by analyzing existing vehicle designs and ODV vehicle concepts. Table 5 shows the four selected groups.

1. The small ODV, e.g., a Nuro-type[3] concept, that is used to deliver small packages. It is small in size with a low gross vehicle weight rating (GVWR).
2. The mid-size ODV is larger in size and GVWR and can be used for transporting goods and deliveries to customers and is based on a concept presented by Mercedes.[4]
3. The large-size ODV, such as the Einride T-Pod,[5] is a concept that can be used to transport larger cargo such as lumber or pallets of food and drinks, for example.
4. The tractor trailer ODV, such as the Volvo Vera[6] design, would be used for interstate cargo transportation.

Initially, ODV vehicle maximum speeds are expected to be lower than for traditional human-driven vehicles. To represent a range of ODD categories, different impact speeds were selected for the different ODV categories, ranging from 35 km/h for the small ODV to 50 km/h for the tractor ODV.

[3] [Editor's note: Nuro, an American robotics company in Mountain View, California, designs and develops autonomous delivery vehicles. It was the first company to receive an exemption from NHTSA since its vehicles are designed to carry goods instead of humans. An R2 is its second-generation self-driving vehicle designed with no steering wheel, side-view mirrors, or pedals.]

[4] [Editor's note: The Mercedes concept called "Vision" includes the "Urbanetic" autonomous driving platform with switchable bodies based on a self-driving, electrically powered chassis that can become a ride-sharing vehicle for up to 12 passengers, or a cargo module shown in Table 5.]

[5] [Editor's note: Stockholm-based Einride AB is a Swedish transport company that specializes in electric and self-driving vehicles known as Einride pods, formerly called T-pods, electric trucks remotely controlled by drivers and are notable for lack of driver cabs.]

[6] [Editor's note: The Vera is Volvo Trucks Division first autonomous tractor unit for intended for heavy haulage. It is a low-profile, noiseless vehicle with no driver's cab, a "pure" electric power unit, and is emission-free. It is claimed to be well-suited to short, repetitive trips where large volumes of goods can be transported from ports, factory sites, and large logistics centers that operate together in a fleet network connected by a cloud-based management center. For safety reasons Veras move at low operating speeds and when the batteries runs low, they return automatically to charging stations.]

Table 5. Four ODV categories

	Generic FE Model	**Reference Concept**	
Small ODV	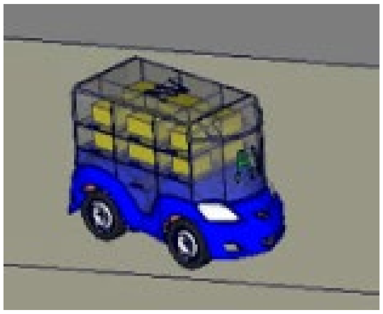		"Nuro" (Nuro, 2018)
Mid-size ODV	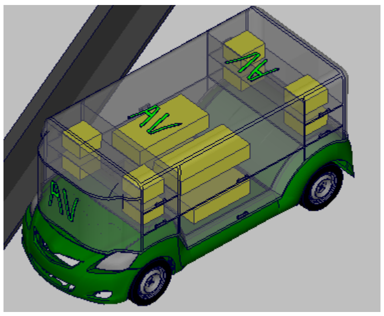		"Mercedes Vision" (Davies, 2018)
Large ODV	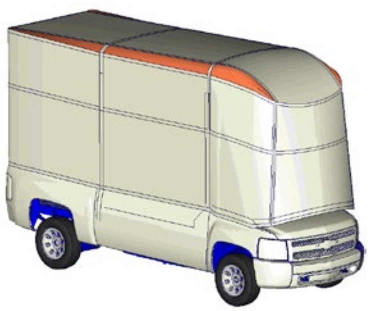		"Einride T-Pod" (Sawers, 2017)
Tractor Trailer ODV	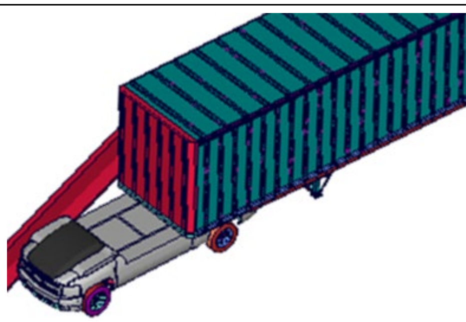		"Volvo Vera" (Sawers, 2017)

Crash Scenarios for the ODV Delivery Vehicle Groups and ODDs

For all four ODV categories, impact scenarios with a full overlap were studied to evaluate the effect of compatibility compliant and compatibility non-compliant ODV designs, as shown in Figure 8. Criteria for evaluating compatibility are outlined in Chapter 4. Selected impact velocities for the respective ODDs are outlined in Chapter 6.

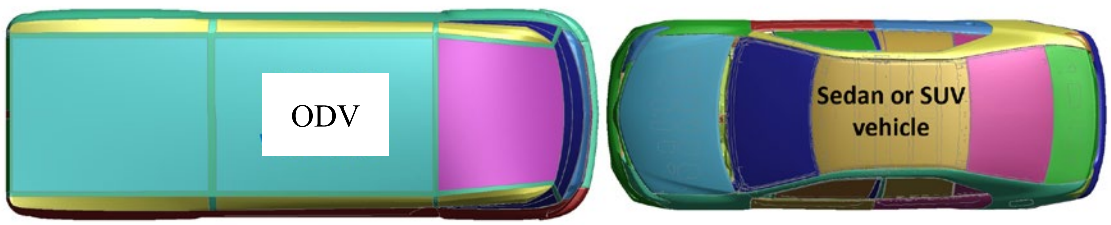

Figure 8. Impact configuration 1 – full-frontal

In addition, analyses for frontal oblique configurations with partial overlap were conducted, as shown in Figure 9. A 50-percent overlap at a 10° oblique angle was considered a reasonable configuration based on the conducted crash data analyses and existing impact scenarios. This would represent a crossing the centerline or left turn crash scenario. The same impact speeds as for the full-frontal impact scenarios were selected for the crash partner and ODV vehicles, as outlined in Chapter 6.

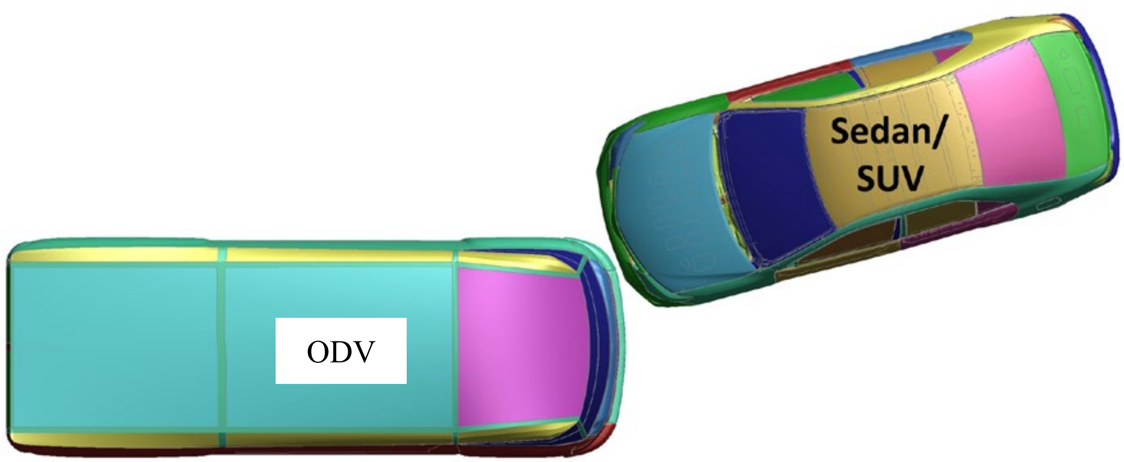

Figure 9. Impact configuration 2 – frontal oblique

In the determined side impact configuration, the respective ODV vehicles impact a stationary passenger vehicle perpendicularly at the center of the vehicle's side profile, as shown in Figure 10. Impact angle and location were based on the previously conducted crash data analyses and existing crash test configurations. As with the frontal impact configurations, different impact velocities were defined for the different ODV vehicle groups, as outlined in Chapter 6.

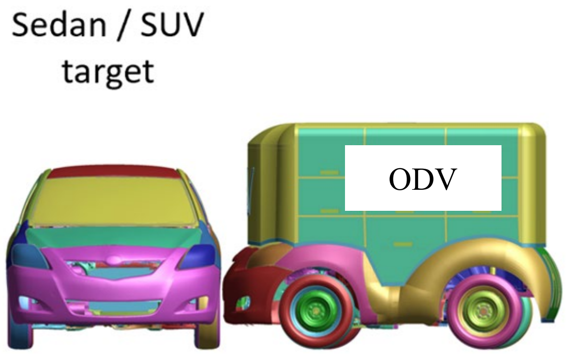

Figure 10. Impact configuration 3 – side crash

The defined impact configurations, i.e., frontal full overlap, frontal oblique partial overlap, and side impact, were conducted for all four ODV vehicle groups.

This page intentionally left blank.

3. Evaluation of Crash Test Configurations

We evaluated the relevance of Federal Motor Vehicle Safety Standard and NCAP crash test configurations to the vehicle-to-vehicle incidents identified in Chapter 2, Identification of Real-World Crash Scenarios, for consideration in the evaluations of ODV. Since existing crash test configurations were not exactly applicable for all identified ODV-to-LPV scenarios, appropriate modifications were also applied. It was planned to define a minimum of two test configurations for each ODV ODD, in which the front-end of the ODV contacts another occupied vehicle. It was decided that in addition to the full-frontal co-linear and the ODV striking the side of another occupied vehicle, the frontal oblique offset configuration would be a beneficial additional research load case.

For the full-frontal configuration, the NCAP full overlap and a ODV-to-vehicle full overlap frontal impact were compared. Different metrics, such as deformation, force levels of primary and secondary load paths, OLC, and crush work stiffness (KW400) were considered as structural compatibility metrics.

Recent research as outlined in Chapter 2 has indicated that an increase in intersection crashes can be anticipated with the introduction of ADS vehicles. A possible side-impact scenario could therefore be that a moving occupied vehicle is being struck by an ODV from the side. Side impact scenarios with ODV vehicles of different shapes, masses, and frontal structure compatibility characteristics and their respective ODD were defined, as outlined in Chapter 6. We compared the results with existing side impact configurations, such as NHTSA's FMVSS No. 214 MDB impact and IIHS side impact configurations.

Approach

First, a thorough literature search was conducted to identify previous relevant research for vehicle compatibility in front and side impact configurations. Important references[7] are documented in Appendix A.

Second, the relevance of FMVSS and NCAP crash test configurations to the vehicle-to-vehicle incidents identified in Chapter 3 was determined.

The process used, as well as crash test configurations chosen to simulate the identified real-world crash scenarios for each ODD, are summarized below.

1. Identification of Real-World Crash Scenarios
2. Include existing rating or regulation crash scenarios that have a similar PDOF in the simulation matrix as Reference 1. For example, for a frontal oblique impact scenario, NHTSA's OMDB[8]-to-vehicle frontal oblique configuration would be used as Reference 1 for a real-world frontal oblique impact scenario. Reference 1 means that the occupant's kinematics and injury metrics would be determined in the existing impact scenario, for which injury metrics or injury assessment research values (IARV) are known. The

[7] Alliance of Automobile Manufacturers, 2003); Barbat et al., 2007; Brewer et al., 2011; Delannoyet al., 2004; Enhanced Vehicle-to-Vehicle Crash Compatibility Technical Working Group, 2009; Hobbs, 1998; Insurance Institute for Highway Safety, 2014; Mohan, 2007; Mohanet al., 2007; Mohan, & Smith, 2007; NHTSA, 1990; Patel et al., 2007, 2009; Powell et al., 1999; Side Airbag Out-of-Position Injury Technical Working Group, 2003; Subramaniam et al., 2007; Teoh & Nolan, 2012

[8] Offset moving deformable barrier

Reference 1 results served as an initial reference for the identified real-world frontal oblique crash scenario, which differed in impact angle or overlap.

3. Conduct ODV-to-vehicle simulation(s) according to the identified real-world crash scenarios. The results from the previously conducted "known" impact scenarios served as Reference 2 for the ODV-to-vehicle baseline simulation.
4. Ultimately, study how a ODV vehicle's front-end structural design can affect the occupants in a crash partner vehicle, across a range of expected ODV ODDs for the respective impact scenarios.

To evaluate occupant kinematics and injury metrics with modified boundary conditions compared to existing test configurations, the baseline ODV-to-vehicle simulation results of an impact scenario of interest was compared with results from existing crash scenarios (Reference 1 and Reference 2) to demonstrate differences and similarities.

Configuration 1: Full-Frontal Co-Linear

A frontal impact, with vehicle damage across the entire front of the vehicle, was identified as one relevant impact scenario from the real-world crash data analysis. A representative ODV-to-vehicle configuration is shown in Figure 15.

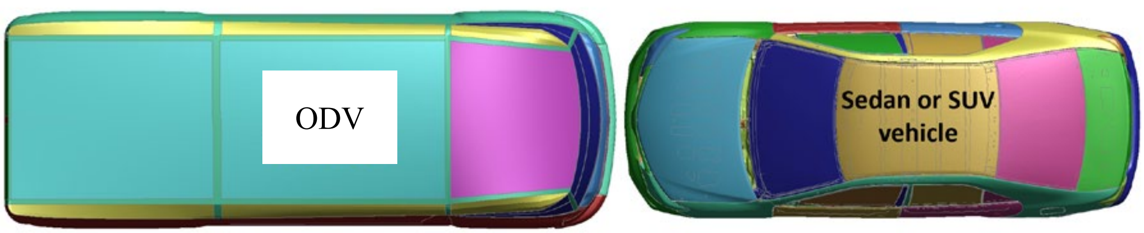

Figure 11. Real-world impact scenario 1 – full-frontal

The FMVSS No. 208/NCAP configuration, as shown in Figure 12, simulates this type of full overlap co-linear crash scenario. This is an example of Reference 1.

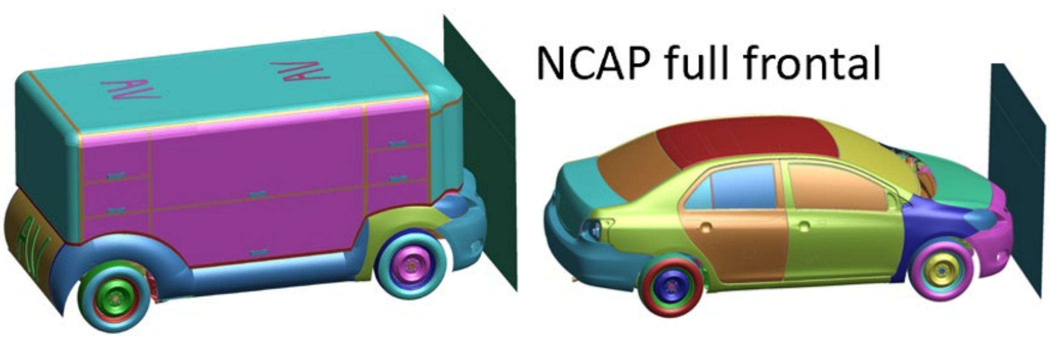

Figure 12. FMVSS No. 208/NCAP full-frontal reference

Recorded load cell data from the impact of a vehicle into a rigid wall has been used in previous research efforts related to compatibility and vehicle structure performance characteristics. Some citations (Brewer et al., 2011; Mohan, 2007; Mohan et al., 2007; Mohan & Smith, 2007; Patel et al., 2009; Patel et al., 2007) have been listed in Appendix A.

The NCAP full-frontal configuration captures the same co-linear nature and overlap percentage as the identified full-frontal ODV-to-vehicle impact and was therefore used as the standardized reference (Reference 1) for the identified real-world crash scenario with full-frontal vehicle damage. Impact speeds were determined to best capture the most meaningful scenarios for the respective ODV vehicle categories and ODDs, as outlined in Chapter 6.

Configuration 2: Frontal Moderate Overlap

A frontal impact with a partial frontal vehicle damage was identified as another relevant impact configuration from the real-world crash data analysis. An example is shown in Figure 13.

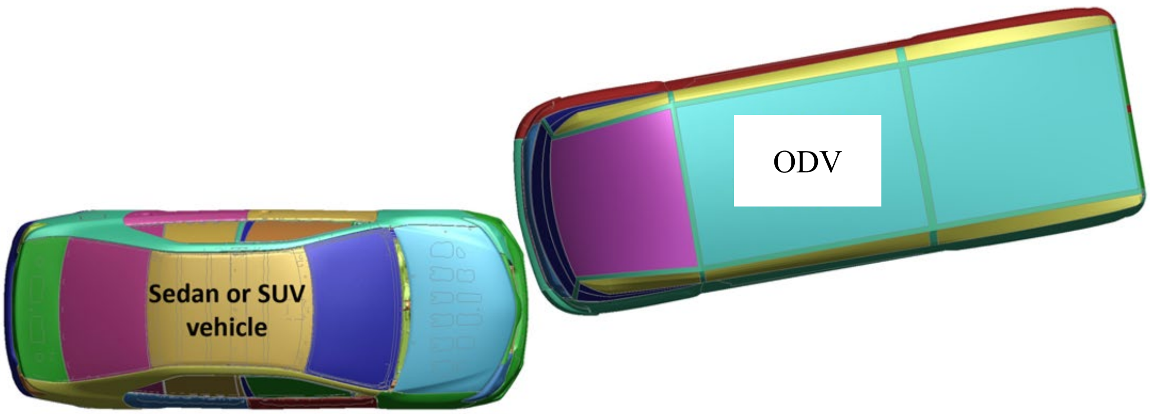

Figure 13. Real-world impact scenario 2: frontal oblique

A 50-percent overlap at a 10° oblique angle was found to be a representative configuration based on the conducted crash data analyses and existing impact scenarios. This can represent a crossing-the-centerline or left- or right-turn crash scenario.

The first relevant existing test configuration for this real-world crash scenario is NHTSA's frontal oblique impact, where the OMDB strikes a stationary vehicle. The OMDB weighs 2,486 kg and strikes the vehicle at 90 km/h. The vehicle is placed at a 15° angle from the OMDB longitudinal axis. The impact is set up such that a 35-percent overlap occurs between the OMDB and the front end of the struck vehicle at initial contact, as shown in Figure 14.

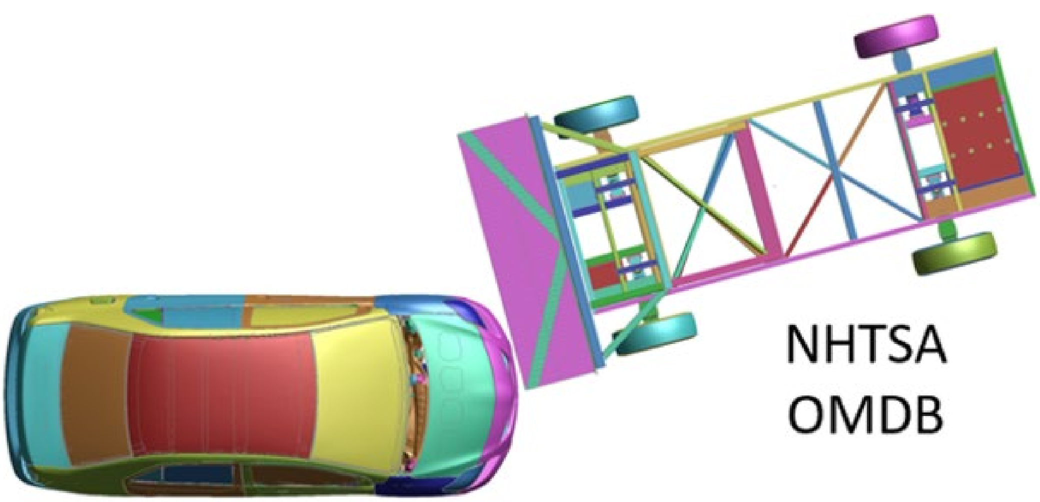

Figure 14. NHTSA frontal oblique OMDB impact reference

A second selected, relevant existing test configuration is EuroNCAP's MPDB-to-car impact, shown in Figure 15.

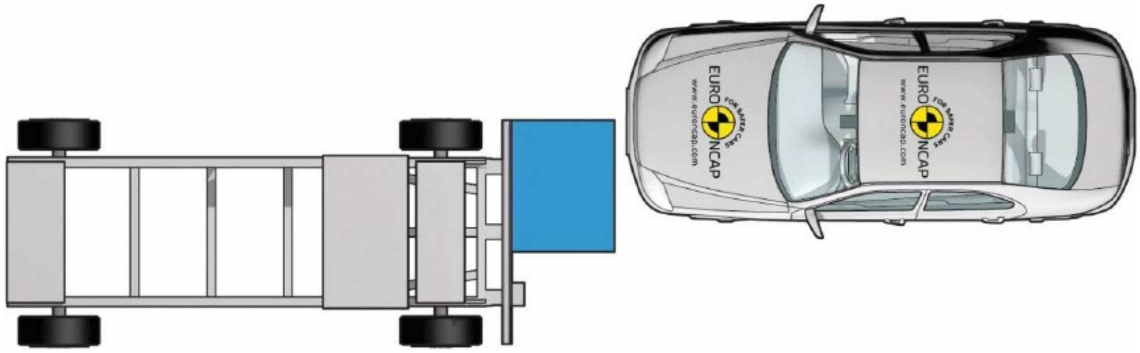

Figure 15. EuroNCAP MPDB reference, © Euro NCAP 2021

In the full-scale MPDB test, the test car travels at 50 km/h with a 50-percent overlap into a deformable barrier face mounted on an oncoming 1,400 kg trolley, also traveling at 50 km/h. The barrier represents the front end of another vehicle, getting progressively stiffer the more it is deformed. The test replicates a crash between the test vehicle and a mid-size family car.

The EuroNCAP compatibility assessment is based on three parameters that are determined using the results of the MPDB-to-car impact. The three parameters are the standard deviation (SD) of the post-test barrier face measurements, the OLC, and whether the vehicle has "bottomed-out" the MPDB face. According to EuroNCAP Technical Bulletin 027 (Ellway, 2019), *Compatibility Assessment*, "Bottoming out is defined as an area of the barrier that has been penetrated by 630mm or more that is 40mm x 40mm in height and width."

The NHTSA frontal oblique and EuroNCAP moderate overlap test configurations were used as a reference for the identified real-world crash scenario with partial frontal vehicle damage and oblique PDOF characteristics. Impact speeds were carefully determined to best capture the most meaningful scenarios for the respective ODV vehicle categories and ODDs. The EuroNCAP MPDB configuration (co-linear, 50% overlap) uses the same overlap percentage as the identified real-world scenario. NHTSA's OMDB impact configuration (15° oblique, 35% overlap) takes the oblique nature of the identified real-world crash scenario (10° oblique, 50% overlap) into account.

Side Impact Configuration

Based on the conducted real-world crash data analysis, a side impact scenario where ODV vehicles of different size, GVWR, and ODD impact a stationary passenger vehicle at a 270° angle at the center, as shown in Figure 16. Small differences in impact angle, i.e., +/- 10° (260°/280°) were also found to be likely crash scenarios. While many crashes occurred with the bullet vehicle striking the front third of the target vehicle, the center impact location is considered the more critical scenario and was therefore chosen.

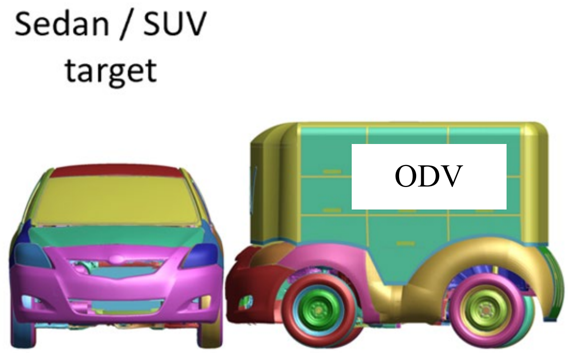

Figure 16. Real-world impact scenario 3 – side crash

The existing FMVSS No. 214 MDB and the IIHS side impact test conditions were determined to best simulate and represent the identified real-world impact scenarios. They are shown in Figure 17.

Figure 17. Side impact references (a) NHTSA MDB; (b) IIHS MDB, © Insurance Institute for Highway Safety.

The MDB's have different mass, height, and deformation characteristics. The NHTSA and IIHS side impact MDB configurations were used as a reference for the identified real-world crash scenarios with lateral PDOF characteristics. Again, impact speeds were carefully determined to best capture the most meaningful scenarios for the respective ODV vehicle categories and ODDs.

This page intentionally left blank.

4. Crash Partner FE Models

Background

We have identified two appropriate FE models for LPVs to be used as crash partners for the scenarios identified in Chapter 2. The models selected for this study represent the sedan and SUV vehicle classes. Existing candidate sedan and SUV FE vehicle models of different types, sizes, and masses are listed below and shown in Figure 18.

- 2010 Toyota Yaris
- 2014 Honda Accord
- 2015 Toyota Camry
- 2018 Dodge Ram (Pickup)
- 2020 Nissan Rogue (SUV)

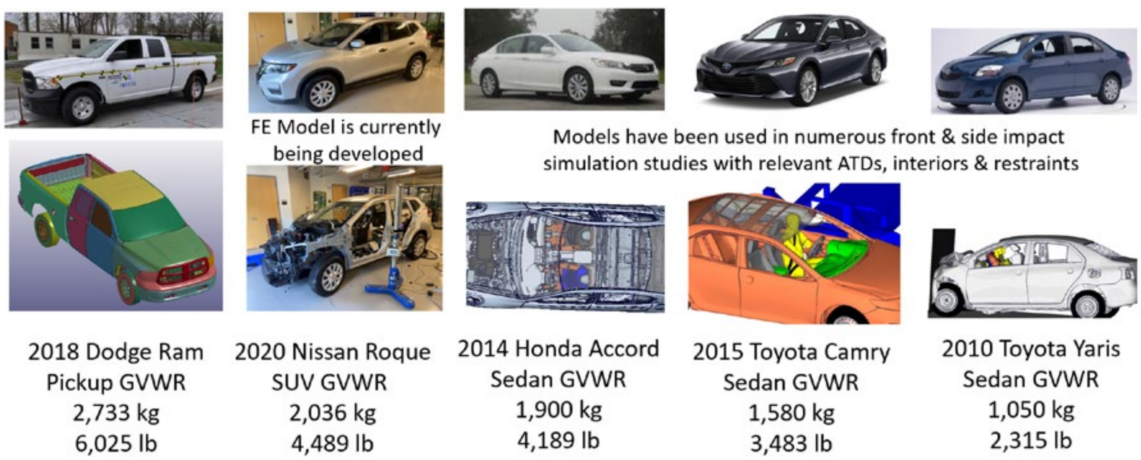

Figure 18. Candidate crash partner vehicle FE models

All candidate crash partner LPV FE models have been or can be used in combination with publicly available or third-party interior and restraint systems. Many research and student projects have been conducted using these models for full-frontal, frontal oblique, partial overlap, and side impact simulation studies.

The LPV FE model selection considered the increasing trend in the U.S. market toward SUVs, pickup trucks, and heavier vehicles with electric or hybrid drive. The crossover vehicle class -- a type of SUV with unibody construction -- is often based on a platform shared with a passenger car, in contrast to a truck-based SUV with a body and a ladder-type frame. The crossover vehicle segment represented by far the largest U.S. market share in 2019 with 39.4 percent, as shown in Figure 19 (a). The annual U.S. sales numbers for this vehicle segment increased by 75 percent from 2013 to 2018, as shown in Figure 19 (b).

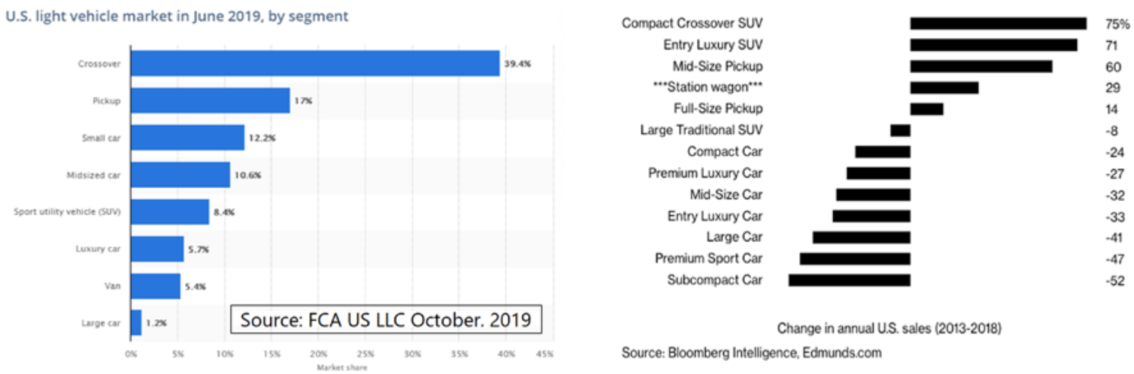

Figure 19. U.S. vehicle segment (a) market share; (b) change in annual sales (2013-2018)

An FE model based on a 2020 Nissan Rogue crossover SUV was recently developed for another completed NHTSA research project, *Crash Simulation of FMVSS No. 214 Safety Performance* (Reichert et al., 2022).

Compatibility Metrics

The use of accepted compatibility metrics and assessment procedures is considered essential for the successful completion of this study. We determined two methods and performance criteria to evaluate the energy absorption capabilities of the crash partner and ODV vehicles. Considered methods and related research are listed below.

- EuroNCAP compatibility assessment using the results of the MPDB-to-car impact. The three parameters are the SD of the post-test barrier face measurements, the OLC and whether the vehicle has bottomed out the MPDB face (Ellway, 2019; EuroNCAP, 2019)
- Assessment using full width deformable barrier
- Part 581 bumper zone for low-speed impacts (NHTSA, 1990)
- Assessment using NCAP load cell wall (Barbat et al., 2007)
- Geometric compatibility metrics "average height of force 400," abbreviated AHoF400 (Subramaniam et al., 2007)
- Stiffness compatibility metrics evaluating the initial slope of the force-deflection curve from NCAP tests over about 200 mm of crush, and stiffness-related crush energy absorbed by a vehicle in the first 400 mm of crush, called "crush work stiffness" (KW400) (Subramaniam et al., 2007).
- Voluntary industry commitment defining geometric alignment options for designing light trucks with respect to PEAS and SEAS (AIAM, 2003; Enhanced Vehicle-to-Vehicle Crash Compatibility Technical Working Group, 2009).
- Results from different resolution of the barriers were compared and found that the compatibility metrics (KW400/AHoF400) were higher in the high-resolution barrier (Patel et al., 2007).

For the EuroNCAP compatibility evaluation, we used a recently developed FE model of the EuroNCAP MPDB, as shown in Figure 20. The FE model was developed and validated by Gesellschaft fuer Numerische Simulation (Benito Cia et al., 2020).[9]

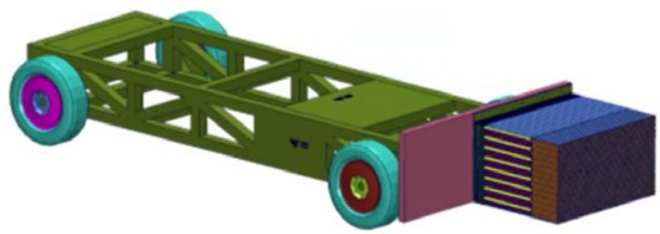

Figure 20. MPDB FE model

Front-to-side impact compatibility aspects were based on previous research and recommendations from the Enhancing Vehicle Compatibility Technical Working Group (Delannoy et al., 2004; Powell et al., 1999; Hobbs, 1989; Teoh & Nolan, 2012; IIHS, 2014).

Geometric compatibility with respect to bumper height, as described in Part 581, the OLC criteria used by EuroNCAP (described in Chapter 4), and KW400 (described in Chapter 5), were selected to evaluate compatibility of the LPV crash partner and ODV FE models.

2015 Toyota Camry Sedan Validation

A model year (MY) 2012 mid-size sedan vehicle was purchased and its mass, center of gravity (CG) location, and inertial properties were determined. A digitizing device was used to scan all relevant components including their internal structure. At the time of model development, Geomagic software, which was subsequently purchased by 3D Systems, was used to create accurate CAD surfaces and HyperMesh and ANSA were used for FE mesh generation.

All components were positioned relative to a defined reference coordinate system and checked for correct position and penetrations. Spot-welds, bead welds, bolts, and joints were used for respective part connections. Material thicknesses and mass distribution were assigned to the individual parts and components. Measured CG location and inertial properties of the entire vehicle were verified. Material property data for most structural parts was obtained by cutting specimens from the actual vehicle components and conducting material coupon tests.

Analysis of a physical MY 2015 mid-size sedan and information from the manufacturer was used to determine differences between the MY 2012 and MY 2015 vehicles. To improve performance in the IIHS small overlap test from POOR to ACCEPTABLE, the vehicle manufacturer added a spacer beyond the bumper reinforcement to the front side member. This spacer directs crash energy through the side member into the reinforced A-pillar, which diffuses it through the roof rail, rocker panel, and floor pan. The available FE model was updated accordingly to reflect the vehicle OEM’s design direction.

To validate the developed MY 2015 vehicle model, a variety of load cases, including frontal oblique impact configurations, side barrier, and side pole impacts were configured, and then compared to respective full-scale crash test results. First, visual analysis of test pictures, test

[9] Gesellschaft Fuer Numerische Simulation [Society for Numerical Simulation] mbH, Braunschweig, Germany, is an engineering company that provides simulation services and software products to the automobile, aeronautical, and chemical industries. GNS serves customers in Germany.

movies, and simulation animations was used to compare overall vehicle kinematics and crash characteristics. For the IIHS small and moderate overlap impacts, the lower and upper occupant compartment intrusion data was evaluated according to the respective test protocols. For NHTSA's full overlap and oblique impact configurations, available intrusion data from the simulation model and respective full-scale tests was compared.

Time history data plots, in combination with test videos and simulation animations, were used to evaluate crash modes and structural energy absorption mechanisms. CORrelation and Analysis (CORA) software was used to rate how well test and simulation results compare. CORA was developed by the Partnership for Dummy technology and Biomechanics[10] and takes phase shift, size, and shape, as well as the comparison of values at each time increment, into account. Using these methods, an objective rating is given that indicates how well a curve (e.g., simulation) compares to a reference curve (e.g., test). CORA rating scores range between 0 and 1, where 0 means no correlation and 1 means (close to) perfect correlation. Specifically, a CORA rating (Barbat et al., 2013) greater than 0.94 was considered excellent correlation, values greater than 0.8 and smaller than or equal to 0.94 represented good correlation, and values greater than 0.58 and smaller than or equal to 0.8 represented fair correlation.

As described, a spacer was added beyond the bumper reinforcement to the front side member for the MY 2015. This spacer directs crash energy into the reinforced A-pillar, which diffuses it through the roof rail, rocker panel, and floor pan. Figure 21 (a) shows a bottom view of the finite element model with an enlarged view of the added bumper reinforcement extension and spacer for the physical vehicle and the simulation model. Figure 21 (b) the effect of the bumper reinforcement and spacer in the IIHS small overlap impact. Due to the minor overlap of 25 percent with the vehicle, the longitudinal rail is not activated when no spacer exists. The frontal rail remains undeformed and no crash energy is absorbed. The effect of the added bumper reinforcement extension and spacer can be seen in Figure 21 (b) on the right. The added components interact with the IIHS small overlap barrier and activate the frontal rail on the driver side. The deformation of the longitudinal rail contributes to the structural crash energy absorption. Available full-scale test results show that the design changes mainly affected performance in the IIHS small overlap impact, while other crash configurations, such as NCAP full overlap and NHTSA left oblique impact, showed similar results for the 2012 and 2015 models.

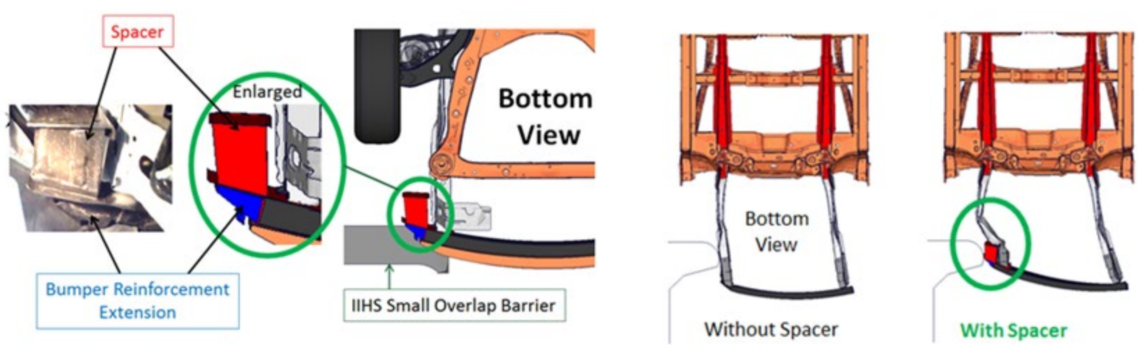

Figure 21. 2015 Camry design changes (a) Bumper extension; (b) Effect of "spacer"

[10] Partnership for Dummy Technology and Biometrics, Gaimersheim, Germany

The resulting Toyota Camry FE model contains relevant structural and interior components, such as body in white, engine, drivetrain, steering, suspension, seats, trims, etc., which are represented by more than 1,000 parts and approximately 2.25 million nodes and elements. Most components were modeled using shell elements with an average element size of 6 mm. The model was evaluated and validated using the nonlinear, explicit FE code LS-DYNA with a minimum time-step of 0.7 microseconds using 16 cpu on a Hewlett-Packard high-performance computer system. The results of the conducted simulations using the MY 2015 sedan FE model are outlined below. Simulation results were compared to available full-scale crash test data for NHTSA's left and right oblique impacts, NCAP full overlap, and IIHS small and moderate overlap configurations. In addition, test and simulation results for side impact and roof crush configurations were compared.

Validation for the NCAP Full Overlap Configuration

NHTSA test #8545 (Walsh & Dutton, 2014) was used to evaluate the developed FE model in the 56 km/h NCAP full overlap impact into a rigid barrier. Figure 22 compares overall vehicle deformation, occupant compartment intrusion values, and vehicle pulse in test and simulation. Figure 22 (a) shows good agreement in overall vehicle deformation in the simulation on the top and in the full-scale crash test on the bottom. Similar deformation of the frontal structure, door frame, and roof was observed. No significant deformation of the roof, A-pillar, or door sill occurred in either test or simulation.

Figure 22 (b) compares the vehicle acceleration pulse. Test results are shown using a black solid line and simulation results using a blue dashed line. The objective CORA rating value of 0.86 documents the good correlation between test and simulation.

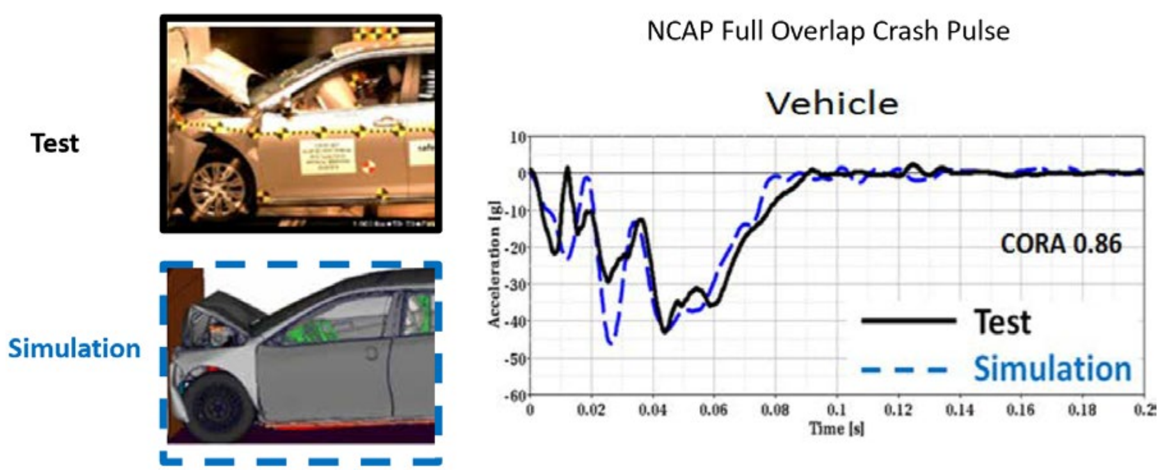

Figure 22. NCAP test versus simulation (a) Deformation; (b) Vehicle pulse

Validation for the IIHS Small Overlap Impact

IIHS Small Overlap (SO) test CEN1349 of a MY 2015 Toyota Camry traveling at 64 km/h into a fixed rigid barrier with a 25-percent overlap was used to evaluate the developed simulation model. Figure 23 (a) shows the overall vehicle deformation in the simulation and in the full-scale crash test. Similar deformation of the frontal structure, door frame, and roof was observed. The A-pillar showed noticeable buckling in both test and simulation. Failure mechanism of the wheel-to-control-arm connection and overall wheel kinematics were well captured. In the later stages of the impact, after maximum intrusion and occupant injury values have occurred, additional material failure of various components in the rocker pillar, door, and sill area were observed in the test that were not completely captured in the simulation. Consequently, some differences in the rebound phase exist.

Figure 23 (b) the intrusion for the lower and upper occupant compartment according to the IIHS SO rating protocol. MY 2015 test results are shown using a black solid line and simulation results using a blue solid line. Respective results correlate well, resulting in an ACCEPTABLE structural rating for both test and simulation. Occupant compartment intrusion characteristics were well captured in the simulation.

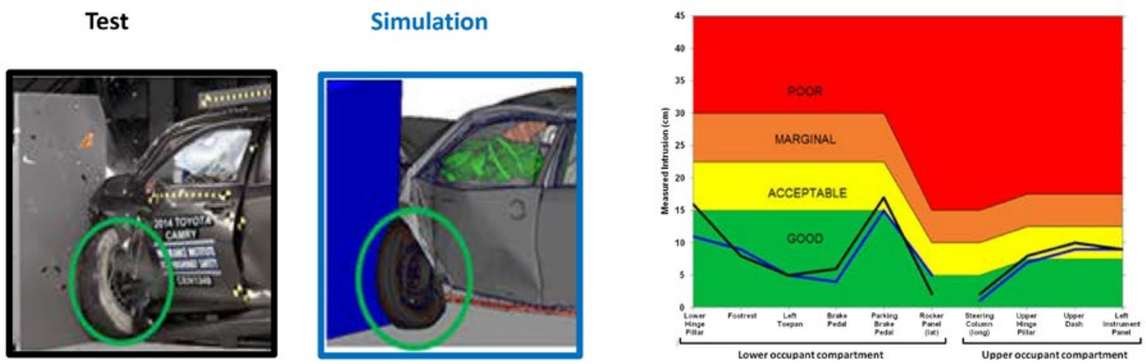

Figure 23. IIHS small overlap test versus simulation (a) Wheel kinematics; (b) Intrusion

Validation for NHTSA's Frontal Oblique Impact Configuration

NHTSA's left oblique full-scale impact test #8790 (Walsh, 2015), consisting of a OMDB traveling at a speed of 90 km/h into the front driver side of the stationary mid-size sedan, was used to evaluate the developed FE model.

Figure 24 the overall vehicle deformation and specific occupant compartment intrusion values in test and simulation. Figure 24 (a) shows the overall vehicle deformation in the baseline simulation on the top and in the full-scale crash test on the bottom. Similar deformation of the frontal structure, door frame, and roof were observed. There was no significant door sill deformation in either test or simulation. Intrusion along the rocker pillar and minor buckling of the A-pillar area were well captured in the simulation. Toe-pan intrusion was recorded for measurement points in five rows, consisting of four points each, in test and simulation. The maximum intrusion values for each row are visualized in the adapted structural rating chart, derived from the IIHS moderate overlap evaluation protocol. Figure 24 (b) visualizes the maximum intrusion for row one to row four, brake-pedal, left and right instrument panel, and A- to B-pillar closure. MY 2015 test results are shown in black and simulation results in blue. The highest values were documented for row one, which is the most forward and upward location at the toe-pan. Values decreased for more rearward locations in both test and simulation. A maximum intrusion of 94 mm was observed in the simulation, versus 99 mm in the test. Lower and upper occupant compartment intrusion, including toe-pan deformation from the full-scale crash test, was well captured in the simulation.

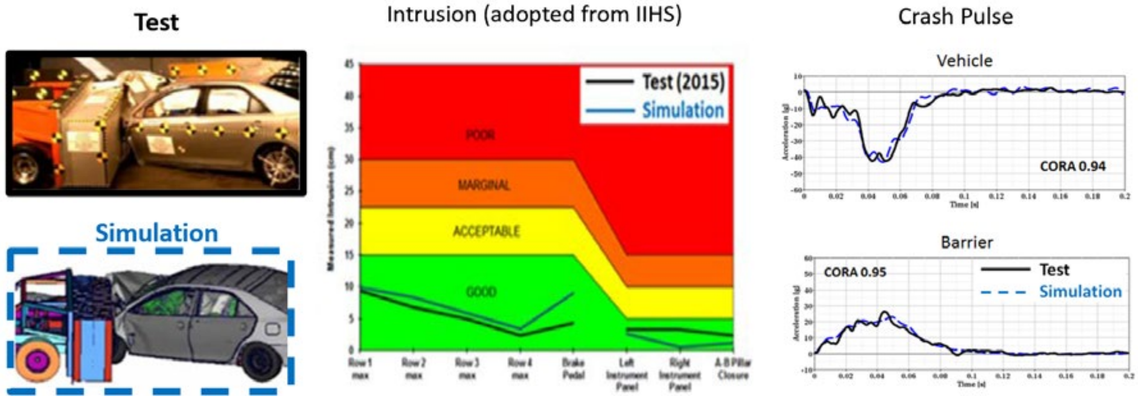

Figure 24. Frontal oblique test versus simulation (a) Deformation; (b) Intrusion; (c) Pulses

The developed FE model represents the structural intrusion characteristics of the MY 2015 sedan in the left oblique impact configuration well. Figure 24 (c) shows the vehicle acceleration pulse for the MY 2015 sedan in the left oblique impact configuration for test and simulation. Test results are shown using a black solid line and simulation results using a blue dashed line. Good overall correlation, with a CORA rating value of 0.94, was observed. Figure 24 (c) at the bottom the OMDB acceleration pulse. Test data is shown using a black solid line and simulation data using a blue dashed line. Excellent correlation between test and simulation, with a CORA rating value of 0.95, was observed. The FE model represents the vehicle and barrier pulse characteristics of the MY 2015 Toyota Camry sedan in the left oblique impact configuration very well.

Validation for Side Impact Configurations

Test results from NHTSA's 62 km/h crabbed barrier and 32 km/h oblique pole side impact configurations, as well as the IIHS 50 km/h 90° barrier side impact, were used to evaluate and validate the developed FE model. Intrusions and velocity profiles play an important role in side impacts, since occupant injury patterns are mainly influenced by direct interaction with the intruding vehicle structure, interior, and restraints. Besides engineering judgement of vehicle kinematics, intrusion behavior, and accelerometer output data, CORA was used to objectively rate the correlation of test and simulation.

No structural changes relevant for side impact performance occurred between the MY 2012 and MY 2015 vehicles. NHTSA test #7517 (Janovicz & Fischer, 2011), a 62 km/h crabbed barrier side impact test into the stationary sedan vehicle, was used to validate the FE model. Weight and vehicle CG location were closely matched between test and simulation. Test vehicle exterior crush measurements were evaluated after the crash at the height of the sill top, the occupant hip point, mid-door, windowsill, and window top. The different measurement heights are shown with yellow markers on the tested vehicle in Figure 25 (a) on the top. The measured intrusion profiles from the test were extracted and overlaid with the simulation. The lines, shown in blue, represent intrusions measured in the full-scale crash test and correlate well with the intrusions seen in the simulation. Similar deformation patterns and intrusion depth in the roof, door, and sill areas were observed. The comparison of vehicle and barrier kinematics in test and simulation showed good correlation, with a CORA rating of 0.92 for the vehicle velocity time history data and 0.87 for the barrier pulse, as shown in Figure 25 (b).

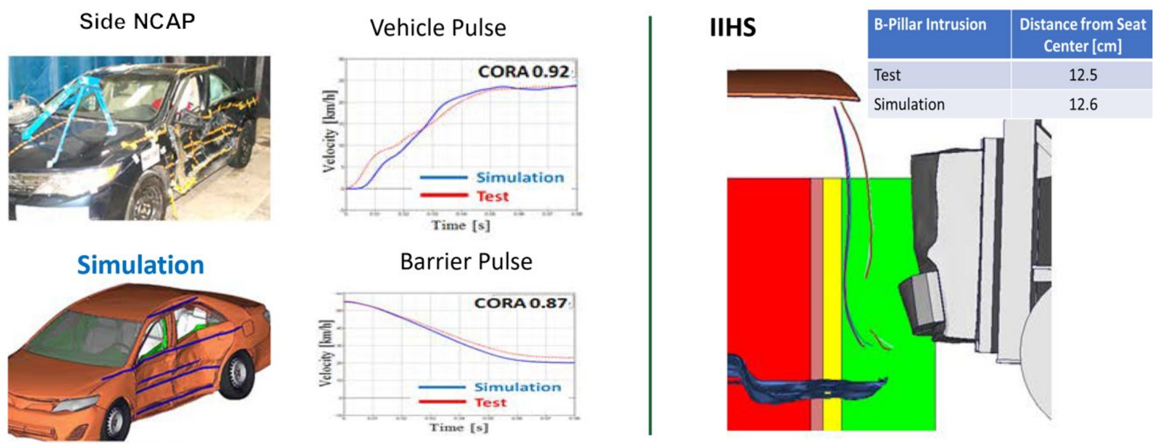

Figure 25. Side impact test versus simulation (a) Side NCAP; (b) Pulses; (c) IIHS

The developed sedan vehicle model was tested in the IIHS side crash configuration by Toyota. In this test a moving deformable barrier with a mass of 1,500 kg hits the stationary vehicle at an angle of 90° and a velocity of 50 km/h. No technical time history data was accessible from the conducted test. The maximum B-pillar intrusion measurement was available and was closely matched, resulting in a GOOD structural rating in test and simulation. In the test, the maximum B-pillar intrusion was 12.5 cm away from the driver seat center line. In the simulation, the maximum intrusion point was 12.6 cm away from the seat center line, as shown in Figure 25 (c).

2015 Toyota Camry Sedan Compatibility

Part 581 Bumper Zone Criteria

Geometric bumper height zone is defined between 406 mm (16 in) to 508 mm (20 in) above ground level, as established by NHTSA for passenger vehicles in 49 CFR Part 581 (1997) and shown in Figure 26. This zone has been defined as the compliance zone for low-speed bumper tests to ensure that LPV bumpers match up and vehicle damage is minimized during low-speed impacts. This zone has also been proposed by the industry as a compliance zone for the height for force load paths of light trucks and vans. The 2015 Toyota Camry FE model's bumper is located between 407 mm and 570 mm above ground, which overlaps well with the Part 581 bumper zone.

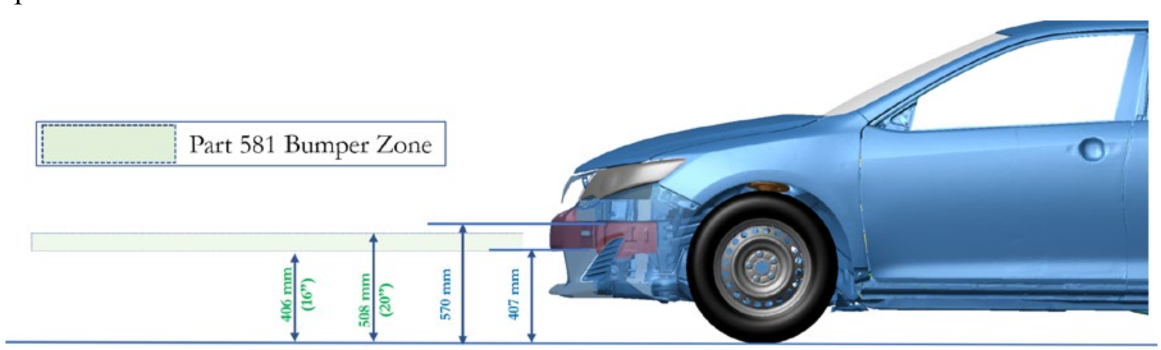

Figure 26. 2015 Toyota Camry Part 581 bumper zone assessment

EuroNCAP Compatibility Assessment

The EuroNCAP compatibility assessment is based upon three parameters that are determined using the results of the MPDB-to-car impact. The three parameters are the SD of the post-test barrier face measurements, the OLC, and whether the vehicle has bottomed out the MPDB face. Until the end of 2021 the compatibility penalty will be halved and added to the overall test score (maximum of 4 points). From the beginning of 2022 the compatibility assessment will be a 0 to 8-point penalty applied to the overall test score. Both the vehicle and MPDB are traveling at 50 km/h and impact each other with a 50-percent overlap, as shown in Figure 27. The presented research focused on two metrics OLC and bottoming out.

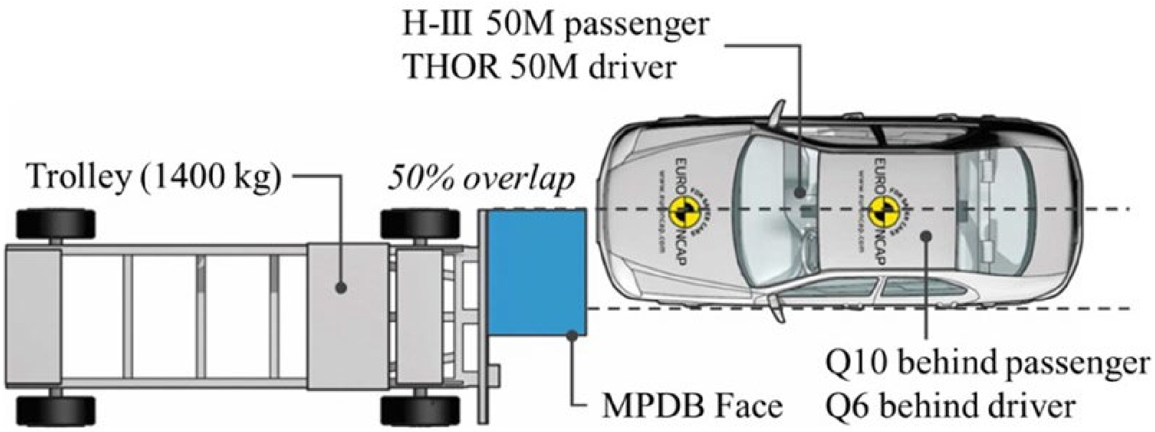

Figure 27. EuroNCAP MPDB-to-vehicle impact configuration, © Euro NCAP 2021.

The OLC metrics are derived from the virtual dummy responses estimated from a governing equation involving an assumed restraint system and a given vehicle crash pulse. This metric is independent of the actual dummy response in tests. It assumes a virtual and uniform restraint system and that a virtual dummy will be in free-flight-phase along a displacement of 65 mm. In the restraining-phase an ideal restraint is assumed that would decelerate the occupant until the relative velocity between the occupant and the vehicle becomes zero. It is assumed that the distance between the vehicle and the occupant at point B is an additional 235 mm, as shown in Figure 28. The OLC is evaluated using a sliding scale between 25 g and 40 g. OLC values below 25 g result in four points and values above 40 g result in zero points.

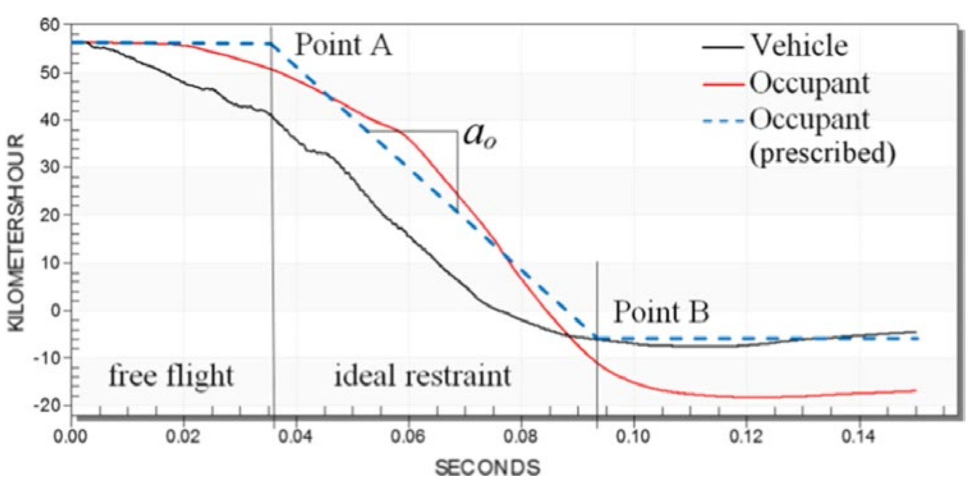

Figure 28. Occupant Load Criterion

Bottoming out is defined as an area of the barrier that is 40 mm x 40 mm high and wide that has been penetrated by 630 mm or more. It is determined from a physical examination of the barrier face and vehicle.

The 2015 Toyota Camry crash partner FE model was evaluated using an FE model of EuroNCAP's MPDB, as shown in Figure 29. An OLC of 27 g for the MPDB indicates good compatibility of the Toyota Camry. No bottoming out of the barrier face was observed.

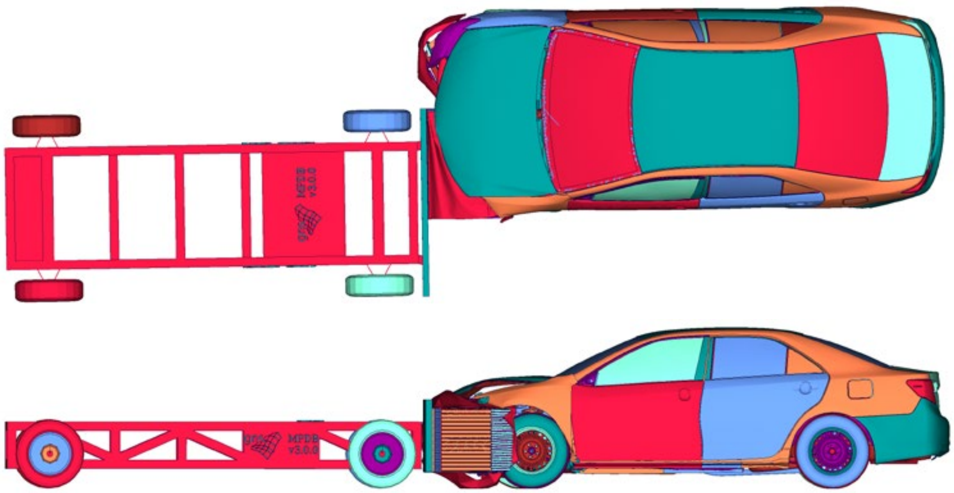

Figure 29. Toyota Camry-to-MPDB evaluation (a) top view; (b) side view

2020 Nissan Rogue SUV Crash Partner FE Model

The Nissan Rogue was the crossover vehicle with the second highest U.S. sales numbers in 2018, as shown in Table 6. It has a GVWR of 4,590 lb, which is higher than the 3,460 lb of the 2015 Toyota Camry mid-size sedan.

Table 6. Crossover vehicles with highest U.S. sales numbers in 2018

#	Type	Size	Make	Model	Sales	GVWR [lb]
1	CUV	Compact crossover SUV	Toyota	RAV4	427,168	4,610
2	CUV	Compact crossover SUV	Nissan	Rogue	412,110	4,590
3	CUV	Compact crossover SUV	Honda	CR-V	379,021	4,695

Source: FCA IS LLC, December 2018

The Nissan Rogue received a 5-star U.S.NCAP side impact and a 4-star U.S.NCAP frontal impact rating. It also received a IIHS Top Safety Pick rating. Existing test data was used to validate this recently developed FE model.

The established reverse engineering process, which was also used for the Toyota Camry sedan FE model development, was adopted to generate the crossover SUV-type vehicle model, as shown in Figure 30.

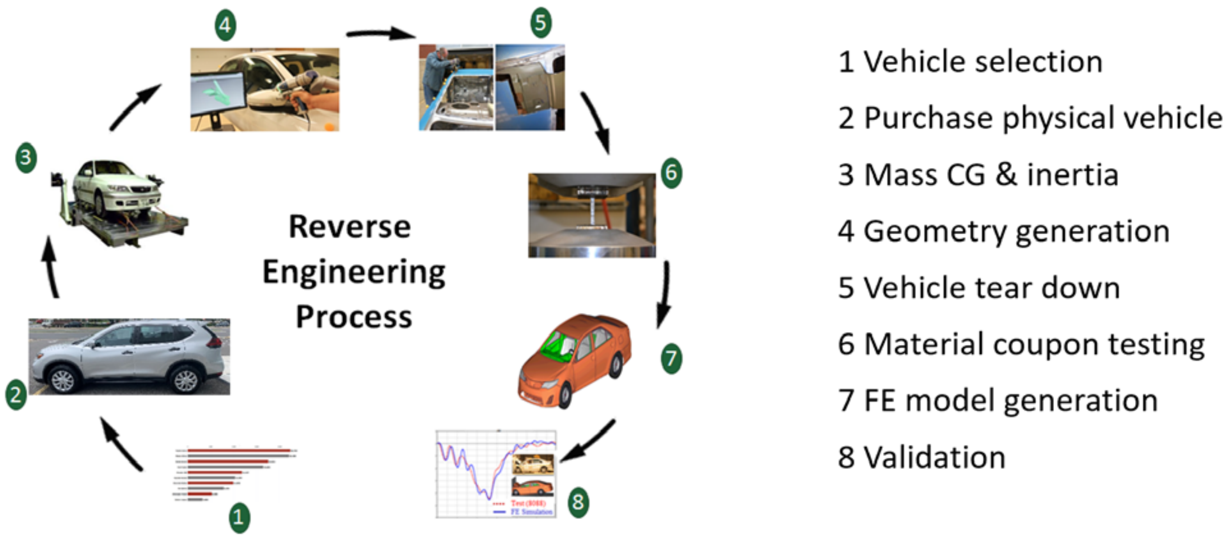

Figure 30. Reverse engineering FE vehicle model development process

Two 2020 Nissan Rogue vehicles were purchased. The first vehicle was used for the FE model development reverse engineering process. The second vehicle was used to conduct non-destructive suspension tests, vehicle CG and inertia measurements, and FMVSS No. 214 static door crush tests. Vehicle CG and inertia measurements were determined in cooperation with the S-E-A[11] Vehicle Inertia Measurement Facility, Columbus, Ohio.

Snapshots of the different stages of the vehicle tear down and FE model development process are shown in Figures 31 and 32. Thickness of all vehicle parts, and type and location of all connections, were recorded and modeled accordingly. Material coupons have been cut for relevant vehicle components to determine the material characteristics.

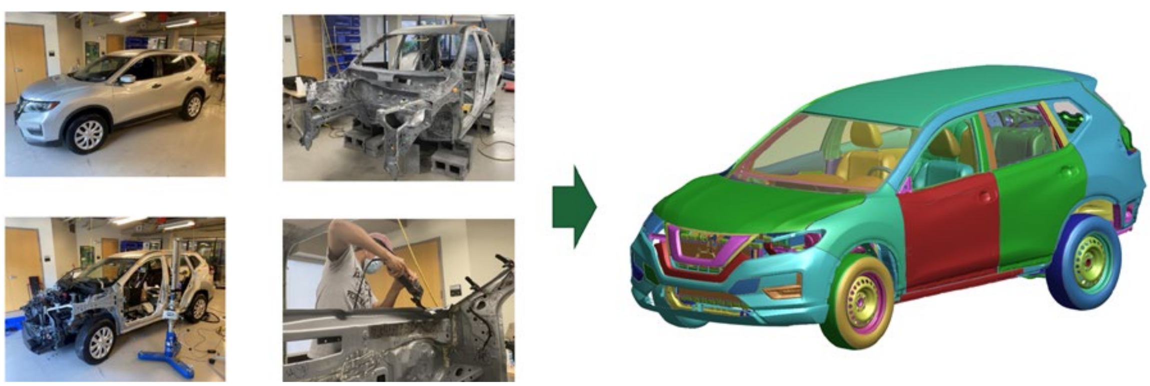

Figure 31. Vehicle tear down and FE model development process

The recently developed FE model, representing the crossover SUV vehicle category based on a 2020 Nissan Rogue, is shown in Figures 31 and 32, and can be downloaded from GMU/CCSA's vehicle model website, www.ccsa.gmu.edu/models/.

[11] [Editor's note: SEA, Ltd., Columbus, OH, uses S-E-A as its common name and logo. See https://sealimited.com/about-us]

Figure 32. 2020 Nissan Rogue FE model for public download

Nissan Rogue Frontal Impact Validation

Validation of the 2020 Nissan Rogue FE model is ongoing. Early results show promising correlation with a good CORA score for the vehicle velocity pulse, as shown in Figure 33, which shows the comparison of vehicle left rear sill crash pulse between test and simulation for the NCAP full-frontal impact configuration and three existing test results.

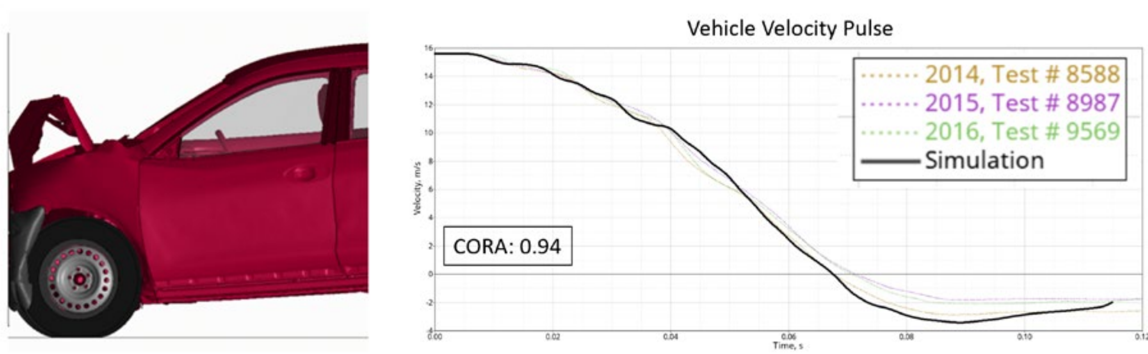

Figure 33. Nissan Rogue – NCAP frontal impact validation

Nissan Rogue MDB Side Impact Validation

Figure 34 (a) shows a side view of the test on the top and simulation on the bottom using the developed 2020 Nissan Rogue FE model for a 53 km/h impact speed, according to the FMVSS No. 214 regulation requirement. Overall vehicle and barrier deformation was well captured, represented by the maximum exterior crush value of 190 mm for the test and 181 mm for the simulation. The relevant y-velocity crash pulse time history data, which is in the dominant perpendicular impact direction, showed excellent correlation, represented by a CORA value of 0.96. The velocity time history measured at the CG of the MDB, showed excellent correlation with a CORA value of 0.96, as well.

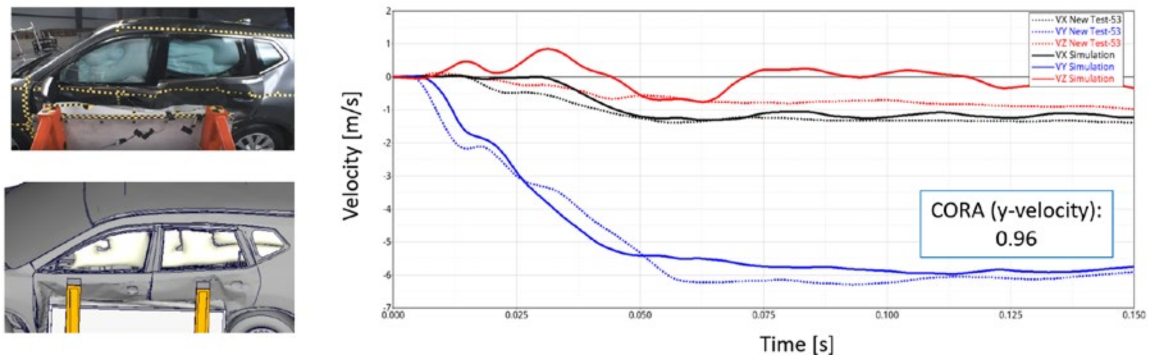

Figure 34. Side impact MDB validation (a) side view; (b) velocity crash pulse

The developed 2020 Nissan Rogue FE model was also exercised at an impact velocity of 62 km/h according to the Side NCAP rating procedure and compared to results from an existing full-scale test, NHTSA test #9786 (TRC, 2016b). Good correlation of FE model and respective test data was observed also for the higher impact speed. The maximum exterior crush was 220 mm and 234 mm in test and simulation. The lateral velocity crash pulse time history compared well, represented by a good CORA value of 0.90. The MDB's velocity pulse time-history showed excellent correlation, characterized by a CORA value of 0.95.

Nissan Rogue FVMSS No. 214 Pole Impact Validation

A FMVSS No. 214 pole side impact test using a 31 km/h impact speed with a 2020 Nissan Rogue was recently conducted at Calspan (TRC, 2016b) to generate data for FE model validation.

A perspective and side view of the conducted FMVSS No. 214 pole test is shown in Figure 35 (a) and (b).

Figure 35. Nissan Rogue pole side crash (a) perspective view; (b) side view

Figure 36 (a) is a side view of test and simulation using the developed 2020 Nissan Rogue FE model. Figure 36 (b) shows the y-velocity crash pulse time history comparison between test and simulation, which showed good correlation based on a CORA value of 0.87. Overall vehicle deformation was reasonably well captured, represented by the maximum exterior crush of 420 mm for the simulation and 379 mm for the test. NTHSA test #9780 (TRC Inc., 2016a), which was conducted at 32 km/h, showed a maximum exterior crush of 390 mm.

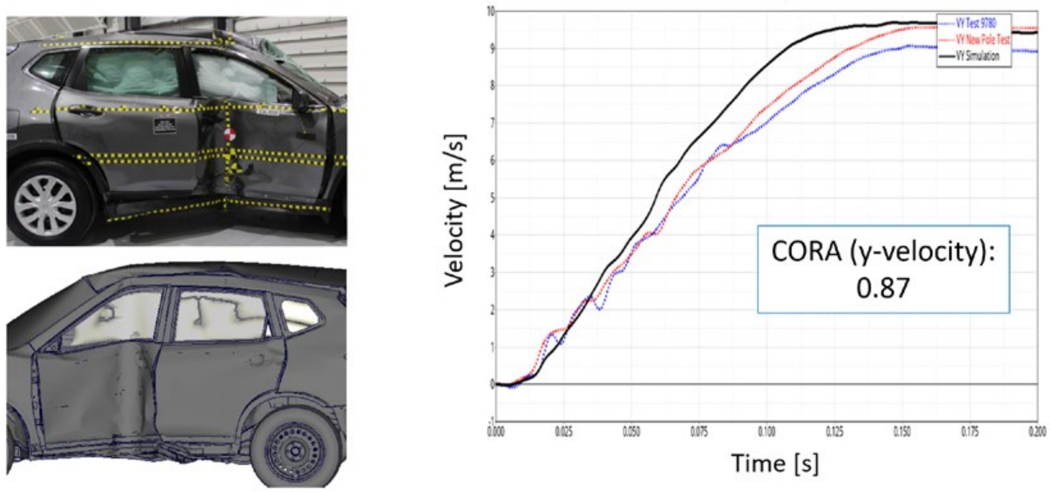

Figure 36. FMVSS No. 214 pole test versus simulation (a) Side view; (b) Crash pulse

The validated FE model, representing the SUV crossover vehicle class with higher sill and occupant seating position, was found to be well suited to be used in a similar manner to the Toyota Camry sedan vehicle, to study the crash compatibility of ODV vehicles.

2020 Nissan Rogue SUV Compatibility

Geometric bumper height zone is defined as 406 mm (16 in) to 508 mm (20 in) above ground level, as established by NHTSA for passenger vehicles in 49 CFR Part 581 (1997) and shown in Figure 37. The 2020 Nissan Rogue marginally overlaps Part 581 bumper zone, as shown in Figure 38.

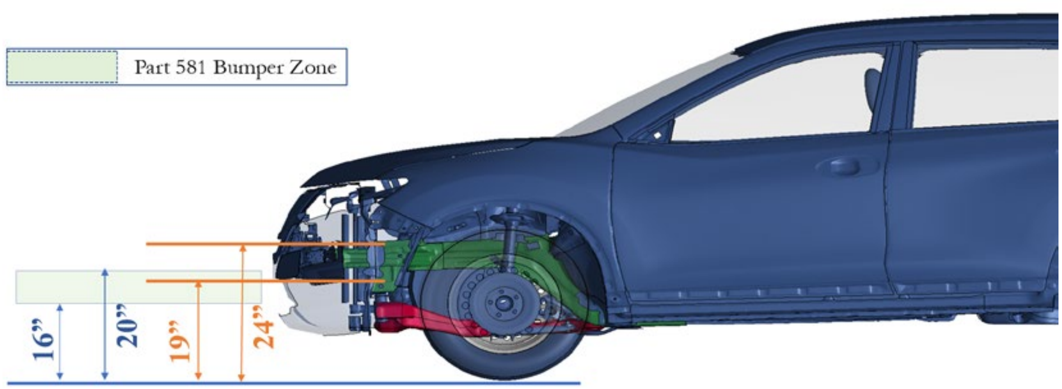

Figure 37. Nissan Rogue Part 581 bumper zone assessment

The frontal structure of the Nissan Rogue with PEAS and SEAS is shown in Figure 38. PEAS components include the bumper and longitudinal rails, shown in blue. SEAS components include the sub-frame and additional structural components connected to the longitudinal rails, shown in red.

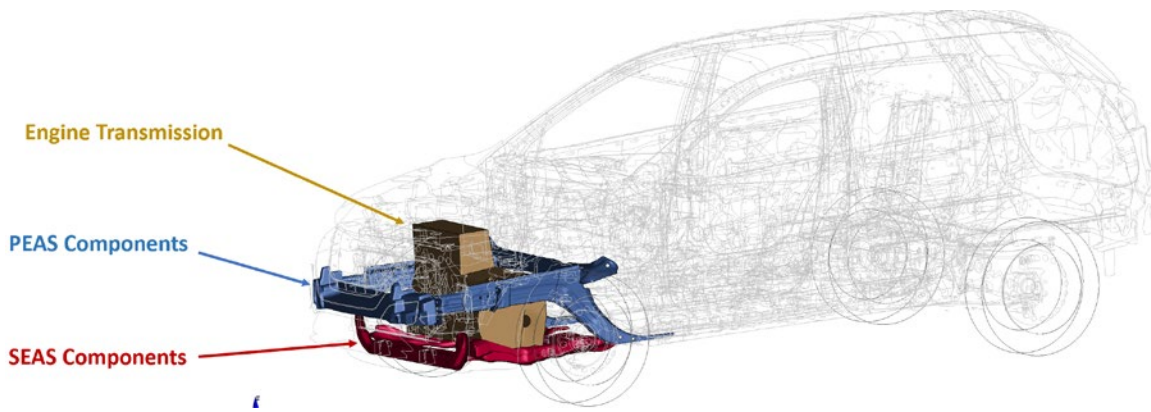

Figure 38. Nissan Rogue PEAS and SEAS components

NHTSA's override rigid barrier (Patel et al., 2009) configuration defines a requirement for the SEAS to withstand a minimum force of 100 kN before 400 mm deflection. Figure 39 (a) a side view of the Nissan Rogue FE model striking the ORB and engagement of the SEAS. Figure 39 (b) shows the force versus displacement, as measured at the ORB. Note that the force exceeds the 100 kN threshold before 400mm of displacement.

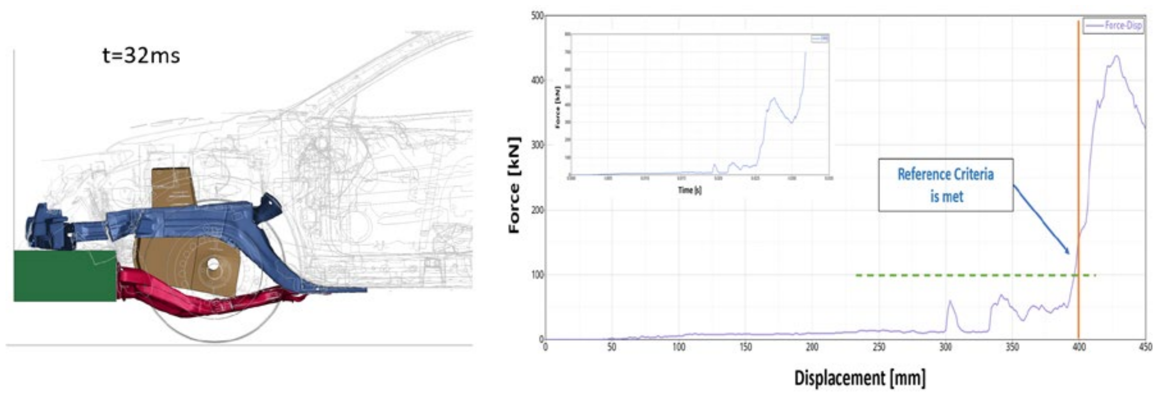

Figure 39. Nissan Rogue (a) ORB; (b) Force versus displacement

The 2015 Toyota Camry sedan and the 2020 Nissan Rogue SUV crash partner FE models represent LPV with different geometrical and frontal structure energy-absorbing characteristics and will allow for a thorough study of crash compatibility for ODV vehicles.

This page intentionally left blank.

5. ODV FE Models

ODV Baseline Vehicles

We conducted a thorough literature review to identify FE vehicle models that could be selected or updated for use for ODV research. From the models identified, at least one model for each ODV ODD, for a total of at least four ODV models, were adapted. The ODV FE model's compatibility was evaluated using existing criteria and performance requirements.

The selected baseline FE models, which have been developed by CCSA at GMU in a previous research project (Reichert et al., 2020), are shown in Table 5, which is copied here for convenience.

	Generic FE Model	Reference Concept	
Small ODV	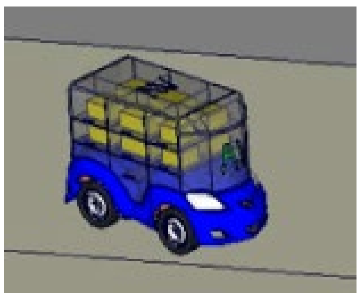		"Nuro" (Nuro, 2018)
Mid-size ODV	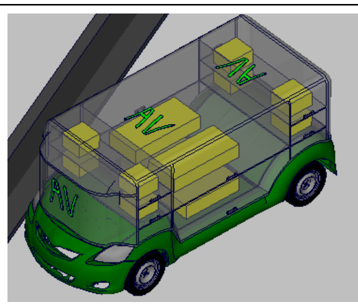		"Mercedes Vision" (Davies, 2018)
Large ODV	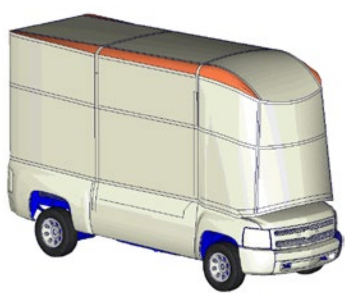		"Einride T-Pod" (Sawers, 2017)
Tractor Trailer ODV	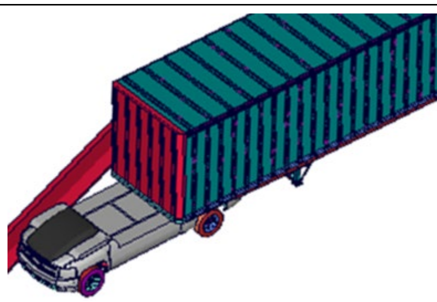		"Volvo Vera" (Sawers, 2017)

Copy of Table 5: Four ODV categories

Many electric vehicles and ADS vehicle concepts use a new type of platform referred to as a "skateboard." As an example, the General Motors' concept of the skateboard platform is shown in Figure 40.

Figure 40. Example of a "skateboard-type" vehicle platform

The "skateboard-type" platform is generally defined by a flat battery located at a lower area of the vehicle at a similar level to the wheels.

FE models of generic non-occupied ADS vehicles were developed according to the 4-phase process shown in Figure 41.

First, a validated FE model of an existing traditional vehicle was selected. For example, a sedan vehicle was chosen as the basis for developing small- and mid-size non-occupied ADS vehicle models.

Second, a skateboard-type chassis was developed by removing seats, restraints, vehicle interior, vehicle body, and other occupant related components. Wheels, suspension, and main vehicle structure were not changed.

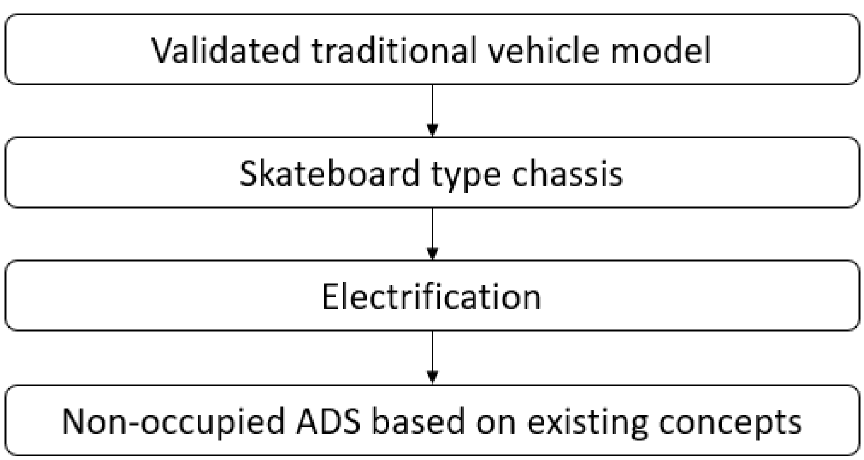

Figure 41. Generic ODV vehicle FE model development process

Third, the combustion engine, radiator, and transmission were removed. Instead, an electric battery, representing the appropriate mass for a respective vehicle size, was added. Furthermore, components representing electric motors were added. The simple modeling approach for the battery pack was applied to mainly represent the mass, i.e., the battery packs are not modeled in detail and no supporting vehicle structure, and active or passive cooling systems have been added. The spaces occupied by the combustion engine and radiation components were not used by other components.

Forth, in the final step a generic vehicle body based on existing ADS vehicle concepts was modeled and integrated with the skateboard-type chassis. In addition, cargos with various mass were also added to the model.

Figure 42 demonstrates the development process for the small- and mid-size ODV vehicles. A validated FE-model of a Toyota Yaris was selected as the basis. A skateboard-type chassis was created by removing seats, interiors, engine, transmission, radiator, and the body of the occupant compartment. Battery pack and motors, shown in red, were added. For the small size ADS vehicle, length and width were reduced (scaled down) compared to the baseline vehicle. A generic vehicle body with optional cargo was modeled based on existing ODV vehicle concepts.

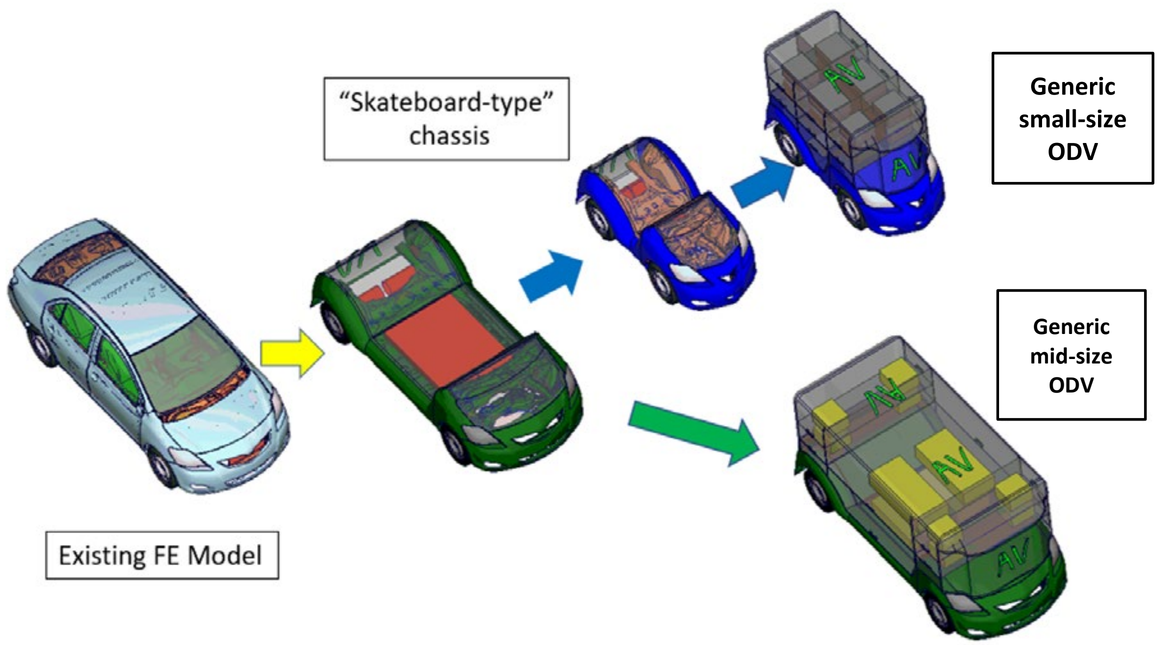

Figure 42. Development process for generic small and mid-size ODV

Similarly, models for a large ODV and a tractor trailer ODV vehicle were developed based on a 2007 Chevrolet Silverado pickup truck. The four ODV models can be downloaded from CCSA's/GMU's FE vehicle model website (Center for Collision Safety and Analysis, n.d.).

Compatibility Assessment Metrics

Existing compatibility metrics were evaluated, including (1) bumper height assessment, which aims to enhance partner protection primarily through geometric matching of front structural components of cars and light trucks and vans; (2) AHoF, which is calculated from NCAP load cell measurements to quantify vertical geometric alignment of a vehicle; (3) crush work stiffness

(KW400), a metric to quantify the front-end stiffness related to the crush energy absorbed by a vehicle in the first 400 mm of crush when striking a rigid wall; (4) criteria used by EuroNCAP, such as the OLC) calculated from the velocity pulse of a MPDB, as described in Chapter 4.

The crush work stiffness (KW400) was selected as one metric to evaluate the baseline ODV vehicles and develop variations with different compatibility characteristics. as shown in Figure 43. The resulting stiffness K value is termed KW400, based on the equation outlined in Figure 43 (b), where F is the average of the total force on the barrier between 25 mm and 400 mm of vehicle front-end crush in a NCAP full-frontal impact configuration. The first 25 mm of crush is ignored to account for soft materials and noise in the measured data. The maximum crush is limited to 400 mm to isolate the high inertial forces on the load cell wall due to potential engine contact for a traditional vehicle.

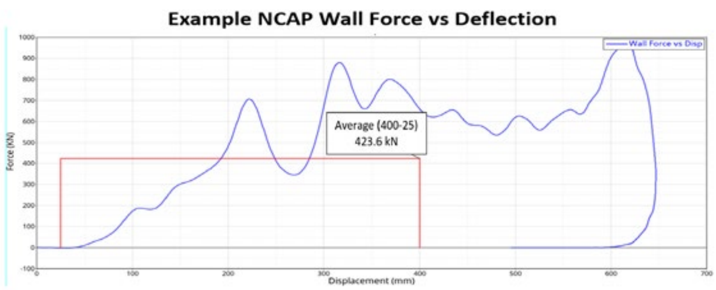

$$\int_{25}^{400} F\,dx = \frac{1}{2}\,Kw400\,[(400)^2 - (25)^2]$$

$$Kw400 = \frac{2F}{425}$$

Figure 43. (a) Crush Work Stiffness compatibility metric basis; (b) KW400 equation

EuroNCAP's OLC metric, outlined in Chapter 4, was selected as a second compatibility metric to evaluate the energy-absorbing characteristics of the baseline ODV and their variations.

For reference, recent rating results from compatibility research (EuroNCAP, 2022), where a commercial van of the N1 category (up to 3.5 metric ton or 3,500 kg) was examined, is shown in Figure 44. An OLC of 34 g was measured by the MPDB and bottoming out of the barrier face was observed, when colliding with the commercial van. It was concluded that "the post-crash barrier deformation analysis demonstrates that the van's lack of compatibility is worrying: the structure bottoms out the barrier face and does not do enough to mitigate high loading of the opponent vehicle."

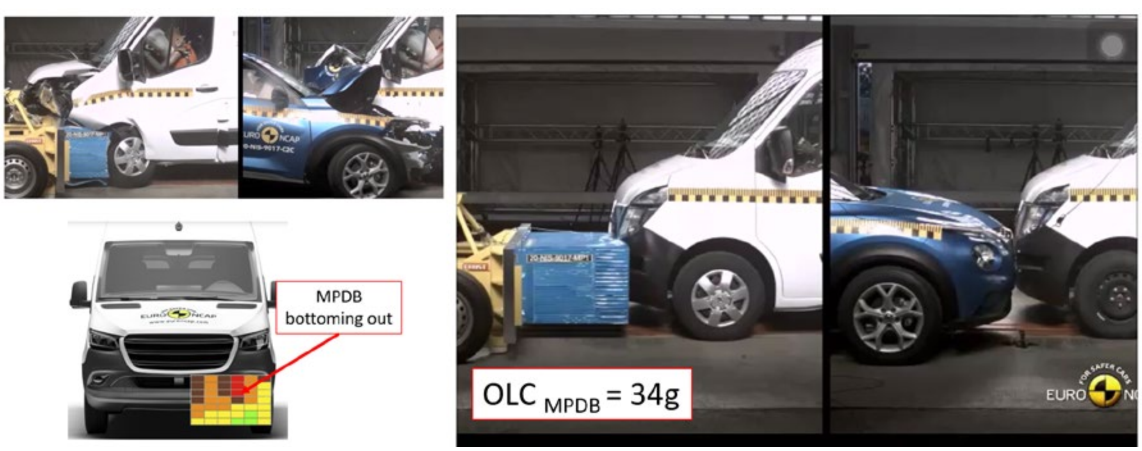

Figure 44. Commercial van compatibility tests, © Euro NCAP 2022

ODV Baseline and Model Variations

After evaluating the baseline ODV models' compatibility and energy absorption, each ODV model was modified to create versions that change the compatibility characteristics based on the identified metrics. As shown in Figure 45, we used an iterative process of changing the material thickness and strength of relevant parts was used to vary the front-end structural compatibility and energy absorption into two separate designs: Design 1 (D1) and Design 2 (D2). For select cases, in particular the mid-size Design 2 and tractor Design 1, the vehicle mass was changed while maintaining the front structural characteristics. For the mid-size ODV Design 2, 800 kg secured cargo was added to represent a heavier mid-size ODV vehicle. The vehicle mass of tractor Design 1 was reduced by using a battery pack with half of the mass compared to the baseline model. This can represent a tractor with more efficient battery concepts, or a tractor design that is designed for a medium-duty tractor trailer category with a GVWR of 7.5 t compared to a heavy-duty tractor trailer with a 15 t GVWR, for example.

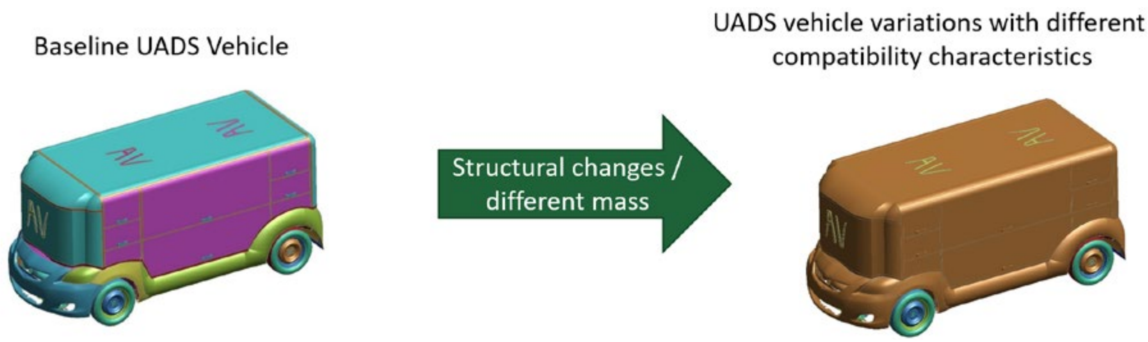

Figure 45. Development of ODV variations

The structural characteristics and performance of each ODV model relative to the crash compatibility and energy-absorbing criteria for the four ODV categories are outlined below with additional details documented in Appendix A.

Small ODV

Figure 46 shows a perspective and side view of the small ODV vehicle. The baseline model has a mass of 804 kg and was based on a validated Toyota Yaris small size sedan. The bumper height matches the Part 581 height definition. Select components, such as the longitudinal rails and bumper design were adapted from the existing traditional vehicle frontal structural design and the combustion engine was removed. The width of the small ODV is smaller than the width of the reference sedan. Less compatible variations of the small ODV baseline model were developed by changing the material strength and material thickness for select parts, as outlined in Appendix A1 and B2. The mass of the Design 1 (812 kg) and Design 2 (834 kg) increased marginally compared to the baseline model.

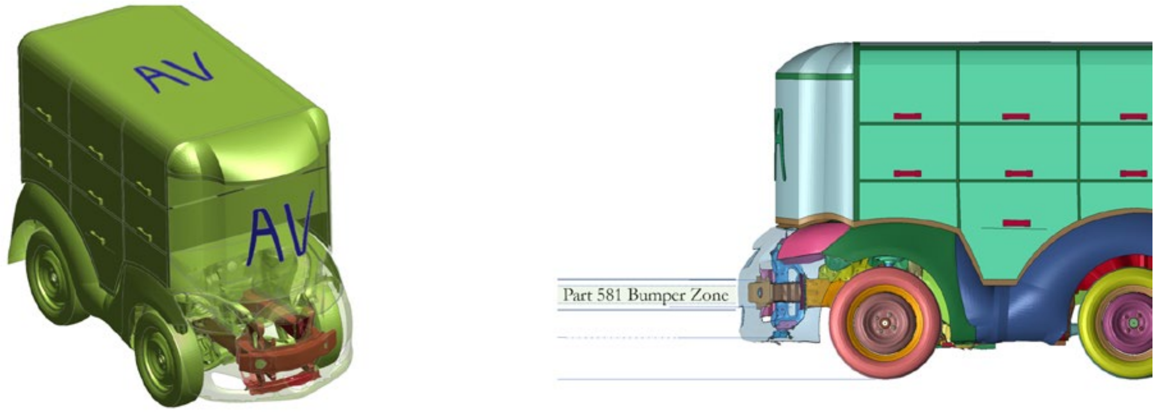

Figure 46. Small ODV frontal structure and bumper height

Figure 47 (a) shows a bottom view of the baseline and a modified Design 2 for the frontal offset impact configuration. Significant differences with respect to structural deformation of the rails, bumpers, and barrier honeycomb face can be observed. The front of the longitudinal rails for the least compatible Design 1 did not buckle and resulted in a more severe MPDB crash pulse and higher deformation of the honeycomb face at the height of the rails. Figure 47 (b) shows a cross-section view of the small ODV Design 2 when striking the NCAP rigid wall. Note that no buckling occurs in the frontal longitudinal rails, resulting in a stiff behavior.

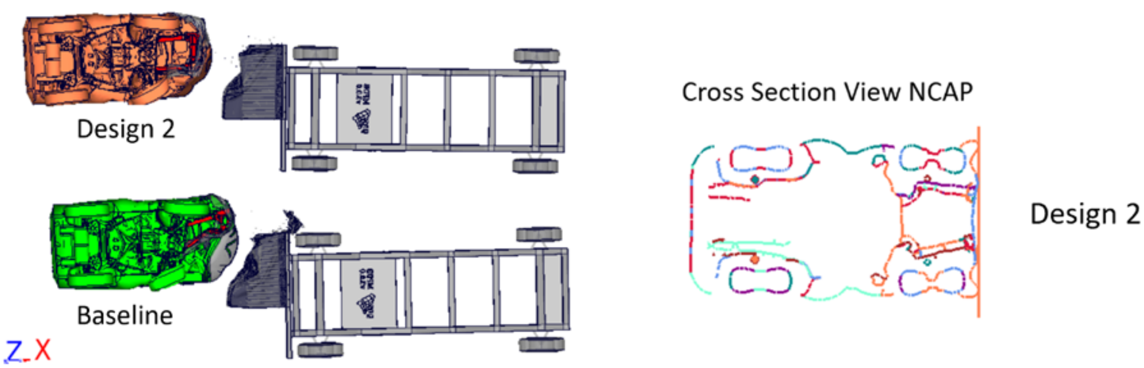

Figure 47. Small ODV (a) Bottom view; (b) Cross section view

The NCAP full overlap and EuroNCAP offset configurations, which the compatibility metrics, KW400 and OLC, are based on, complement each other. While the impact into the rigid wall engages the entire width and frontal structure of the vehicle, only part of the vehicle, e.g., one frontal rail, is engaged in the 50-percent offset condition. The differences in energy absorption and respective compatibility metrics for the baseline model and two variations with different characteristics are summarized at the end of this chapter.

Mid-size ODV

Figure 48 (a) shows a perspective and cross-section view for the mid-size ODV in the offset impact configuration. The baseline model had a mass of 1,467 kg. In addition to the OLC criteria, bottoming out of the barrier honeycomb face is typically evaluated. Clear bottoming out occurred for Design 2, as shown in Figure 48 (a) at the bottom. Figure 48 (b) shows the bumper height matching the zone defined in Part 581 on the top and a perspective view of the NCAP full overlap crash configuration at the bottom.

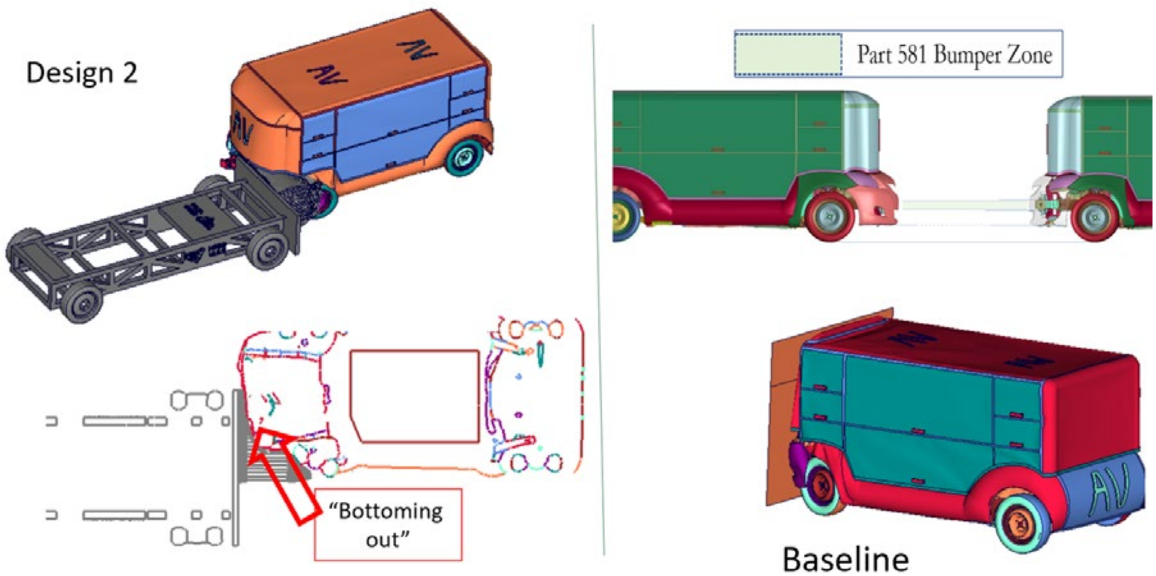

Figure 48. Mid-size ODV (a) Offset impact; (b) Bumper height and full-frontal impact

For the mid-size ODV Design 1, the thickness of the longitudinal rails and bumper was significantly increased create a less compatible model variation. The vehicle mass increased from 1,467 kg for the baseline model to 1,513 kg for Design 1, as summarized in Appendix A3. For the mid-size ODV Design 2, the vehicle mass was increased by 800 kg while keeping the frontal stiffness characteristics the same as for Design 1. The model variations developed for the mid-size ODV allowed to study the effect of different compatibility characteristics due to a stiffer frontal structure and due to increased vehicle mass.

Large ODV

Figure 49 (a) shows a bottom view of the large ODV, with a baseline mass of 4,000 kg, in the frontal offset impact configuration.

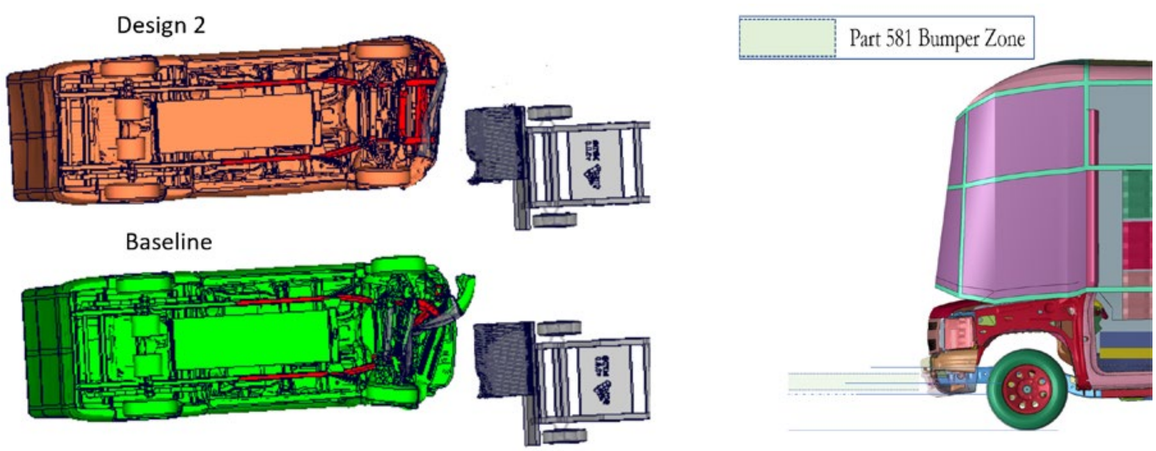

Figure 49. Large ODV (a) Offset impact Design 2 and baseline; (b) Bumper height

The picture on the top represents the modified Design 2, shown in orange, with a stiffer frontal structure that showed different deformation and energy absorption characteristics than the baseline model, shown in green. Significant differences in longitudinal rail and bumper buckling, due to modified material strength and material thickness for select parts, were observed. Differences between the baseline model, the Design 1 with better compatibility characteristics and a mass of 3,810 kg, and the less compatible Design 2 with a mass of 4,021 kg, are summarized in Appendix A4 and Appendix A5. Figure 49 (b) shows, how the bumper of the large ODV, which was based on a Chevrolet Silverado vehicle, overlaps with the bumper zone defined in Part 581. Respective metrics are summarized at the end of this chapter.

Tractor ODV

Figure 50 (a) shows a perspective and cross-section view of the frontal offset impact configuration for the tractor ODV with a baseline mass of 3,400 kg.

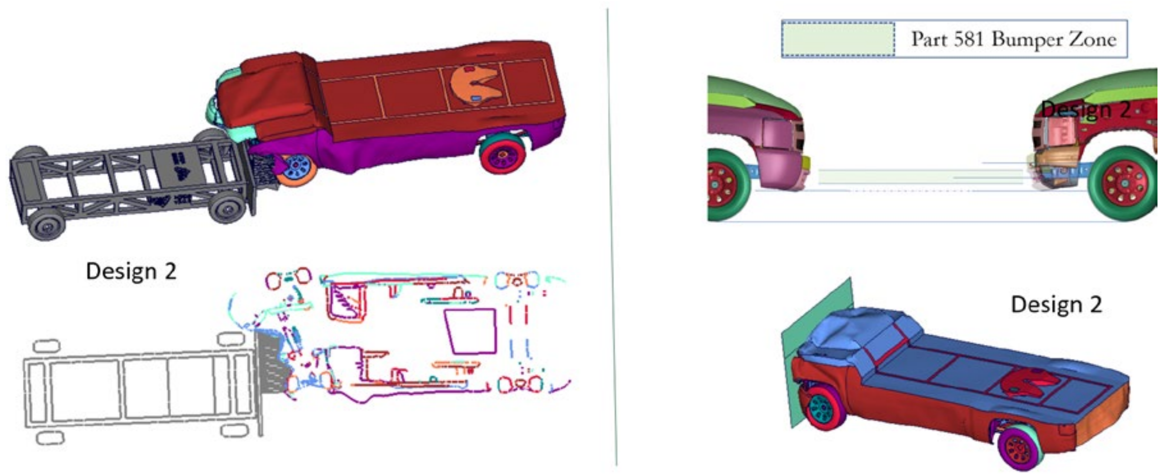

Figure 50. Tractor ODV design 2 (a) offset impact; (b) bumper height and rigid wall impact

Figure 50 (b) illustrates how the bumper overlaps with the Part 581 bumper zone on the top, and a snapshot of the impact into a rigid wall on the bottom. Like for the other three ODV categories, select components of the frontal structure, such as the bumper and longitudinal rails, were modified to create a less compatible model variation Design 2, as documented in Appendix A6. Design 1 has the same frontal structure as the baseline model but a battery with half the weight (1 t instead of 2 t), as described at the beginning of this chapter. Respective metrics are summarized in the next section.

ODV Compatibility Metrics Summary

Two variations in addition to the baseline model for each of the four ODV categories were developed by modifying the material strength and material thickness of relevant frontal structural components or by changing the vehicle mass.

Figure 51 (a) summarizes the compatibility characteristics for the small, mid-size, large, and tractor ODV categories, based on the OLC, calculated from the MPDB barrier pulse in the offset impact configuration.

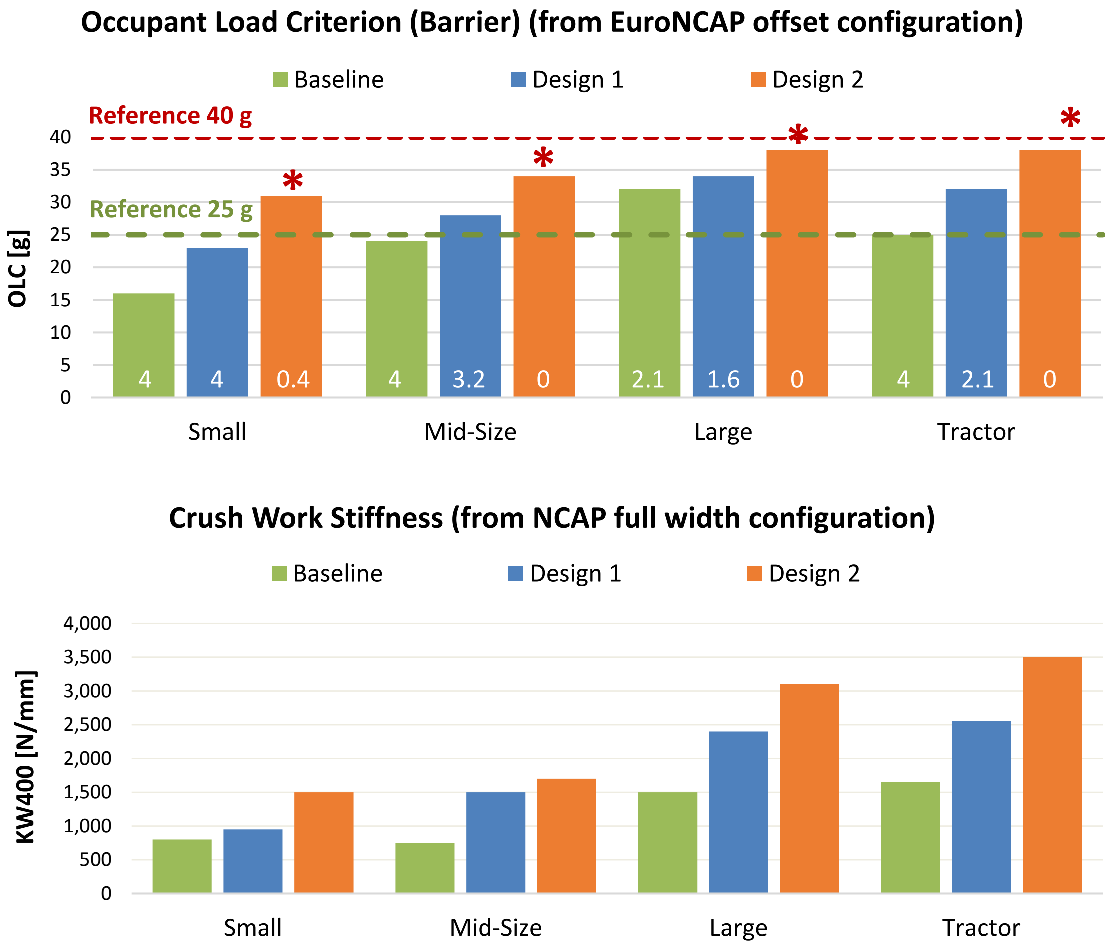

Figure 51. Summary of compatibility metrics for 4 ODV categories (a) OLC; (b) KW400

Reference lines representing an OLC of 25 g and 40 g are shown in green and red. They are based on the sliding scale used by EuroNCAP, where OLC values below 25 g would give 4 points and values above 40 g would give 0 points for the overall compatibility rating assessment. In addition to the OLC, barrier bottoming out is evaluated. If bottoming out occurs, a 2-point penalty modifier applies. For example, if a vehicle generates an OLC of 32.5 g and barrier face bottoming out is observed, zero points would be given for the overall rating and the vehicle would be considered to have bad compatibility characteristics. The red asterisk on top of the design variations of the four ODV categories with the highest OLC values indicates that bottoming out was observed and that the model can be considered “non-compliant” with respect to the defined compatibility metrics, i.e., the vehicles would receive 0 points for the EuroNCAP compatibility assessment. The respective EuroNCAP score based on the OLC value and the bottoming out penalties is documented by the numbers, shown in white at the bottom of each bar in Figure 51 (a). For example, the mid-size ODV baseline model, with an OLC value of 23 g and no bottoming out, would receive 4 points. The mid-size ODV Design 2 with an OLC of 34 g would receive 1.6 points without modifier and 0 points with the 2-point penalty applied.

Figure 51 (b) summarizes the crush work stiffness (KW400) values for the respective baseline models and ODV variations, as calculated from the force versus deformation characteristics in the NCAP full overlap impact. Similar trends can be observed for the OLC and KW400 metrics.

In summary, model variations with substantially different compatibility characteristics, based on the selected metrics, were developed. The ODV categories span a wide range of potential future ODV designs with respect to size, geometry, and frontal structure compatibility. Different strategies when generating the model variations were applied, as previously outlined. These included (1) iterative modification of relevant parts using different material strength and thickness; (2) substantial reinforcement of relevant components to represent a vehicle with a very stiff vehicle front that does not deform and absorb energy; and (3) reducing and increasing vehicle mass without changing the vehicle structure.

The ODV baseline models and model variations with different compatibility characteristics were used in combination with the previously described occupied crash partner FE models to conduct the ODV-to-vehicle compatibility simulation studies.

6. ODV-to-Vehicle Simulation Plan

Impact Configurations and Assessment Metrics

For each of the four ODV vehicles, i.e., the small, mid-size, large, and tractor vehicles, a FE simulation plan was developed based on the conducted crash data analyses and the selected occupied crash partner vehicles.

The following three impact configurations were identified, as described in Chapter 2 Identification of Real-World Crash Scenarios, and Chapter 3 Evaluation of Crash Test Configurations.

1. Co-linear frontal impact with full overlap
2. Frontal 10° oblique, 50-percent offset impact
3. 90° side impact aligned with B-pillar of target vehicle

The effect of different compatibility characteristics of the described ODV vehicles on two different occupied crash partner target vehicles was studied. Two occupied LPV FE models will be used as crash partner vehicles, as described in Chapter 4.

1. 2015 Toyota Camry, mid-size sedan
2. 2020 Nissan Rogue, crossover SUV

Defined vehicle metrics, recorded from the occupied crash partner vehicles, were assessed. For the full-frontal and frontal oblique impact configurations, the vehicle pulse using the OLC metric and toe pan intrusion were evaluated to understand the effect of impacts with ODV vehicles with different compatibility characteristics. Structural metrics were compared to existing crash test configurations at various speed, i.e., the NCAP full-frontal impact of the occupied crash partner vehicles into a rigid wall, and NHTSA's frontal oblique impact configuration, where the occupied crash partner vehicle is struck by an OMDB. For the side impact configuration, maximum absolute velocity, recorded at the near-side B-pillar, and maximum exterior crush were used as structural metrics. Side impact results were compared against existing crash test configurations, i.e., NHTSA crabbed MDB and the IIHS MDB side impact load cases using different impact velocities.

Similarly, occupant metrics were used to document the effect of different ODV compatibility characteristics. Established injury metrics for the head, chest, and pelvis/femur were used. The crash partner FE models were occupied with state-of-the-art anthropomorphic test device models seated in the driver seat.

- 50th percentile male Hybrid III
- 50th percentile WorldSID
- 5th percentile female Hybrid III (select cases)

The 5th percentile female Hybrid III occupant was studied in addition to the 50th percentile male Hybrid III to understand differences and similarities for the two dummy sizes. The validated Hybrid III dummy models have been developed by a company called ATD-Models GmbH[12]and

[12] Weißwasser, Germany

the validated WorldSID FE model has been developed by the Partnership for Dummy Development and Biomechanics and is being distributed by Humanetics and DYNAmore.[13] The dummy models, shown in Figure 52, are widely used during the vehicle development process by many car manufacturers.

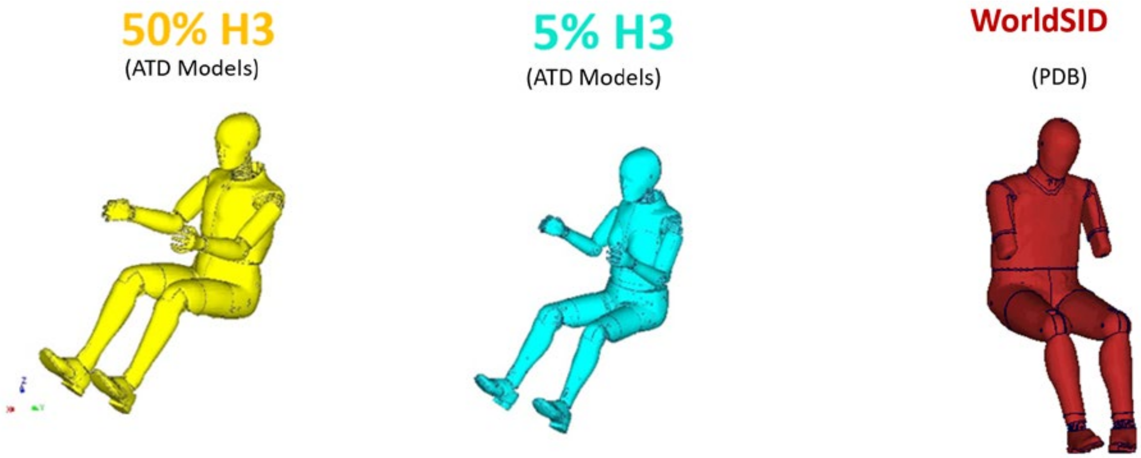

Figure 52. Dummy models (a) 50-percent male Hybrid III; (b) 5-percent female Hybrid III; (c) WorldSID

Integrated ODV-to-vehicle simulations, where the ODV vehicles struck the occupied crash partner FE models, equipped with relevant interiors and restraints, were conducted for frontal and side impact configurations. Established analyses methods, such as accelerometers and injury risk assessment instrumentation, were exercised for both target vehicles when struck by the four ODV categories.

The defined approach allowed for understanding of how variations in an ODV vehicle's design can affect the occupants in a crash partner vehicle, across a range of expected ODDs.

Comparison of the structural and occupant metrics, as recorded during the (1) Reference 2 ODV-to-vehicle and (2) Reference 1 existing barrier-to-vehicle reference configurations, allow the readers to compare the severity of evaluated configurations to known existing load cases. The ODV vehicles' structural compatibility, as outlined in Chapter 5, was documented.

Full-frontal Impact Simulation Plan

A ODV-to-vehicle full impact with vehicle damage at the entire frontal width was identified as an important real-world crash configuration. Hence, ODV-to-vehicle load cases with 100-percent overlap was studied for all four ODV categories. It was assumed that fully unoccupied vehicles will be designed for different ODDs. For example, the existing NURO vehicle, which is being used for grocery deliveries, has an implemented maximum speed of 25 mph. Larger ODV vehicles, which are anticipated to transport cargo long-distance, for example, are anticipated to allow higher maximum velocities than the small ODV. For this research, different impact speeds were defined for the different ODV categories. Impact velocity of 35 km/h (22 vehicles. Therefore, the full-frontal impact configuration simulation study was executed according to the plan illustrated in Figure 53.

[13] DYNAmore FEM Ingenieurdienstleistungen GmbH, Stuttgart, Germany

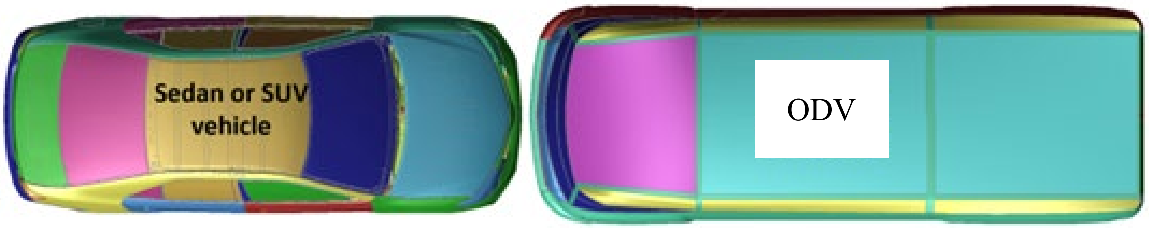

Initial Velocity of ODV and LPV [km/h (mph)]	LPV into Rigid Wall	Small ODV into LPV (Baseline, Design 1+2)	Mid-size ODV into LPV (BL, Design 1+2)	Large ODV into LPV (BL, Design 1+2)	Tractor ODV into LPV (BL, Design 1+2)
35 (22)	✓	✓✓✓			
40 (25)	✓		✓✓✓		
45 (28)	✓			✓✓✓	
50 (31)	✓				✓✓✓
56 (35)	✓				

Figure 53. Full-frontal impact ODV-to-LPV simulation plan

All configurations were exercised using the baseline ODV FE vehicle model and the two developed ODV variations with different compatibility metrics, as illustrated by the three check marks in Figure 53, for the respective ODV categories. For example, simulations where the small ODV and the sedan LPV impact, each traveling at a ground speed of 35 km/h (22 mph), under co-linear conditions with a 100-percent overlap were conducted for the three ODV variations, the baseline, the Design 1, and the Design 2 FE models. Similarly, simulations were conducted where the small ODV and the cross-over SUV LPV impact each other. In addition to the ODV-to-LPV simulations, the impact of the LPV into a rigid wall, based on NHTSA's NCAP rigid barrier test, were conducted at respective velocities, for reference. Hence, 12 ODV-to-LPV and 5 LPV-into-rigid-wall simulations were conducted using either a 2015 Toyota Camry sedan or a 2020 Nissan Rogue SUV vehicle FE model. A minimum of 34 (17 sedan and 17 SUV) simulations were defined for the full-frontal impact configuration.

Frontal Oblique Impact Crash Simulation Plan

Oblique ODV-to-vehicle impacts with partial overlap were identified as another important real-world crash configuration, as described in Chapter 2. Hence, ODV-to-vehicle load cases with 50-percent overlap and 10° oblique orientation, relative to the co-linear axis, were studied for all four ODV categories. For this compatibility research, different impact speeds were defined for the various ODV categories. Impact velocities of 35 km/h (22 mph), 40 km/h (25 mph), 45 km/h (31 mph), and 50 km/h (35 mph) were defined for the small, mid-size, large, and tractor ODV vehicles. Like for the full-frontal simulation study, impact scenarios with both vehicles moving at the same speed were studied. The frontal oblique configuration simulation study was executed according to the plan illustrated in Figure 54.

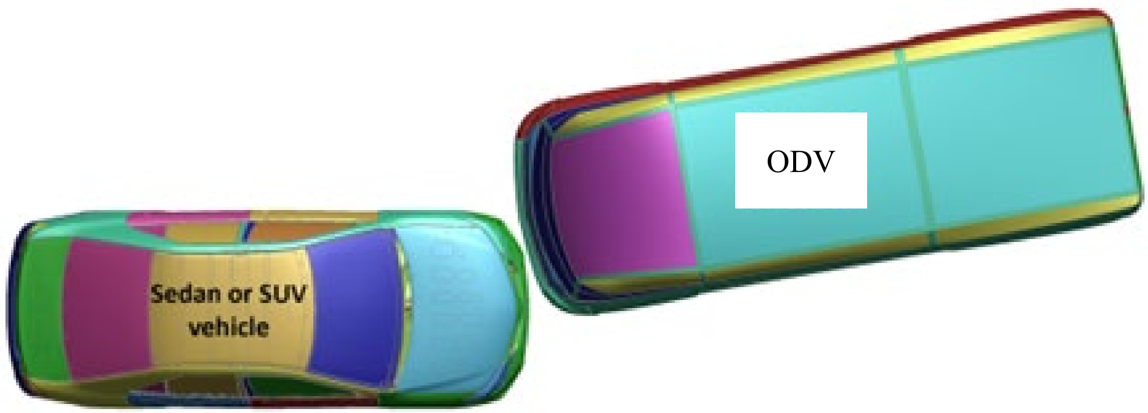

Initial Velocity of ODV and LPV [km/h (mph)]	LPV into EuroNCAP MPDB	Small ODV into LPV (Baseline, Design 1+2)	Mid-size ODV into LPV (BL, Design 1+2)	Large ODV into LPV (BL, Design 1+2)	Tractor ODV into LPV (BL, Design 1+2)
35 (22)	✓	✓✓✓			
40 (25)	✓		✓✓✓		
45 (28)	✓			✓✓✓	
50 (31)	✓				✓✓✓

Figure 54. Frontal oblique impact ODV-to-LPV simulation plan

All configurations were exercised using the baseline ODV FE vehicle model and the two developed ODV variations with different compatibility metrics, as illustrated by the three check marks in Figure 54, for the respective ODV categories. For example, simulations where the large ODV and the 2015 Toyota Camry sedan vehicle impact, each traveling at a ground speed of 45 km/h (28 mph), at a 10° oblique angle with a 50-percent overlap were conducted for the three ODV variations, the baseline, the Design 1, and the Design 2 FE models. Similarly, simulations were conducted where the large ODV and the 2020 Nissan Rogue cross-over SUV impact each other. For reference, LPV-to-MPDB simulations were carried out, based on the EuroNCAP compatibility test. In addition, impacts of the OMDB traveling at 80 km/h (50 mph) and 85 km/h (53 mph) into the stationary LPV, based on NHTSA's oblique impact test, were conducted for reference. Hence, 12 ODV-to-LPV, four MPDB-to-LPV, and two OMDB-to-LPV simulations were carried out using the respective ODV, sedan, and SUV vehicle models.

Select additional simulations with different impact velocities were defined. For example, a higher impact velocity of 40 km/h (25 mph) was studied for the small ODV. Furthermore, select cases, where the LPV vehicle travels at a 16 km/h (10 mph) higher speed than the ODV, such as the mid-sized ODV traveling at 40 km/h (25 mph) and the LPV travels at 56 km/h (35 mph), was evaluated. This represents a scenario where an LPV vehicle drives on a road with a 35-mph speed limit and the ODV is required to have at least a maximum speed of 25 mph, i.e., 10 mph less than the speed limit. More than 40 (20 sedan and 20 SUV) simulations were conducted for the frontal oblique impact configuration, which includes both the simulations noted in Figure 54 and the select additional simulations.

Side Impact Crash Simulation Plan

Side impacts with a close to perpendicular PDOF were identified as another important real-world crash configuration, as described in Chapter 2. Hence, ODV-to-vehicle load cases, where the ODV impacts the stationary LPV at a 90° angle, were studied for all four ODV categories. For this compatibility research, different impact speeds were defined for the different ODV categories. Impact velocities of 35 km/h (22 mph), 40 km/h (25 mph), 45 km/h (31 mph), and 50 km/h (35 mph) were defined for the small, mid-size, large, and tractor ODV vehicles. The side impact configuration simulation study was executed according to the plan illustrated in Figure 55.

Initial velocity of ODV (LPV stationary) [km/h (mph)]	NHTSA & IIHS MDB	Small ODV into LPV (Baseline, Design 1+2)	Mid-size ODV into LPV (BL, Design 1+2)	Large ODV into LPV (BL, Design 1+2)	Tractor ODV into LPV (BL, Design 1+2)
35 (22)	✓✓	✓✓✓			
40 (25)	✓✓		✓✓✓		
45 (28)	✓✓			✓✓✓	
50 (31)	✓✓				✓✓✓

Figure 55. Side impact ODV-to-LPV simulation plan

All configurations were carried out using the baseline ODV FE vehicle model and the two developed ODV variations with different compatibility metrics, as illustrated by the three check marks in Figure 55, for the respective ODV categories. For example, simulations where the tractor ODV impacts the stationary occupied Toyota Camry sedan at a 90°angle with a speed of 50 km/h (31 mph) was conducted for the three ODV variations, the baseline, the Design 1, and the Design 2 FE models. Similarly, simulations were conducted where the tractor ODV vehicles impact the occupied Nissan Rogue cross-over SUV. For reference, NHTSA's crabbed MDB side impact configuration and the IIHS MDB side impact load case was studied. In addition to the simulations outlined in Figure 55, select cases with different velocities, such as the mid-size ODV traveling at a higher velocity of 45 km/h (28 mph), was evaluated. More than 44 simulations (22 sedan and 22 SUV LPV) were defined, which includes both the simulations noted in Figure 55 and the select additional simulations.

In total, about 120 simulations for the full-frontal, frontal oblique, and side-impact configurations were conducted, focusing on crash scenarios between the front-end of a ODV and an occupied crash partner. The results, which will be outlined in the next Chapter, demonstrated how variations in an ODV vehicle's design can affect the crashworthiness and the occupants in an occupied crash partner vehicle, across a range of expected ODDs.

This page intentionally left blank.

7. ODV-to-Vehicle Simulation Results

Frontal, frontal oblique, and side impacts of ODV vehicles with occupied sedan and SUV crash partner FE models were conducted according to the previously defined simulation plan. For each of the four ODV categories, three model variations with different compatibility characteristics were studied, as outlined in Chapter 5.

Evaluation Metrics

Structural and occupant metrics were defined to evaluate the effect of ODV compatibility on an occupied sedan and SUV LPV. The team chose to use three structural responses to measure the effect of ODV compatibility in the frontal impact conditions: Vehicle CG acceleration, as shown in Figure 56 (a), and two toe pan intrusion measurements near the driver's right and left feet, as shown in Figure 56 (b). In addition, the LPV's OLC was calculated.

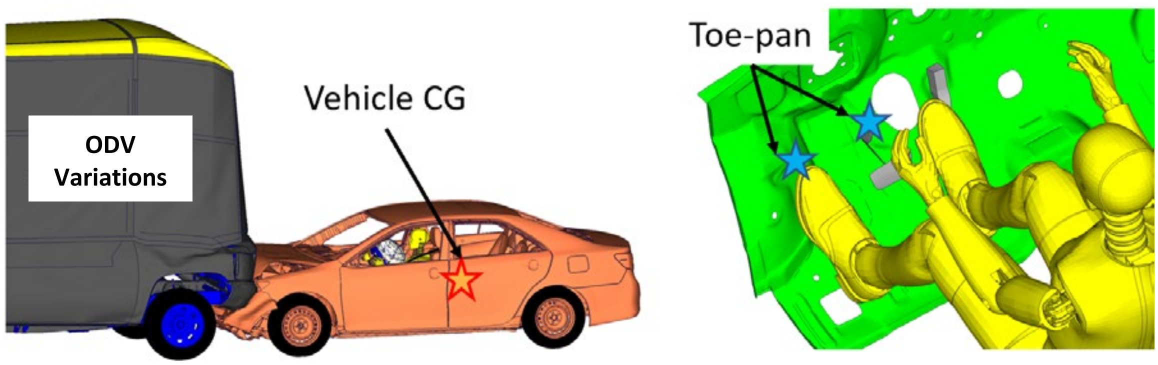

Figure 56. LPV frontal impact structural metrics (a) Vehicle CG pulse, (b) Toe-pan intrusion

Head, chest, and femur loads were extracted from the frontal impact simulations, as shown in Figure 57 (a). Color coding was used to illustrate if measured values for HIC, BRIC, thorax deflection, and femur forces were below, in between, or above defined reference values, as shown in Figure 57 (b). For example, an HIC value below 500 was highlighted using the green color, HIC values between 500 and 700 were colored in yellow, and values above 700 were color coded using red. Upper and lower reference values are based on a NCAP Request for Comments (NHTSA, 2015) document. Most simulations were conducted with a 50th percentile male Hybrid III seated on the driver seat. The 5th percentile female Hybrid III ATD was also used for select cases. For illustration purpose, the same color scheme and IARVs were used for both frontal impact dummies.

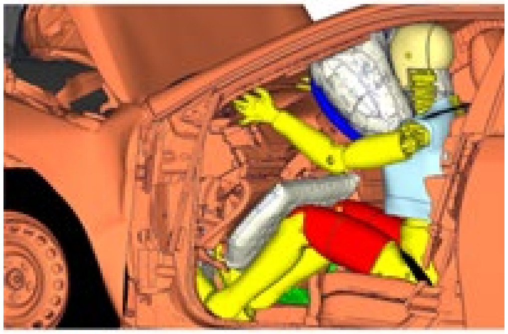

50% Hybrid III Color Coding*	Lower Limit		Upper Limit
HIC	< 500	500 -700	> 700
BRIC	< 0.71	0.71 - 1.05	> 1.05
Thorax [mm]	< 22	22 - 42	> 42
Femur [N]	< 5331	5331 - 8588	> 8588

*mainly based on NCAP TFC [Docket No. NHTSA-2015-0119. Same color coding is used for 5% Hybrid III

Figure 57. LPV frontal impact occupant metrics (a) ATD body regions, (b) Hybrid III injury metrics / IARV color coding

Different vehicle and occupant metrics apply for side impact crash evaluations. Maximum exterior crush at the pelvis, thorax, and head locations, as well as the maximum absolute vehicle velocities at the vehicle CG and the near-side B-pillar, were recorded for all conducted simulations, as shown in Figure 58. The yellow stars denote exterior crush, and the red stars denote absolute velocity.

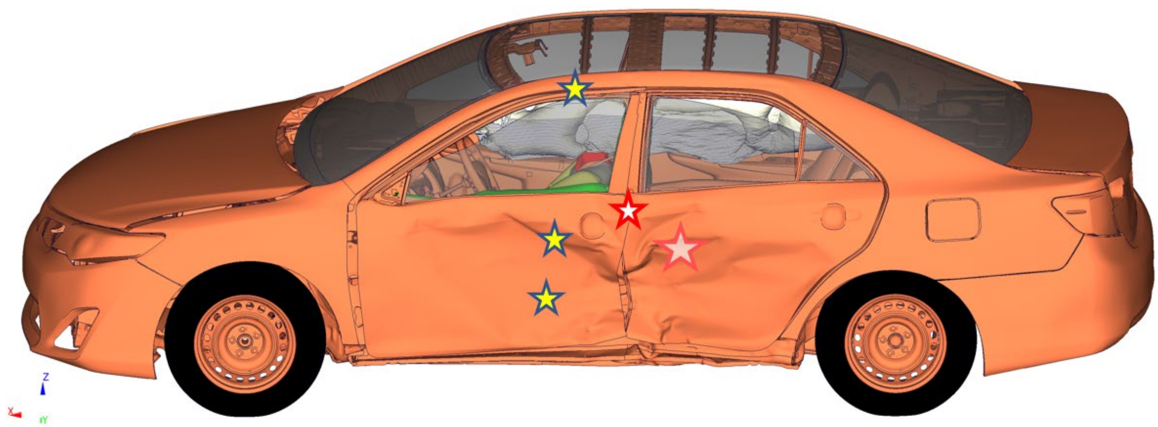

Figure 58. Locations of LPV side impact structural metrics including exterior crush and absolute B-pillar velocity

From the author's experience working in industry and with major car manufacturers, it is known that the B-pillar thorax location is used by some OEMs to judge the structural side impact performance of a vehicle. An accelerometer positioned at the middle of the B-pillar provides important information with respect to occupant loads caused by vehicle deformation and vehicle kinematics. In frontal impact configurations, interaction of the occupant with the seat and seat belt results in deceleration of the occupant coupled with the vehicle deceleration, called ride-down effect. Side impact injury mechanisms are different. In a collision where an occupied stationary vehicle is struck by a striking vehicle from the side, occupant loads are mainly induced by the deformation of the vehicle structure and interior and the motion of the near side structure. The absolute B-pillar velocity describes the combination of the vehicle deformation and vehicle motion and is therefore a good indicator for loads relevant for occupant injury risk, which are then mainly mitigated by optimized air bags and interior components. To further explain the side impact characteristic, we can assume two extreme cases, (1) a small vehicle with low mass and no significant deformation, and (2) a heavy vehicle with a significant amount of deformation. The light vehicle would be pushed away during an impact and the heavy vehicle would not move but experience near-side structural deformation, while the occupant predominantly remains at the initial location without significant ride-down effect. The absolute velocity measured at the B-pillar is a good structural metric in side impact, because it captures well the load the occupant experiences for both cases, in the first case caused by vehicle motion, and in the second case mainly caused by vehicle deformation. Similarly, absolute velocities measured at the doors can be a good indicator for a vehicle's side impact performance, while measurements from the doors are more likely to show questionable data in full-scale testing, due to local buckle effects and higher oscillations, compared to the B-pillar location.

In addition to the described structural LPV metrics, occupant metrics based on the measurements from the 50th percentile WorldSID dummy were studied. Head, thorax, and abdominal loads were extracted from the side impact simulations, as shown in Figure 59 (a). Color coding was used to illustrate if measured values for HIC, BRIC, thorax, and abdominal deflections were below, in between, or above defined reference values, as shown in Figure 59 (b). For example, maximum thorax deflection below 27 mm was highlighted using green, values between 27 mm and 50 mm were colored in yellow, and values above 50 mm were color coded using red. Upper and lower reference values are based on the previously referenced NCAP Request for Comment document (NHTSA, 2015).

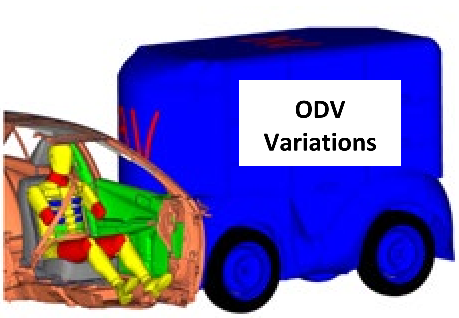

WorldSID 50th Color Coding*	**Lower Limit**		**Upper Limit**
HIC	< 500	500 - 700	> 700
BRIC	< 0.65	0.65 – 0.85	> 0.85
Thorax [mm]	< 27	27 - 50	> 50
Abdomen [mm]	0 - 47		47

*based on NCAP RFC [Docket No. NHTSA-2015-0119

Figure 59. LPV side impact occupant metrics (a) ATD body regions, (b) WorldSID injury metric color coding

ODV-to-Sedan Full-Frontal Impact Results

In order to put the study results into perspective, the existing frontal impact configuration, where the LPV impacts a rigid wall with full overlap, was conducted first. The load case represents the impact of two identical vehicles travelling at the same speed. Both the LPV-to-LPV and LPV-to-Wall scenarios were examined, as shown in Figure 60.

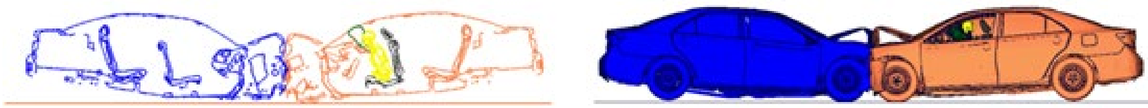

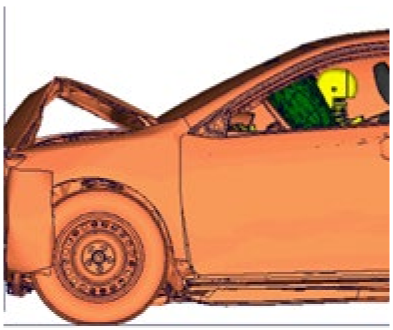

		Camry2Camry	Camry2Wall				
	Velocity [km/h]	56	56	50	45	40	35
Structure	OLC Camry	33	35	30	27	25	20
	Max. Acc. Camry	60	60	55	49	29	32
	Intrusion Left Foot	39	41	24	16	15	9
	Intrusion Right Foot						
Occupant	HIC	342	294	289	198	189	162
	BRIC	0.47	0.39	0.4	0.42	0.42	0.51
	Chest	33	34	34	32	30	29
	Femur left	2461	2702	2363	2351	2368	1835
	Femur right	2163	2364	2244	2113	1982	1795

Figure 60. Sedan reference scenarios (a) LPV-to-LPV and LPV-to-Wall images in top and left, and (b) Occupant and structural response values.

The vehicle deformation using a cross-section and side view for an impact of two Toyota Camrys traveling at 56 km/h is shown on the top. The impacts of the occupied sedan LPV into a rigid wall at 35, 40, 45, 50, and 56 km/h were also conducted, for reference. The characteristic values describing the vehicle structure and occupant loads are summarized. The same maximum acceleration (60 g), measured at the vehicle CG, was recorded for the vehicle-to-vehicle and vehicle-to-rigid wall impact at 56 km/h, as highlighted by the green circles. The maximum acceleration correlated with velocity for the vehicle-to-rigid wall impacts at different impact speed. Similarly, maximum toe-pan intrusion was comparable for the vehicle-to-vehicle and the vehicle-to-rigid wall impacts for the same speed and correlated with impact velocity for different speeds. For example, a maximum intrusion of 9 mm was recorded for the 35 km/h impact, and a maximum intrusion of 41 mm was recorded for the 56 km/h impact into a rigid wall, as highlighted by the light blue frame. Similarly, occupant loads for the head, chest, and femur all correlated with impact speed. HIC values increased from 162 for the 35 km/h impact to 294 for the 56 km/h impact, for example.

The same occupied Toyota Camry sedan LPV was then struck by the small and mid-size ODV variations, representing different compatibility characteristics. Figure 61 (a) shows a cross-section view for the scenario, where both vehicles travel at a ground speed of 35 km/h in a full-frontal configuration. Note that the small ODV with good compatibility metrics, shown at the bottom and marked with baseline (BL), behaved softer and experienced more crush than the Design 2 (D2) with less compatible characteristics, shown on top. Similar observations were made for collision of the mid-size ODV and the LPV, both traveling at 40 km/h, as shown in

Figure 61 (b). More deformation can be seen for the BL model with good compatibility metrics compared to D2 with less compatible performance.

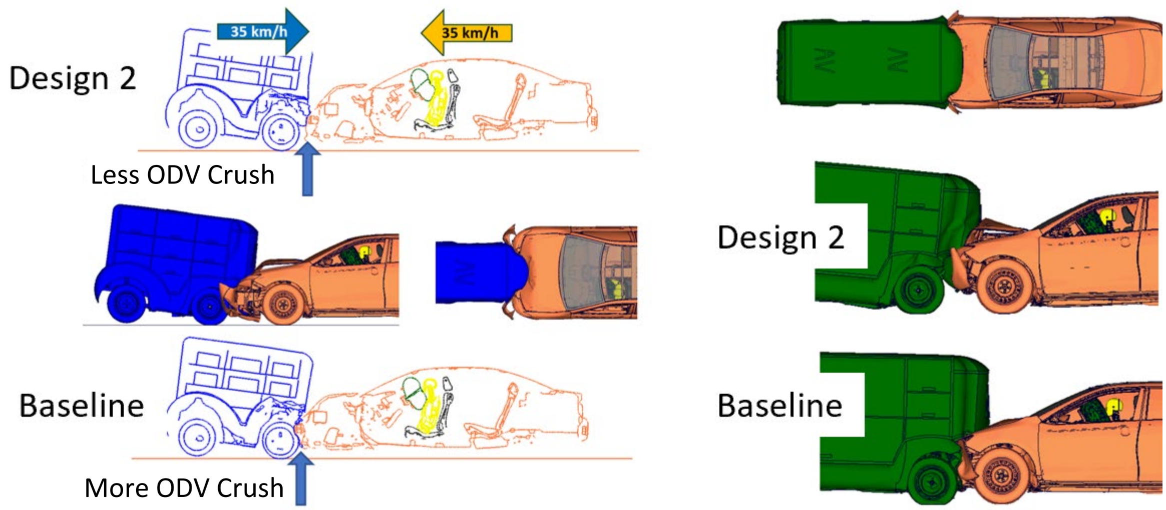

Figure 61. Comparison of good and bad compatibility (a) small ODV; (b) mid-size ODV

Small and mid-size ODV compatibility correlated with LPV structural and occupant metrics, as summarized in Table 7.

Table 7. Small and mid-size ODV full-frontal impact into sedan - characteristic values summary, with vehicles traveling at identical ground speeds.

		Camry2Wall		**Small-ODV-to-Camry 35 km/h**			**Mid-size-ODV-to-Camry 40km/h**		
		40		BL	D1	D2	BL	D1	D2
Structure	OLC Camry	25	OLC-Camry	9	11.2	11.6	15,0	21.6	24.6
	Max. Acc. Camry	29	Acc-Camry	20	32	29.8	22.5	38	40.8
	Intrusion Left Foot	15	intru-left	2	4	4	7	22	28
	Intrusion Right Foot	12	intru-right	2	4	4	7	18	22
Occupant	HIC	189	HIC	33	78	84	91	146	182
	BRIC	0.42	BRIC	0.47	0.52	0.52	0.49	0.4	0.49
	Chest	30	Chst	18	25	26	24	32	32
	Femur left	2368	fem-le	1269	1198	1329	1698	2153	2181
	Femur right	1982	fem-ri	1233	1359	1372	1553	1952	2107
ODV	EuroNCAP Compatibility		OLC [g]	16	26	31	23	28	34
ODV	NCAP Crush Work Stiffness		KW400 [kN/mm]	709	955	1501	775	1543	1760

While most loads for the small and mid-size ODV impacts were smaller than for the rigid wall reference scenario due to the low mass and low speed, a clear correlation between compatibility and loads was observed. The occupied LPV pulse, represented by the OLC and maximum acceleration, the toe-pan intrusion, HIC, BRIC, chest, and femur load values all correlated with ODV compatibility. For example, the maximum chest deflection increased from 18 mm to 26 mm for the small ODV and from 24 mm to 32 mm for the mid-size ODV, as highlighted by the orange circles. The compatibility metrics were based on impacts of the ODV with the EuroNCAP MPDB (OLC metric) and an impact into a rigid wall (KW400) metric, as described in Chapter 4. The characteristic compatibility metrics for the ODV vehicles are shown in the bottom two rows for the respective ODV designs. For example, the impact of the mid-size ODV baseline design with good compatibility metrics, represented by an OLC of 23 g and a KW400 value of 775 kN/mm, resulted in lower injury risk than the mid-size ODV Design 2, represented by an OLC of 34 g and a KW400 value of 1760 kN/mm, as highlighted by the orange circles. Another example is the increase of maximum vehicle acceleration from 22.5 g to 40.8 g and the increase in HIC values from 91 to 182, for the most and least compatible designs. While most absolute values were small due to the relatively low energy impact, ODV compatibility had a substantial effect on LPV occupant loads.

Figure 62 (a) shows side view of the impact of the large ODV baseline design and the Toyota Camry, where both vehicles traveled at 45 km/h. Note the difference in vehicle geometry and height. As for the small and mid-size ODV, structural changes were applied to components at the lower section of the large ODV, such as the bumper and longitudinal rails. Figure 62 (b) shows a cross-section view of the less compatible tractor ODV Design 2 on the top, and the more compatible Design 1 on the bottom. Note the mass effect and different stiffness characteristics of the frontal ODV structure, demonstrated by the different longitudinal rail buckling modes.

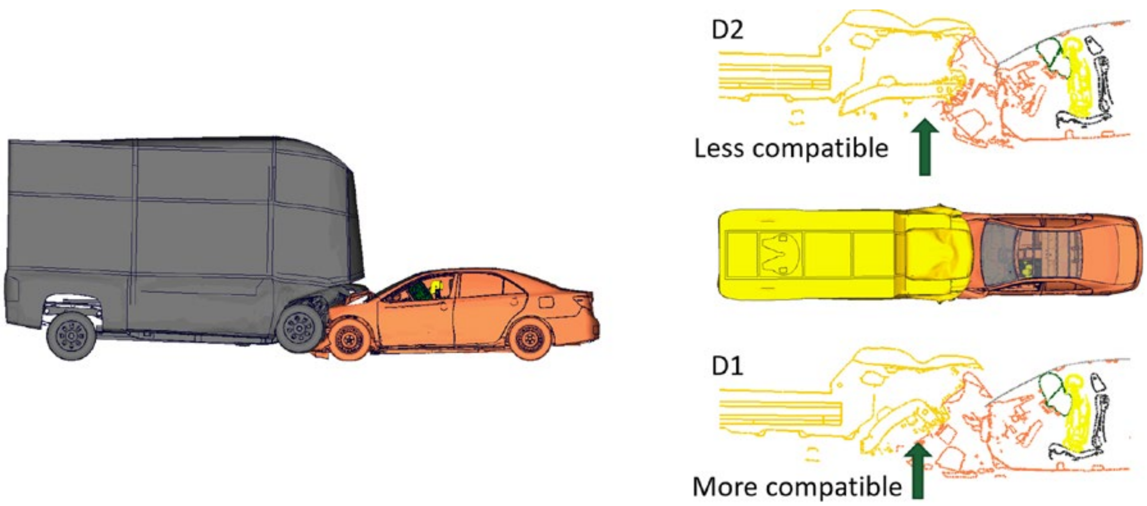

Figure 62. ODV-to-sedan deformation (a) 45 km/h large ODV; (b) 50 km/h tractor ODV

Table 8 summarizes the characteristic values for the large and tractor ODV. Similar to the small and mid-size ODV vehicles, correlation between ODV compatibility and LPV structural and occupant loads can be observed. Less compatible ODV designs resulted in higher deformation and higher injury risk. For example, maximum chest deflection increased from 28 mm for the most compatible to 31 mm for least compatible large ODV and from 28 mm for the most compatible to 34 mm for the least compatible tractor ODV, as highlighted by the orange circles.

Table 8. Full-frontal ODV-to-sedan impact characteristic values, with vehicles traveling at identical ground speeds.

		50% male Hybrid III			**50% HIII**		**5% female HIII**	**50% HIII**		
		Large ODV to Camry 45 km/h			Camry 50 to Large ODV 35		Large ODV to Camry 45 km/h	Tractor ODV to Camry at 50 km/h		
		D1	BL	D2	D1	D2	D2	D1	BL	D2
Structure	OLC Camry	20.7	23.6	23.2	19.1	24.3	25.3	18.9	24.3	25.1
	Max. Acc. Camry	38.4	47.5	45.6	35.5	44.3	45.1	38.9	46.5	47.7
	Intrusion Left Foot	20	30	22	17	20	22	13	26	51
	Intrusion Right Foot	13	26	18	13	15	17	9	22	54
Occupant	HIC	148	147	161	109	162	101	116	181	400
	BRIC	0.53	0.5	0.51	0.54	0.47	0.48	0.55	0.52	0.34
	Chest	28	30	31	28	31	20	28	32	34
	Femur left	1846	3200	2690	1428	2694	1956	1935	2760	3367
	Femur right	1732	2998	2238	1715	2140	2419	2221	2193	2902
ODV	EuroNCAP Compatibility	28	32	36	28	36	36	25	32	38
ODV	NCAP Crush Work Stiffness	1524	2389	3064	1524	3064	3064	1690	2520	3462

In addition to the 50th percentile male Hybrid III, the 5th percentile female Hybrid III dummy was placed on the LPV driver seat for the impact with the large ODV Design 2 at 45 km/h. Compared to the impact with the LPV occupied with the 50th percentile male ATD, similar structural loads were observed. Minor differences were caused by the difference in occupant weight and position, which resulted in marginally different occupant to vehicle interaction. Head and chest loads were smaller, while the maximum femur load was higher for the 5th compared to the 50th percentile Hybrid III for the specific simulations. Different occupant posture and interaction with the restraints were the reason for the observed differences.

Furthermore, the researchers studied how an impact in which both vehicles traveled at 45 km/h compared to a scenario where the sedan LPV traveled at 50 km/h and the ODV at 35 km/h. Similar LPV structural and occupant loads were observed and the correlation between ODV compatibility and occupied vehicle loads was confirmed.

The tractor ODV-to-sedan impacts at 50 km/h showed the highest values compared to the previously analyzed ODV categories, due to the higher impact velocity.

ODV-to-Sedan Frontal Oblique Impact Results

NHTSA's frontal oblique offset and EuroNCAP's co-linear frontal offset test configurations were evaluated using the selected occupied Toyota Camry FE model, as shown in Figure 63.

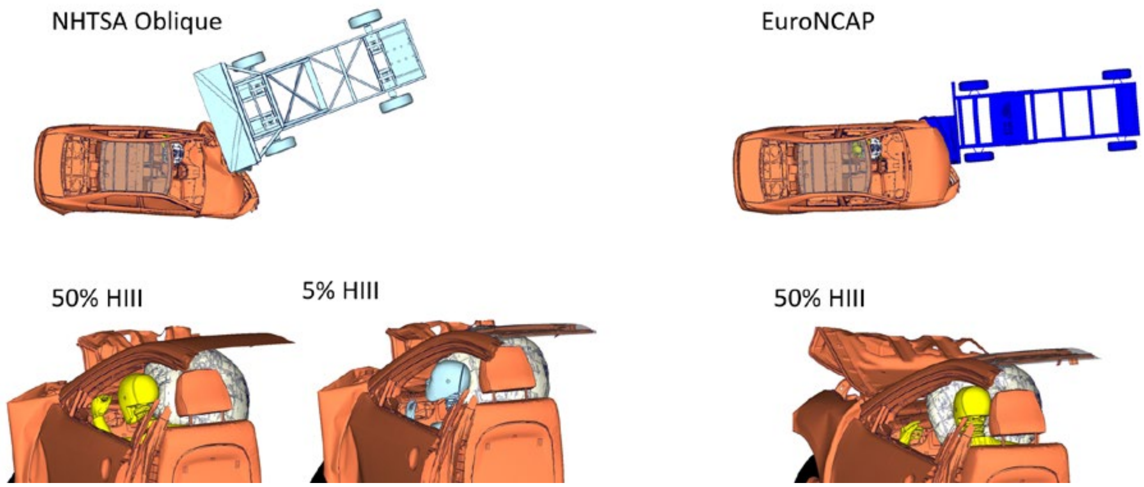

Figure 63. Frontal oblique reference configurations (a) NHTSA oblique; (b) EuroNCAP MPDB

The reference load-cases showed different structural deformation and occupant kinematics. Higher structural deformation was observed for NHTSA's oblique impact with a 2,500 kg OMDB compared to the impact with the 1,400 kg EuroNCAP MPDB. More significant head motion towards the A-pillar was seen for the oblique compared to the co-linear impact. Significant differences in 5-percent and 50-percent Hybrid head kinematics were observed. The 5th percentile ATD experienced higher head rotation caused by the different initial occupant position and interaction with the restraints, as shown in Figure 63 (a).

The characteristic values for the frontal oblique and frontal offset reference configurations are summarized in Table 9.

Table 9. Sedan frontal oblique references characteristic values

			NHTSA Oblique			**EuroNCAP**	
			80 km/h	85 km/h	85 km/h	40 km/h each	45 km/h each
			50% male H3		5% female H3	50% male H3	
Structure	OLC Camry	24.3	22.2	24.5	25	17.8	21
	Max. Acc. Camry	46.5	38.3	40.6	42.1	25	30.5
	Intrusion Left Foot	26	29	41	41	24	32
	Intrusion Right Foot	22	27	37	37	14	21
Occupant	HIC	181	670	623	117	124	118
	BRIC	0.52	1.11	1.22	1.67	0.62	0.6
	Chest	32	27	28	14	27	27
	Femur left	2760	2212	2561	3214	1596	1884
	Femur right	2193	1856	2084	1957	1538	1863

While the struck vehicle is stationary during NHTSA's oblique impact, vehicle and MPDB travel at the same speed during the EuroNCAP test. Note that structural and injury values were smaller for the EuroNCAP test, which can mainly be attributed to the lower barrier mass. NHTSA's oblique impact condition at 85 km/h was simulated once with the 50th percentile male and once with the 5th percentile female ATD. Structural loads were similar for the two cases, as expected, and occupant loads tended to be lower for most body regions of the 5th percentile Hybrid III, except for the BRIC. The higher BRIC value is caused by the more significant head rotation of the 5th percentile Hybrid III, as shown in Figure 63. BRIC values of 1.22 and 1.67 were recorded for the respective ATDs in NHTSA's oblique impact, while a much lower BRIC value of 0.6 for the 50th percentile ATD was recorded during the EuroNCAP's load case, as highlighted by the white circles in Table 9. OLC, maximum acceleration, and intrusion correlated with impact speed for NHTSA's oblique impact, as documented in the first two columns. Correlation of impact speed and occupant loads was not as clear as for the full-frontal impact condition. Only femur loads showed a clear correlation. Occupant kinematics, which play a more significant role in the oblique impact condition, were the reason for the observed injury metric trends, especially for the head.

Figure 64 (a) and (b) show a top view of the small and mid-size ODV, striking the occupied Toyota Camry in the frontal oblique condition. The smaller dimensions, mass, and impact velocity of the small ODV resulted in significantly less LPV damage.

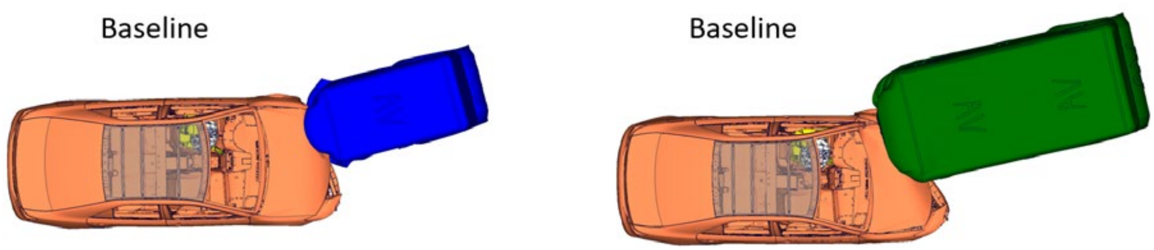

Figure 64. Frontal oblique impact (a) small ODV-to-sedan, (b) mid-size ODV

Table 10 summarizes the characteristic values for the 35 km/h small and 40 km/h mid-size ODV frontal oblique impact simulations, together with two reference load cases.

Table 10. Small and mid-size ODV frontal oblique impact into sedan - characteristic values summary

		NHTSA Oblique	EuroNCAP	Small ODV into Camry 35km/h each			Mid-size ODV into Camry 40 km/h each		
		80 km/h	40 km/h each	BL	D1	D2	BL	D1	D2
Structure	OLC Camry	22.2	17.8	7.4	8.6	9	13.1	17.6	19.7
	Max. Acc. Camry	38.3	25	16.5	19.3	18.3	23.1	29.7	30.9
	Intrusion Left Foot	29	24	8	15	17	10	39	48
	Intrusion Right Foot	27	14	5	5	6	7	19	25
Occupant	HIC	670	124	27	45	50	90	92	106
	BRIC	1.11	0.62	0.44	0.52	0.5	0.51	0.65	0.74
	Chest	27	27	14	19	19	22	25	26
	Femur left	2212	1596	1299	1322	1357	1270	1614	1760
	Femur right	1856	1538	1332	1495	1496	1392	1710	1669
ODV	EuroNCAP Compatibility OLC [g]			16	26	31	23	28	34
ODV	NCAP Crush Work Stiffness KW400 [kN/mm]			709	955	1501	775	1543	1760

Most LPV structural and occupant values were smaller than for the reference load cases due to the lower vehicle mass. A correlation between ODV compatibility and LPV loads was observed for all metrics. For example, the chest deflection increased from 14 mm to 19 mm for the small ODV and from 22 mm to 26 mm for the mid-size ODV when comparing the least and most compatible ODV designs, as highlighted by the orange circles. The effect of better LPV crash pulse, toe-pan intrusion, lower BRIC values and femur loads for a more compatible ODV design, was generally more substantial for the mid-size ODV.

Figure 65 (a) and (b) show the vehicle deformations for the large and tractor ODV striking the occupied sedan.

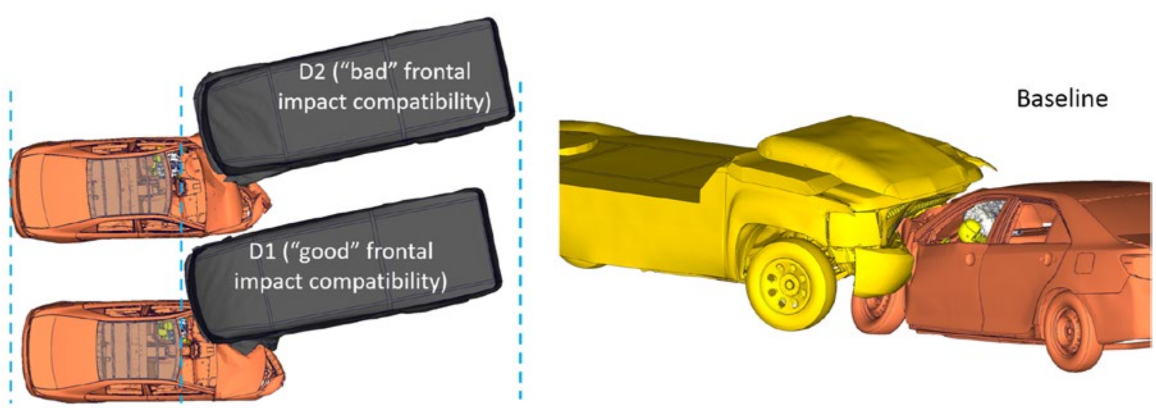

Figure 65. Frontal oblique impact (a) large ODV-to-sedan, (b) tractor ODV BL

The less compatible large ODV Design 2 with higher frontal structural stiffness pushes the Toyota Camry further back compared to the large ODV Design 1 with good compatibility characteristics, indicated by the dashed blue vertical reference lines. LPV damage for all simulations conducted with the large and tractor ODV was higher compared to the impacts with the small and mid-size ODV, due to the different frontal structure as well as higher mass and impact velocity. Occupant kinematics were like NHTSA's oblique impact configuration, characterized by head kinematics directed toward the A-pillar.

The characteristic values for the 45 km/h large ODV and 50 km/h tractor ODV frontal oblique impact simulations and three reference load cases are summarized in Table 11.

Table 11. Large and tractor ODV frontal oblique impact into sedan - characteristic values summary

					Large-ODV-Camry 45 km/h each				**Tractor-ODV-Camry 50 km/h each**		
				50%-M HIII			5%-F HIII				
	NHTSA Oblique		EuroNCAP	D1	BL	D2	D1	D2	D1	BL	D2
	85 km/h	85 km/h	45 km/h each								
Structure OLC Camry	24.5	25	21	17.7	21.5	21.7	21.2	24.3	18.1	22.5	24.6
Max. Acc. Camry	40.6	42.1	30.5	22.2	37.2	42.1	35.3	44.3	25.1	28.3	43.9
Intrusion Left Foot	41	41	32	32	39	84	21	23	17	32	129
Intrusion Right Foot	37	37	21	16	32	61	11	19	8	22	103
Occupant HIC	623	117	118	98	279	397	40	58	139	159	156
BRIC	1.22	1.67	0.6	0.53	0.98	1.05	0.51	1.2	0.79	1.05	0.46
Chest	28	14	27	24	26	25	15	16	24	29	29
Femur left	2561	3214	1884	1597	4043	3611	1776	2981	1660	2571	3656
Femur right	2084	1957	1863	1129	3305	2605	1381	2019	1773	2096	4823
ODV EuroNCAP Compatibility OLC [g]				28	32	36	28	36	25	32	38
ODV NCAP Crush Work Stiffness KW400 [kN/mm]				1524	2389	3064	1524	3064	1690	32	3462

The 5th percentile female ATD was used in addition to the 50th percentile male ATD using the large ODV vehicles. Structural and occupant loads clearly correlated with ODV compatibility characteristics. The effect was most substantial for the toe-pan intrusion when struck by the different tractor ODV designs, the 50th percentile male HIC, and BRIC, when struck by the large ODV. For example, BRIC increased from 0.53 to 1.05 for the 50th percentile and from 0.51 to 1.2 for the 5th percentile Hybrid III, when comparing the least and most compatible designs.

ODV-to-Sedan Side Impact Results

Like for the frontal impact conditions, existing side impact configurations were used to determine reference values for the ODV-to-sedan side impact studies. The NHTSA crabbed MDB side impact configuration, as well as the previous and updated IIHS MDB side impact configurations, were simulated, as shown in Figure 66.

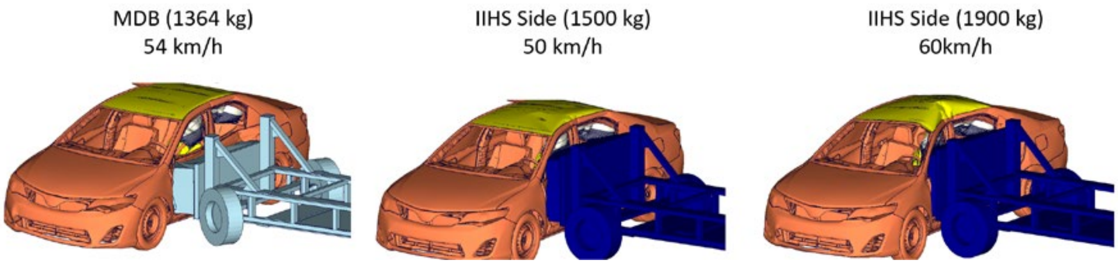

Figure 66. Sedan side impact reference configurations (a) NHTSA MDB (1364 kg, 54 km/h); (b) IIHS MDB (1500 kg, 50 km/h); (c) IIHS MDB (1900 kg, 60 km/h)

The IIHS barrier has a higher honeycomb face compared to NHTSA's MDB, representing a SUV or pickup. The IIHS barrier used to have a mass of 1,500 kg travelling at 50 km/h and was recently updated to 1,900 kg and a speed of 60 km/h, to better capture the current SUV vehicle fleet and more severe crash scenarios. NHTSA's MDB has a mass of 1,360 kg, representing a sedan vehicle, and uses crabbed tire orientations to simulate the impact into a driving target vehicle. Higher structural deformation of the B-pillar and roof can be observed for the IIHS conditions due to greater height and mass compared to NHTSA's MDB. Note the substantial deformation of the roof for the updated IIHS configuration in Figure 66 (c).

Table 12 summarizes the occupant and structural characteristic values for the NHTSA and IIHS MDB impact into the Toyota Camry, occupied with a 50th percentile WorldSID dummy positioned on the front driver seat.

Table 12. Sedan side impact NHTSA and IIHS MDB references - characteristic values summary

		MDB 7 45 km/h	**MDB 54 km/h**	**IIHS 1500kg 50km/h**	**IIHS 1900kg 60km/h**
Occupant	HIC	36	74	239	1789
	BRIC	0.35	0.48	0.7	0.82
	Thorax [mm]	8	26	36	60
	Abdomen [mm]	22	36	46	56
Structure	Roof [mm]	14	26	64	173
	Door Thorax [mm]	173	232	291	387
	Door Pelvis [mm]	218	272	323	395
	B-Pillar [m/s]	7.4	7.6	8	10.8
	CG [m/s]	5.7	6.5	7.6	8.7

Higher impact speed and higher MDB mass correlated with higher vehicle deformation at the door and the roof. Absolute B-pillar velocity also clearly indicated the higher structural loads caused by the higher impact speeds and higher barrier mass for the respective impact configurations. Consequently, higher occupant injury values were observed for the impacts with the IIHS barrier compared to NHTSA's MDB. For example, maximum thorax compression was 26 mm for the 54 km/h NCAP, 36 mm for the 50 km/h IIHS, and 60 mm for the 60 km/h IIHS configurations. Note that occupant's thoracic response exceeded the refence values for the 1,900 kg, 60 km/h IIHS condition, highlighted by the red color for HIC, thorax, and abdominal loads.

Figure 67 (a), (b), and (c) show the side impact of the small ODV traveling at 35 km/h and 50 km/h and the mid-size ODV striking the stationary Toyota Camry at 40 km/h.

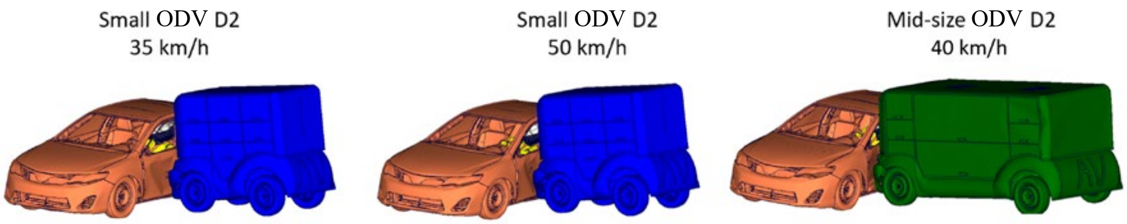

Figure 67. Sedan side struck by (a) small ODV Design 2 at 35 km/h; (b) small ODV Design 2 at 50 km/h; (c) mid-size ODV Design 2 at 40 km/h

Note that little vehicle damage was observed especially for the small ODV for both impact speeds, 35 km/h and 50 km/h, compared to the side impact reference configurations. This can be attributed to the lower ODV vehicle mass.

Table 13 summarizes the characteristic values for the impact with the small and mid-size ODV with different compatibility metrics.

Table 13. Small and mid-size ODV side impact into sedan - characteristic values summary

		MDB 45 km/h	**IIHS 1500kg 50km/h**	**Small ODV into Camry 35 km/h**			**Small ODV 50 km/h**	**Mid ODV into Camry 40 km/h**		
				BL	D1	D2	D2	BL	D1	D2
Occupant	HIC	36	239	5	4	5	44	36	38	74
	BRIC	0.35	0.7	0.21	0.23	0.21	0.55	0.26	0.31	0.47
	Thorax [mm]	8	36	5	5	5	15	10	12	15
	Abdomen [mm]	22	46	12	13	13	28	11	30	34
Structure	Roof [mm]	14	64	5	14	7	33	1	0	1
	Door Thorax [mm]	173	291	101	106	108	212	150	170	197
	Door Pelvis [mm]	218	323	216	222	221	323	174	303	328
	B-Pillar [m/s]	7.4	8	4.8	5.2	5.2	7.7	5.6	5.9	6
	CG [m/s]	5.7	7.6	4	3.9	4	4.8	5.9	6.1	7.1
ODV	EuroNCAP Compatibility			16	26	31	31	23	28	34
ODV	NCAP Crush Work Stiffness			709	955	1501	1501	775	1543	1760

Differences in structural and occupant loads were not substantial for the impact with the small ODV variations at 35 km/h, due to low ODV mass. The effect of higher impact speed for the small ODV resulted in larger differences. For the mid-size ODV, a clear correlation between ODV compatibility and LPV load was observed. Maximum exterior crush at the height of the pelvis was 174 mm for the mid-size ODV with good compatibility metric and 328 mm for the Design 2 with a less compatibility metrics, as highlighted by the orange circles. Consequently, maximum abdominal deflection increased from 11 mm to 34 mm.

The occupied sedan LPV was then struck by the large ODV and tractor ODV with the previously described frontal impact compatibility characteristics, as shown in Figure 68.

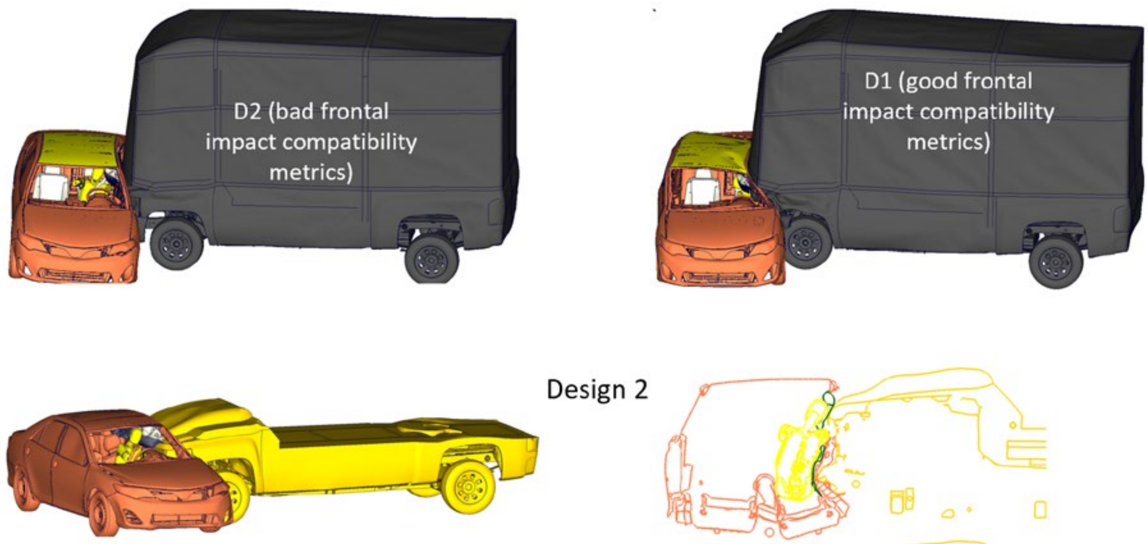

Figure 68. tractor ODV Design 2 at 50 km/h (bottom)

Figure 68 (a) shows a deformed state for the impact with the large ODV Design 2 with bad frontal impact compatibility on the left and for the impact with the large ODV Design 1 with good frontal impact compatibility on the right. Note that the specific large ODV Design 2 with a non-compatible, stiff lower frontal vehicle structure, showed little ODV deformation, illustrated by the large distance between the wheels of the ODV and the sedan. It interacted with the LPV at the sill and door areas, pushing the LPV in the lateral direction. In contrast, the large ODV Design 1 with a softer, lower frontal vehicle structure, experienced more deformation, indicated by the small distance between the ODV wheels and the LPV. Consequently, the interaction of the ODV upper structure and the sedan upper B-pillar and roof became more relevant, resulting in visible exterior crush to the upper portion of the vehicle cabin's structure. This highlights that different compatibility aspects can be relevant for frontal and side impact configurations. The importance of geometry and potential interaction with an occupant's head agrees with previous research and voluntary industry commitments. For example, in the FMVSS No. 201 side pole impact test, the HIC performance requirement of 1000 or less in the driver's seating position resulted in optimized curtain air bag designs that have contributed to real-world occupant safety, for example.

This observation was specific to the large ODV due to the high frontal vehicle structure. The side impact with the tractor ODV striking the stationary Toyota Camry at 50 km/h is shown in Figure 68 (b). Significant exterior crush, especially at the door, can be observed in the cross-section view on the right. No direct contact with the roof occurred due to the smaller height of the tractor ODV compared to the large ODV.

Table 14 summarizes the characteristic values for the impact with the large and tractor ODV with different compatibility metrics and some MDB references.

Table 14. Large and tractor ODV side impact into sedan characteristic values summary

		MDB 54 km/h	IIHS 1500kg 50km/h	IIHS 1900kg 60km/h	Large ODV into Camry 45 km/h			Tractor ODV into Camry 50 km/h		
					D1	BL	D2	D1	BL	D2
Occupant	HIC	74	239	1789	1091	496	387	571	692	1070
	BRIC	0.48	0.7	0.82	1.41	0.71	0.79	0.45	0.6	0.76
	Thorax [mm]	26	36	60	38	49	44	37	35	47
	Abdomen [mm]	36	46	56	27	59	55	57	55	59
Structure	Roof [mm]	26	64	173	143	55	49	40	45	49
	Door Thorax [mm]	232	291	387	166	316	296	300	343	364
	Door Pelvis [mm]	272	323	395	176	422	394	450	501	512
	B-Pillar [m/s]	7.6	8	10.8	8.4	9.2	9.2	9.1	9.9	10.5
	CG [m/s]	6.5	7.6	8.7	6.7	7.2	9	7.4	7.9	7.7
ODV	EuroNCAP Compatibility				28	32	36	25	32	38
ODV	NCAP Crush Work Stiffness				1524	2389	3064	1690	2520	3462

The deformation and loading characteristics for the large ODV, as illustrated in Figure 68, are documented in the characteristic values, highlighted with orange circles in Table 14. Structural and occupant values for the impact with the tractor ODV were higher than for the impacts with the small and mid-size ODV due to the higher mass and impact velocity. A clear correlation was observed between tractor ODV structural compatibility and LPV loads, like the previously described frontal and side impact configurations. For example, absolute B-pillar velocity increased from 9.1 m/s to 10.5 m/s and maximum thorax deflection increased from 37 mm to 47 mm for the large ODV Design 2 with bad compatibility characteristics compared to the tractor ODV Design 1 with good compatibility characteristics.

The results for the large ODV, with respect to roof exterior crush and HIC values, are an exception to the previous findings and showed an opposite trend. Exterior crush of 143 mm and HIC of 1,091 was recorded for Design 1, while exterior crush of 49 mm and an HIC value of 387 was recorded for Design 2, as highlighted by the orange circles in Table 14. Note that the measurements at the door show the expected trend, where the more compatible (with respect to frontal impact) Design 1 experienced a maximum exterior crush of 176 mm and the less compatible Design 2 experienced a maximum exterior crush of 394 mm. The specific case indicated that good frontal impact compatibility does not necessarily provide good side impact compatibility for all body regions, especially for taller striking vehicles where the striking ODV interacts significantly with the upper portion of the occupant cabin in the crash partner. The results indicate that attention to both, the upper and lower portion of a tall vehicle, should be given, when optimizing the frontal structure compatibility and/or front-end geometry. Frontal impact compatibility metrics typically address the lower area of a vehicle and the combination of a relatively soft lower frontal structure, and a relatively stiff upper frontal structure of a tall vehicle can result in high loads to the roof and head, when striking another vehicle on the side.

ODV-to-SUV Full-frontal Impact Results

Similar studies as those for the sedan were conducted using the recently developed FE model of a 2020 Nissan Rogue. Reference simulations, where the occupied SUV struck a rigid wall at different speeds, were conducted first, as shown in Table 15.

Table 15. SUV reference impact into rigid wall (a) Vehicle deformation (b) Characteristic values

		Rogue into rigid wall				
		35 km/h	40 km/h	45 km/h	50 km/h	56 km/h
Structure	OLC - Nissan Rogue	18.5	22.2	25.8	29.7	35.3
	Max. Acc. Rogue	31	34.3	50.4	54.8	59.4
	Intrusion Left Foot	15	31	46	59	66
	Intrusion Right Foot	17	34	53	80	100
Occupant	HIC	185	203	192	255	486
	BRIC	0.78	0.77	0.75	0.8	0.7
	Chest	30	32	33	34	36
	Femur left	1159	923	1012	2334	3329
	Femur right	1243	1497	1712	1827	3676

Vehicle pulse, intrusion, and occupant loads correlated with impact speed, as highlighted by the colored frames. For example, a maximum toe-pan intrusion of 34 mm was recorded for an impact velocity of 40 km/h and a maximum intrusion of 100 mm was recorded for the 56 km/h impact, as highlighted by the orange circles.

The Nissan Rogue FE model was then struck in a full-frontal condition by the small ODV, as shown in Figure 69. Structural damage of the SUV was small due to the low impact energy.

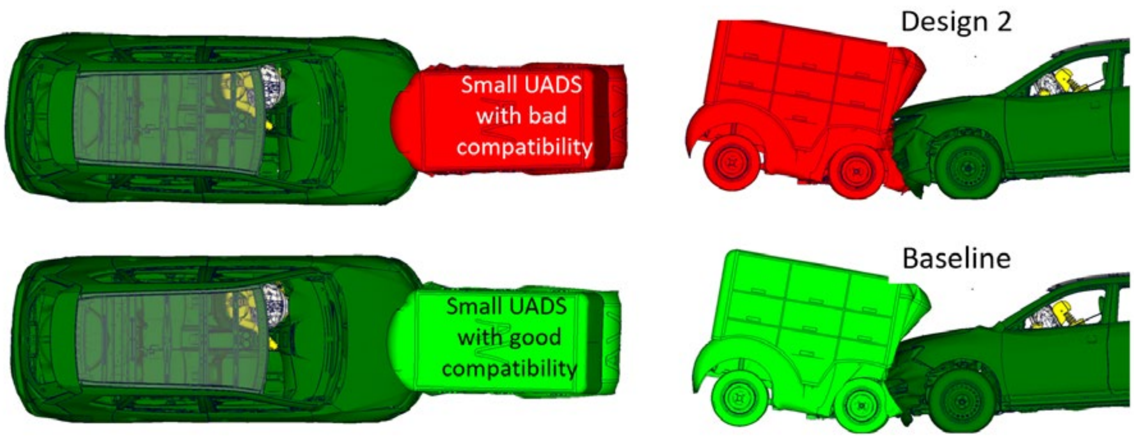

Figure 69. Small ODV with different compatibility metrics striking Nissan Rogue SUV

Figure 70 shows the effect of different compatibility characteristics when struck by the mid-size ODV. Note that the impact with the mid-size ODV with bad compatibility metrics, shown in red at the top, resulted in a more severe SUV vehicle pulse, illustrated by a larger head forward motion, when compared to the impact with the mid-size ODV with good compatibility characteristics, shown in green. At a time of 80ms after impact, the occupant's forward trajectory resulted in a head position in front of the roof cross member, when struck by the least compatible mid-size ODV design, while the head was still positioned behind the roof cross member, when struck by the most compatible mid-size ODV design, shown in green.

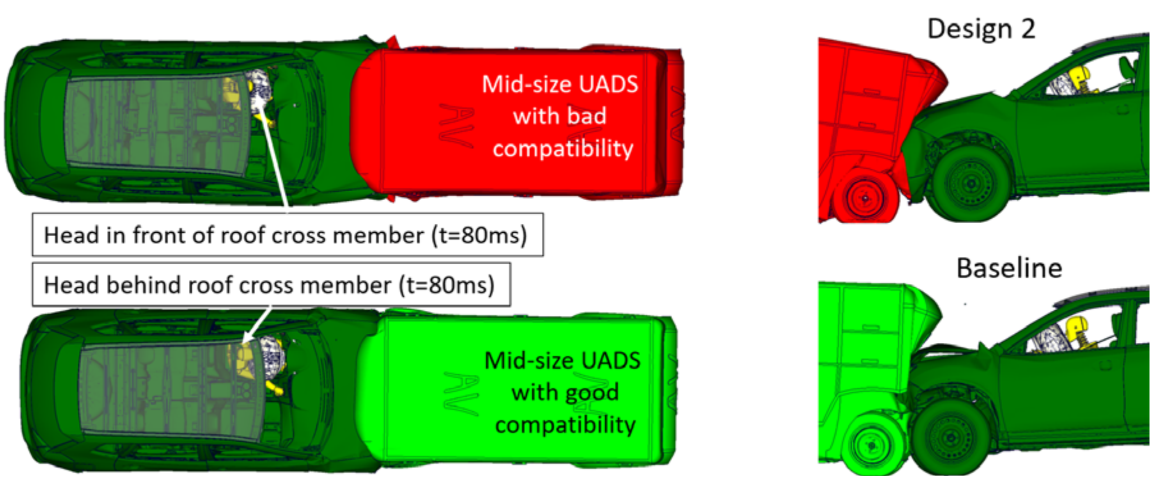

Figure 70. Mid-size ODV with different compatibility metrics striking Nissan Rogue SUV

Small and mid-size ODV compatibility correlated with LPV structural and occupant metrics, as summarized in Table 16. For example, maximum femur loads increased from 772 N to 1,320 N and from 1,271 N to 2,806 N, for the small and mid-size ODV. This is highlighted by the orange circle, when comparing the most and least compatible designs.

Table 16. Small and mid-size ODV full-frontal impact into SUV - characteristic values summary

		Rogue into rigid wall		Small ODV to Rogue			Mid ODV to Rogue			Rogue to ODV
		35 km/h	40 km/h	35 km/h			40 km/h			50 km/h, 30 km/h
				BL	D1	D2	BL	D1	D2	BL
Structure	OLC - Nissan Rogue	18.5	22.2	9.5	10.3	10.5	16.2	23.3	27.5	18.6
	Max. Acc. Rogue	31	34.3	23.3	32.4	36.6	32.7	50.2	52.5	35.6
	Intrusion Left Foot	15	31	3	5	7	6	19	20	5
	Intrusion Right Foot	17	34	4	8	9	6	32	33	6
Occupant	HIC	185	203	69	75	77	154	257	306	191
	BRIC	0.78	0.77	0.73	0.81	0.81	0.73	0.85	0.85	0.8
	Chest	30	32	24	26	26	29	31	31	31
	Femur left	1159	923	892	1126	1162	966	1799	1785	989
	Femur right	1243	1497	772	1226	1320	1271	2649	2806	1439
	shb	4113	4176	4050	4078	4079	4082	4202	4229	4109
	lb	3043	3452	2135	3067	3297	2721	4407	4620	3140
ODV	EuroNCAP Compatibility			16	26	31	23	28	34	23
ODV	NCAP Crush Work Stiffness			709	955	1501	775	1543	1760	775

While most loads for the small and mid-size ODV impacts were smaller than for the rigid wall reference scenario due to the low mass and low speed, a clear correlation was observed between compatibility and loads. The occupied LPV pulse, represented by the OLC and maximum acceleration, the toe-pan intrusion, HIC, BRIC, chest, and femur load values, all correlated with ODV compatibility. The characteristic compatibility metrics for the ODV vehicles are shown in the bottom two rows of Table 16 for the respective ODV designs. For example, the impact of the mid-size ODV baseline design with good compatibility metrics, represented by an OLC_{MPDB} of 23 and a KW400 value of 775, resulted in lower injury risk than the mid-size ODV Design 2, represented by an OLC_{MPDB} of 34 and a KW400 value of 1,760.

Figure 71 compares the crush characteristics for the impact of a tractor ODV and the Nissan Rogue at 50 km/h in the full-frontal condition. The two illustrations on the left side show a Tractor ODV striking the Nissan Rogue crash partner: red denotes the ODV with poor compatibility and green denotes good compatibility. The illustration on the right side shows a section view overlay of the crash partner toe-pan intrusion near the left and right foot. The difference in foot movement from those two impacts is highlighted using the blue arrows. Red denotes the crash partner toe-pan intrusion when struck with a poor compatibility ODV, while green denotes the crash partner toe-pan intrusion when struck with the good compatibility ODV.

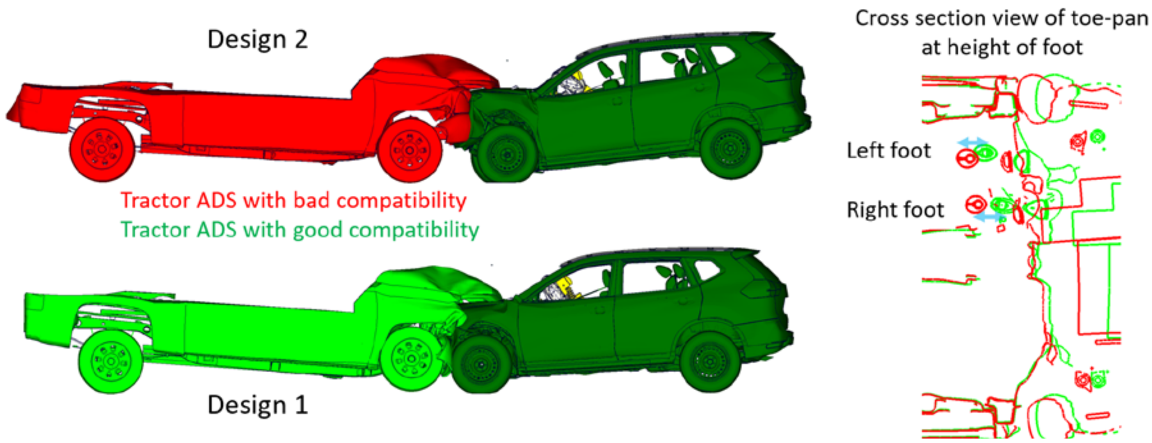

Figure 71. Tractor ODV with different compatibility characteristics striking Nissan Rogue SUV

Table 17 summarizes the characteristic values for the large and tractor ODV. Clear correlation can be observed between ODV compatibility versus SUV structural and occupant loads. Less compatible ODV designs resulted in higher deformation and higher injury risk. For example, maximum femur load increased from 1,786 N for the most compatible to 5,030 N for the least compatible large ODV design. Similarly, maximum femur load increased from 2,836 N for the most compatible to 6,132 N for the least compatible tractor ODV design, as highlighted by the orange circles.

Table 17. Small ADS with different compatibility metrics striking Nissan Rogue SUV

		Rogue to		Large ODV to				Tractor ODV to			
		rigid wall		Camry			Rogue	Rogue			Rogue
		45 km/h	50 km/h	45 km/h			30, 50 km/h	50 km/h			30, 50 km/h
				D1	BL	D2	BL	D1	BL	D2	BL
Structure	OLC - Nissan Rogue	25.8	29.7	20.9	28.8	33.3	27.4	25.5	32.2	40.1	30.8
	Max. Acc. Rogue	50.4	54.8	39.1	47.5	51.3	42.4	50.9	55.7	70.4	50.6
	Intrusion Left Foot	46	59	28	39	71	39	26	81	118	71
	Intrusion Right Foot	53	80	23	48	105	45	33	128	188	99
Occupant	HIC	192	255	151	361	458	323	360	421	961	403
	BRIC	0.75	0.8	0.7	0.79	0.72	0.81	0.89	0.8	0.62	0.8
	Chest	33	34	36	38	36	37	36	38	40	36
	Femur left	1012	2334	1124	3523	5030	3284	2826	4755	6132	5289
	Femur right	1712	1827	1786	2549	3164	2441	2336	3195	5729	2876
ODV	EuroNCAP Compatibility			28	32	36	32	25	32	38	32
ODV	NCAP Crush Work Stiffness			1524	2389	3064	2389	1690	2520	3462	2520

It was further analyzed, how an impact in which both vehicles traveled at 45 km/h and 50 km/h, compared to a scenario in which the SUV LPV traveled at 50 km/h and the ODV at 35 km/h. Structural and occupant values were in a similar range for these impact speed combinations, as documented in the columns marked with BL in Table 17. The tractor ODV-to-sedan impacts at 50 km/h showed the highest values compared to the previously analyzed ODV categories, due to the higher impact velocity. Again, clear correlation between ODV compatibility and LPV loads can be seen.

ODV-to-SUV Frontal Oblique Impact Results

NHTSA's frontal oblique offset and EuroNCAP's co-linear frontal offset test configurations were evaluated using the selected occupied Nissan Rogue FE model, as shown in Figure 72. The reference load-cases showed different structural deformation and occupant kinematics, like the observations described for the sedan vehicle class. Higher structural deformation was observed for NHTSA's oblique impact with a 2,500 kg OMDB compared to the impact with the 1,400 kg EuroNCAP MPDB. More significant head motion towards the A-pillar was seen for the oblique compared to the co-linear impact. Similarly, the maximum femur load of 4,541 N for the 85 km/h NHTSA OMDB impact into the stationary SUV was much higher than the maximum femur load of 1,788 N for the EuroNCAP configuration, where SUV and MPDB travelled at 50 km/h, as highlighted by the orange circles in Figure 72.

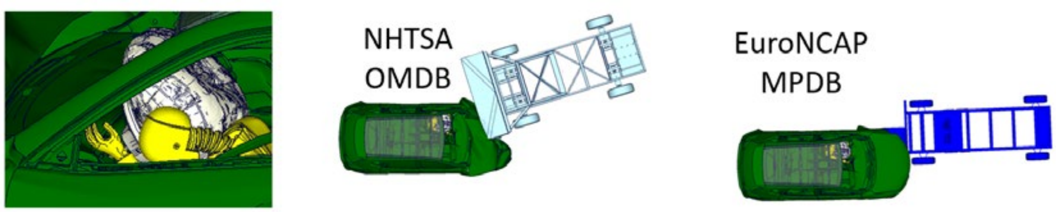

		NHTSA Oblique		EuroNCAP (both vehicles with same speed)		
		Reference		Reference		
		80 km/h	85 km/h	40 km/h	45 km/h	50 km/h
Structure	OLC - Nissan Rogue	21.2	23.5	17.2	20	23.7
	Max. Acc. Rogue	37.2	40.8	29.7	34.6	36.2
	Intrusion Left Foot	96	117	25	46	64
	Intrusion Right Foot	111	143	33	58	88
Occupant	HIC	199	370	196	213	222
	BRIC	1.05	1.19	0.9	0.92	0.9
	Chest	34	36	30	31	32
	Femur left	4073	4541	968	1199	1788
	Femur right	1812	1777	1450	1828	1882

Figure 72. Nissan Rogue SUV frontal oblique reference configurations (a) NHTSA oblique; (b) EuroNCAP MPDB

The structural and injury values tended to be smaller for the EuroNCAP test, which can mainly be attributed to the lower barrier mass. Higher impact velocities correlated with higher LPV, and occupant loads for both reference configurations, as highlighted by the blue and brown frames.

The characteristic values for the 35 km/h small and 40 km/h mid-size ODV frontal oblique impact simulations, together with two reference load cases, are summarized in Table 18.

Table 18. Small and mid-size ODV frontal oblique impact into SUV - characteristic values summary

		NHTSA Oblique	EuroNCAP	Small ODV into			Mid-size ODV into			Rogue
		Ref	Ref	Rogue			Rogue			Small ODV
		80 km/h	40 km/h	35km/h each			40 km/h each			50, 35 km/h
				BL	D1	D2	BL	D1	D2	BL
Structure	OLC - Nissan Rogue	21.2	17.2	7.5	8.8	9.1	14.2	17.9	21.3	10.2
	Max. Acc. Rogue	37.2	29.7	21.6	26.6	30.7	22.5	36.8	36.5	22.9
	Intrusion Left Foot	96	25	8	37	37	13	80	98	8
	Intrusion Right Foot	111	33	7	44	46	11	108	133	8
Occupant	HIC	199	196	51	56	60	100	188	225	80
	BRIC	1.05	0.9	0.74	0.82	0.83	0.65	0.98	0.96	0.76
	Chest	34	30	23	24	24	26	29	30	25
	Femur left	4073	968	793	1045	1075	746	2561	2557	794
	Femur right	1812	1450	1007	1110	1148	1139	1761	1924	1074
ODV	EuroNCAP Compatibility			16	26	31	23	28	34	16
ODV	NCAP Crush Work Stiffness			709	955	1501	775	1543	1760	709

Most of the Nissan Rogue's structural and occupant values were smaller than those of the reference load cases due to the lower ODV vehicle mass. A correlation between ODV compatibility and LPV loads was observed for all metrics, as highlighted by the red and blue frames. The effect of better LPV crash pulse, toe-pan intrusion, lower BRIC values and femur loads for a more compatible ODV design was more substantial for the impact with the mid-size ODV than for the small ODV due to the higher mass and impact speed. For example, the maximum toe-pan intrusion increased from 8 mm for the most compatible to 46 mm for the least compatible small ODV design, while the maximum toe-pan intrusion increased from 13 mm for the most compatible to 146 mm for the least compatible mid-size ODV design, as highlighted by the orange circles.

Figure 73 shows the vehicle deformations for the large ODV striking the occupied SUV. The less compatible large ODV Design 2, shown in red, with higher frontal structural stiffness, experienced less crush and pushed the Nissan Rogue further back compared to the large ODV Design 1, shown in green, with good compatibility characteristics.

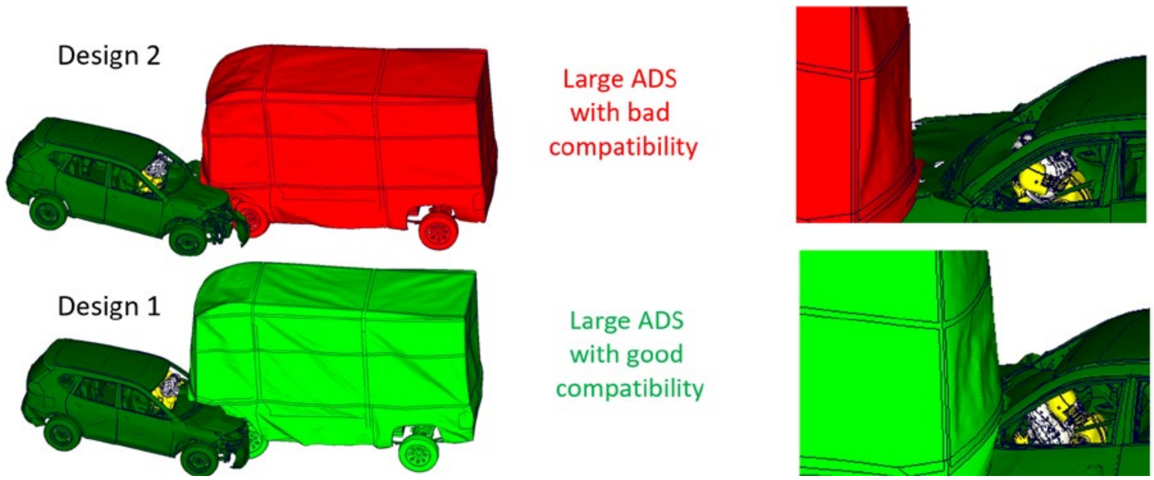

Figure 73. Frontal oblique impact - large ODV-to-SUV

LPV damage for all conducted simulations with the large and tractor ODV was higher compared to the impacts with the small and mid-size ODV, due to the higher mass and impact velocity. Occupant kinematics like NHTSA's oblique impact configuration were observed, characterized by head trajectory directed toward the A-pillar. This was more significant for the impact with the less compatible large ODV, shown in red, due to the more severe vehicle pulse, as illustrated by the snapshots on the right in Figure 73.

Large ODV compatibility significantly affected toe-pan intrusion. The impact with the less compatible Design 2, shown in red, resulted in visibly higher intrusion and pushed the feet further back, as illustrated by the blue arrows in the cross-section view, shown in Figure 74.

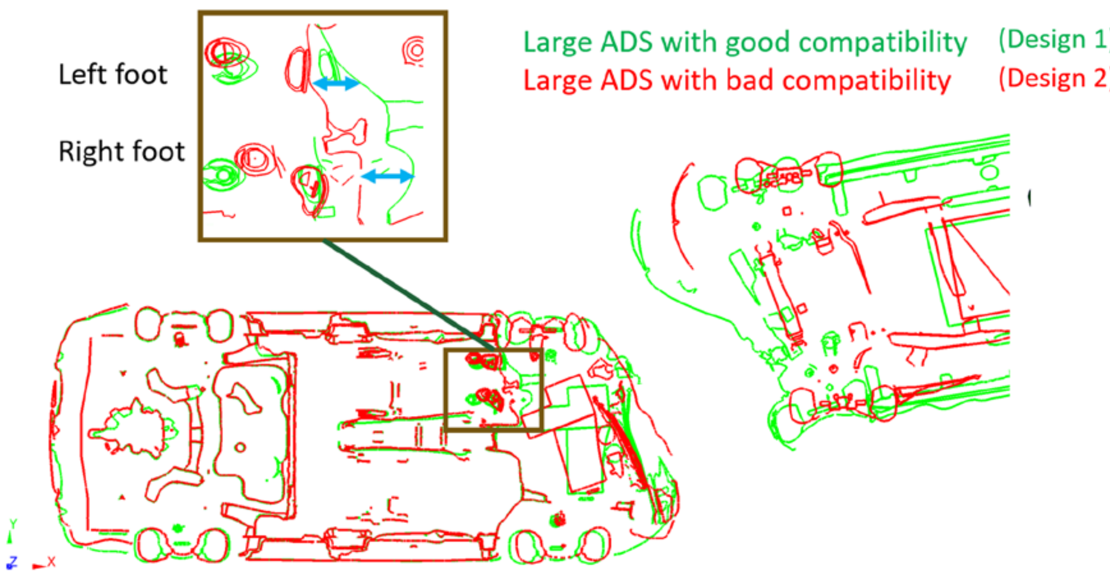

Figure 74. Frontal oblique impact - large ODV-to-SUV cross-section view

Characteristic values for the 45 km/h large, the 50 km/h tractor ODV frontal oblique impact simulations, and two reference load cases are summarized in Table 19.

Table 19. Large and tractor ODV frontal oblique impact into SUV - characteristic values summary

		NHTSA Oblique	EuroNCAP	Large ODV into			Tractor ODV into			Tractor 35 km/h
		Reference	Reference	Rogue			Rogue			into
		85 km/h	50 km/h	45 km/h each			50 km/h each			Rogue 50 km/h
				D1	BL	D2	D1	BL	D2	BL
Structure	OLC - Nissan Rogue	23.5	23.7	19.6	19.6	22.3	18.6	22.7	29.5	16.3
	Max. Acc. Rogue	40.8	36.2	29.6	30.8	35.7	27.7	29.9	41	22.3
	Intrusion Left Foot	117	64	34	127	143	66	103	211	54
	Intrusion Right Foot	143	88	32	139	167	77	127	298	54
Occupant	HIC	370	222	213	224	316	190	235	671	156
	BRIC	1.19	0.9	0.72	0.98	1.01	1	1.05	1.35	0.88
	Chest	36	32	33	31	33	30	32	36	29
	Femur left	4541	1788	1063	4677	5504	2212	4674	4990	1736
	Femur right	1777	1882	1622	1717	1733	1585	1883	6514	1464
ODV	EuroNCAP Compatibility OLC [g]			28	32	36	25	32	38	25
ODV	NCAP Crush Work Stiffness KW400 [kN/mm]			1524	2389	3064	1690	32	3462	1690

Structural and occupant loads clearly correlated with ODV compatibility characteristics. The effect is clearly documented by the characteristic values for the toe-pan intrusion, BRIC, and femur loads, as highlighted by the red, blue, and brown frames. For example, maximum toe-pan intrusion increased from 34 mm for the most compatible large ODV Design 1 to 167 mm for the least compatible large ODV Design 2. Similarly, the maximum toe-pan intrusion increased from 77 mm for the most compatible tractor ODV Design 1 to 298 mm for the least compatible tractor ODV Design 2, highlighted by the orange circles in Table 19. In addition to the compatibility analyses, an impact of the baseline tractor ODV traveling at 35 km/h with the Nissan Rogue traveling at 50 km/h was simulated. Results, shown in the rightmost column, were lower than for the scenario in which both vehicles traveled at 50 km/h, as expected.

SUV Side Impact Results

As was done for the frontal impact conditions, existing side impact crash test configurations were used to determine reference values for the ODV-to-SUV side impact studies. The NHTSA crabbed MDB, as well as the IIHS MDB side impact configurations, were simulated, as shown in Table 20.

Table 20. SUV side impact references (a) NHTSA MDB; (b) IIHS MDB

		MDB 40	MDB 45	MDB 53	MDB 62	IIHS 1900 40	IIHS 1500 45	IIHS 1900 45	IIHS 1500 50
		Ref	Ref	Ref	Ref	Ref	Ref	Ref	Ref
Occupant	HIC	20	25	33	45	132	178	191	310
	BRIC	0.57	0.63	0.69	0.79	0.69	0.75	0.69	0.87
	Thorax [mm]	10	10	10	10	17	21	34	32
	Abdomen [mm]	8	10	12	17	16	21	33	31
Structure	Roof [mm]	16	17	23	29	92	116	139	153
	Door Thorax [mm]	34	38	62	75	189	214	239	260
	Door Pelvis [mm]	104	120	158	191	234	249	260	271
	B-Pillar [m/s]	5.7	6.6	7.2	8.1	7.8	8.7	9	9.6
	CG [m/s]	4.7	5.2	6.2	7	6.1	6	6.6	6.7
						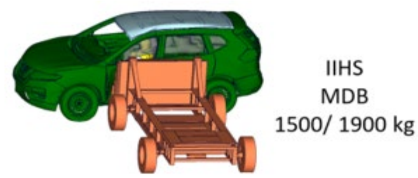			

The IIHS barrier has a higher honeycomb face compared to NHTSA's MDB. Like the sedan reference study, higher structural deformation of the B-pillar and roof can be observed for the IIHS conditions due to greater height and mass compared to NHTSA's MDB.

Table 20 also summarizes the occupant and structural characteristic values for the NHTSA and IIHS MDB impact into the Nissan Rogue, occupied by a 50th percentile WorldSID dummy positioned on the front driver seat. Higher impact speed and higher MDB mass correlated with higher vehicle deformation at the door and the roof. Absolute B-pillar velocity also clearly indicated the higher structural loads caused by the higher impact speeds and higher barrier mass. Consequently, higher occupant injury values were observed for the impacts with the IIHS barrier compared to NHTSA's MDB. For example, a maximum chest deflection was recorded for NHTSA MDB impact, while the maximum chest compression was 21 mm and 34 mm for the 1,500 kg and 1,900 kg IIHS MDB impacts.

Figure 75 (a) and (b) show the side impact of the small ODV traveling at 35 km/h and the mid-size ODV striking the stationary Nissan Rogue at 40 km/h. Compared to the side impact reference configurations, less vehicle damage was observed, especially for the small ODV striking vehicle, due to the lower mass. Exterior crush was higher for the mid-size ODV than for the small ODV, due to the higher vehicle mass. The Nissan Rogue SUV has a higher sill compared to the Toyota Camry sedan, and impact loads were therefore mainly transferred into the rocker and floor components.

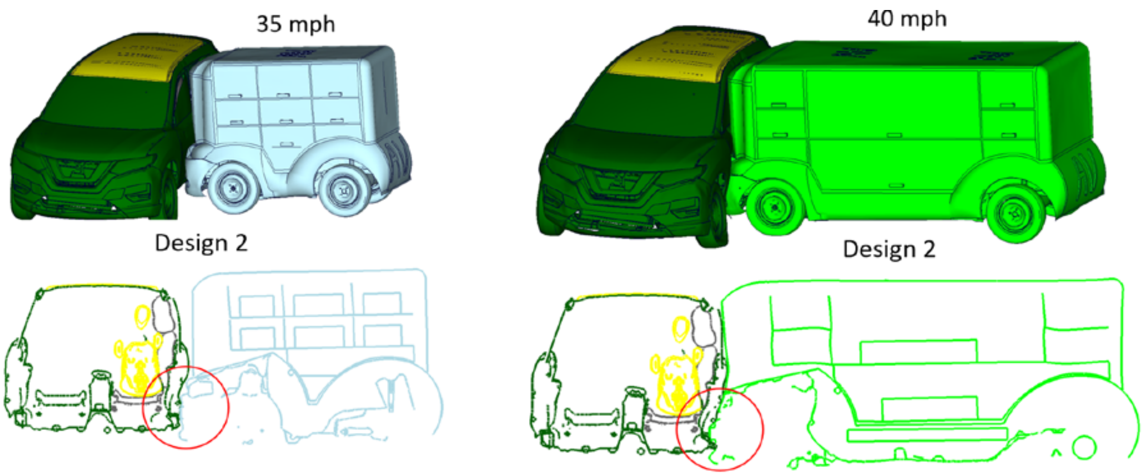

Figure 75. SUV side impact (a) small ODV Design 2 at 35 km/h; (b) mid-size ODV Design 2 at 40 km/h

Table 21 summarizes the characteristic values for the impact with the small and mid-size ODV with different compatibility characteristics, as well as two reference simulations.

Table 21. Small and mid-size ODV side impact into SUV - characteristic values

		MDB 40	**IIHS 1900 40**	**Small ODV into**			**Mid ODV into**		
		Ref	Ref	Rogue at 35 km/h			Rogue at 40 km/h		
				BL	D1	D2	BL	D1	D2
Occupant	HIC	20	132	2	3	3	16	16	30
	BRIC	0.57	0.69	0.22	0.22	0.21	0.44	0.31	0.37
	Thorax [mm]	10	17	10	10	10	10	10	10
	Abdomen [mm]	8	16	4	4	4	15	8	18
Structure	Roof [mm]	16	92	14	15	15	12	20	20
	Door Thorax [mm]	34	189	49	53	57	40	67	77
	Door Pelvis [mm]	104	234	148	175	179	107	179	190
	B-Pillar [m/s]	5.7	7.8	4.9	5.4	5.5	5.6	6.4	6.5
	CG [m/s]	4.7	6.1	3.7	3.7	3.7	5.3	5.9	6.9
ODV	EuroNCAP Compatibility			16	26	31	23	28	34
	NCAP Crush Work Stiffness			709	955	1501	775	1543	1760

Differences in structural and occupant loads were not substantial for the impact with the small ODV variations at 35 km/h, due to low ODV mass. For the mid-size ODV, a clear correlation between ODV compatibility and LPV loads was observed. Maximum exterior crush at the height of the pelvis was 107 mm for the mid-size ODV baseline model with good compatibility and 190 mm for the less compatible Design 2. Similarly, maximum exterior crush at the door at the height of the thorax increased from 40 mm to 77 mm. Maximum absolute B-pillar velocity increased from 5.3 m/s to 6.9 m/s. Occupant loads were relatively small and were mainly controlled by restraints and interiors, due to the high seating position above the main load path at the height of the rocker.

The occupied SUV LPV was then struck by the large ODV and tractor ODV with different frontal impact compatibility characteristics. Figure 76 shows a deformed state for the impact with the less compatible large ODV Design 2 on the top and for the impact with the more compatible large ODV Design 1 on the bottom.

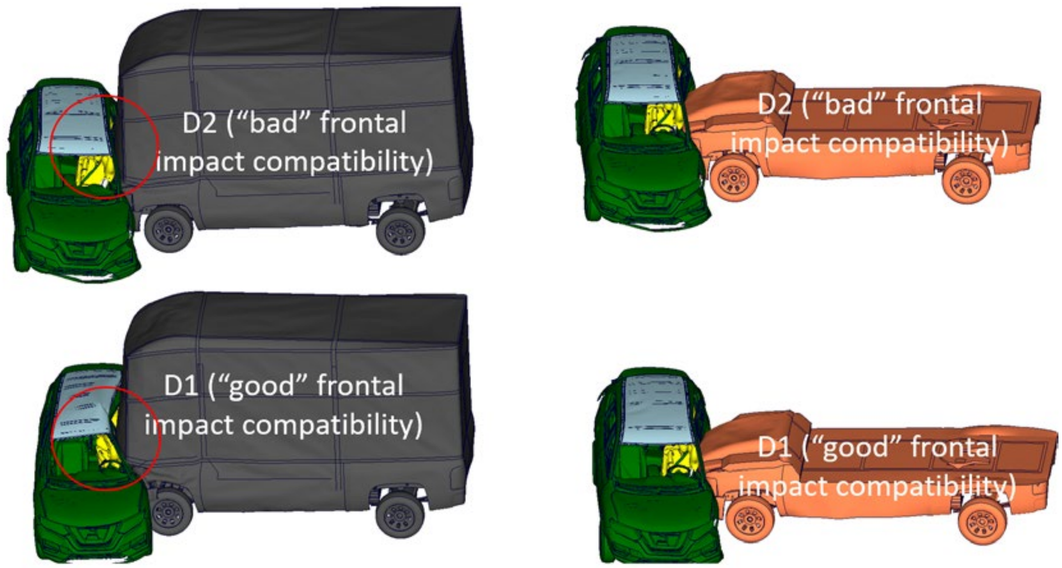

Figure 76. (a) large and (b) Tractor ODV striking Nissan Rogue SUV

Note that the less compatible large ODV Design 2 with a stiff frontal vehicle structure showed little ODV deformation. It interacted with the LPV at the sill and door areas, pushing the SUV in lateral direction. In contrast, the more compatible (with respect to frontal impact compatibility metrics) large ODV Design 1 with a softer lower frontal vehicle structure experienced more deformation, indicated by the small distance between the ODV wheels and the LPV. Consequently, a more substantial interaction of the ODV upper structure and the SUV upper B-pillar and roof areas occurred, resulting in visible exterior crush, and buckling of the roof, highlighted by the red circles in Figure 76 (a).

This observation agrees with the Toyota Camry sedan side impact study, outlined in Chapter 7, and is specific to the large ODV due to the high frontal vehicle structure and the specific frontal structure characteristics. The side impact with the tractor ODV striking the stationary Nissan Rogue is shown in Figure 76 (b). No direct contact with the roof occurred due to the smaller height of the tractor ODV compared to the large ODV.

Figure 77 visualizes the different deformation characteristics for the impact with the large ODV designs using a cross section view. The different structural deformation of the longitudinal rails and the resulting difference in loading of the roof of the SUV due to the interaction with the upper frontal section of the ODV, can be clearly seen, as highlighted by the red circles.

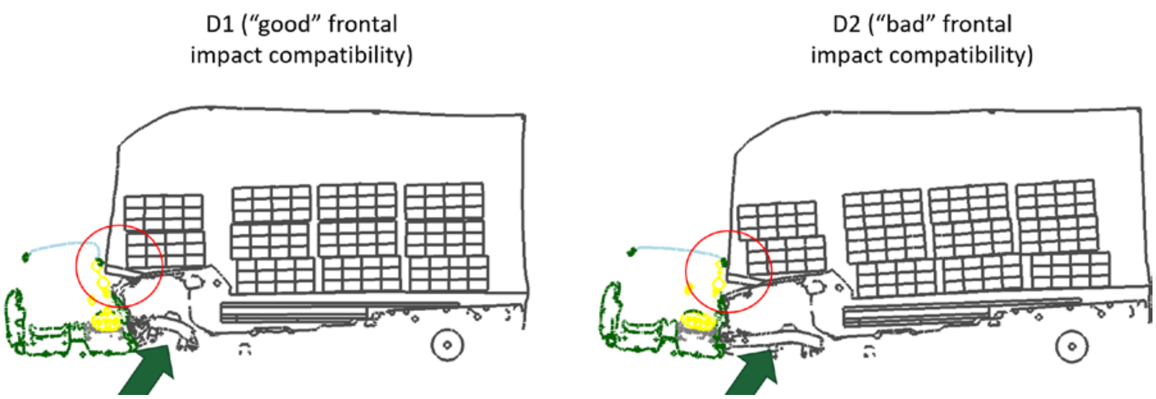

Figure 77. Large ODV-to-SUV cross section view (a) Design 1; (b) Design 2

Table 22 summarizes the characteristic values for the side impact of the Nissan Rogue with the large and tractor ODV with different compatibility metrics and three MDB references.

Table 22. Large and tractor ODV side impact into SUV - characteristic values summary

		MDB	**IIHS 1500**	**IIHS 1900**	**Large ODV into**			**Tractor ODV into**		
		45 km/h	45 km/h	45 km/h	Rogue at 45 km/h			Rogue at 45 km/h		
		Ref	Ref	Ref	D1	BL	D2	D1	BL	D2
Occupant	HIC	25	178	191	658	251	166	126	176	190
	BRIC	0.63	0.75	0.69	0.87	0.72	0.56	0.59	0.66	0.68
	Thorax [mm]	10	21	34	32	28	17	25	35	32
	Abdomen [mm]	10	21	33	27	31	25	27	33	34
Structure	Roof [mm]	17	116	139	308	58	39	54	55	51
	Door Thorax [mm]	38	214	239	300	214	196	195	217	219
	Door Pelvis [mm]	120	249	260	184	309	309	261	291	321
	B-Pillar [m/s]	6.6	8.7	9	8.4	10	8.8	9.3	11	9.5
	CG [m/s]	5.2	6	6.6	7.1	8.9	8.6	7.9	9.4	9.6
ODV	EuroNCAP Compatibility				32	34	36	25	32	38
	NCAP Crush Work Stiffness				1524	2389	3064	1690	2520	3462

Structural and occupant values for the impact with the large and tractor ODV were lower than for the impacts into the Toyota Camry sedan, due to the higher seating position within the SUV and more load transferring into the sill and floor of the SUV.

The results for the large ODV are an exception to the previous findings for the frontal impact configurations and the side impact with the small, mid-size, and tractor ODV. An opposite trend with respect to roof deformation and head injury risk was observed. Higher exterior crush was recorded in the roof area for the large ODV Design 1 with good frontal impact compatibility characteristics. A maximum exterior crush at the roof of 308 mm was recorded for the more compatible Design 1, and a maximum exterior crush of 39 mm was recorded for the less compatible Design 2. Consequently, a higher HIC value of 658 was recorded for the impact with large ODV Design 1 compared to an HIC value of 166 for the less (frontal impact) compatible Design 2. The specific case indicated that good frontal impact compatibility does not necessarily provide good side impact compatibility for all body regions, especially for higher striking vehicles.

8. Conclusion

A thorough compatibility research study was conducted for ODV that are focused on transporting cargo instead of occupants. The approach to study how variations in an ODV vehicle's design can affect the occupants in an occupied crash partner vehicle, across a range of expected ODDs is summarized in Figure 78.

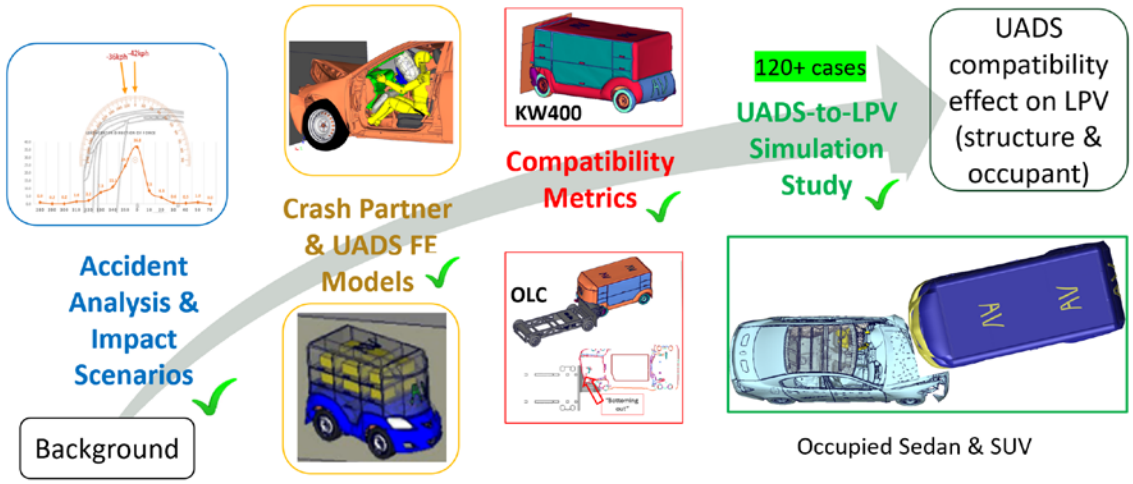

Figure 78. Research approach: crash compatibility evaluations for ODV

First, crash data and existing crash test configurations were analyzed to determine the most appropriate impact configurations for these new types of vehicles. Full frontal, frontal oblique, and perpendicular side impact crash configurations were determined as relevant ODV-to-LPV crash scenarios. Impact scenarios were found to be like existing crash test configurations, such as the NCAP frontal impact, NHTSA side impact, and NHTSA's frontal oblique impact.

Second, existing FE models representing a wide spectrum of ODV categories, ranging from small ODV for grocery delivery to large and tractor ODV for heavy cargo delivery, were selected. Three variations, including the baseline FE model, with different frontal structure compatibility were developed for each of the four ODV categories, capturing different geometry, mass, and stiffness characteristics. Objective metrics, OLC and KW400, were used to develop the ODV variations. Representative occupied 2015 Toyota Camry sedan and 2020 Nissan Rogue SUV crash partner FE models were selected.

Third, a comprehensive simulation study, consisting of more than 120 ODV-to-LPV simulations was conducted. Recorded occupant and structural loads were used to demonstrate, what effect ODV compatibility can have when striking an occupied crash partner vehicle. Respective results from existing crash test configurations were provided for reference.

It was found that better ODV compatibility correlated well with better LPV crash pulses, lower occupant compartment intrusions, and lower occupant injury risk for all four ODV categories, in full frontal and frontal oblique impact configurations. Optimized ODV frontal stiffness characteristics and reduced ODV vehicle mass correlated with better compatibility and reduced crash partner occupant and structural loads.

Better ODV compatibility also correlated with less LPV structural damage and lower occupant injury risk for three of the four ODV categories in side impact. Large and high ODV with a more compatible lower frontal structure and a relatively stiff upper frontal structure produced higher roof deformation and higher head injury risk in the crash partner LPVs.

In addition to reducing ODV mass, existing compatibility metrics, known from traditional vehicles, were found to be suitable for quantifying and optimizing ODV compatibility. These include (1) geometrical metrics, such as the bumper height standard, defined in 49 CFR Part 581; (2) criteria for evaluating potential secondary energy-absorbing structures, defined for NHTSA's ORB barrier test; (3) OLC and compatibility assessment based on EuroNCAP's MPDB configuration; and (4) KW400 derived from NHTSA full overlap rigid wall impact.

While ODV may not need to protect internal occupants, they will likely be designed to protect their cargo, and they do need to interact with other road vehicles. It was found that their mass, design, and structural compatibility can have a substantial effect when colliding with an occupied crash partner vehicle.

Literature Search and References

Citations preceded by an asterisk were found in the literature review.

49 CFR Part 581 - Bumper Standard, May 12, 1997.

* Abraham, H., Reimer, B., & Mehler, B. (2017, October 9-13). *Advanced Driver Assistance Systems (ADAS): A consideration of driver perceptions on training, usage & implementation.* Human Factors and Ergonomics Society 2017 Annual Meeting, Austin, Texas.

* Alliance of Automobile Manufacturers. (2003). *Enhancing vehicle-to-vehicle crash compatibility: A set of commitment for progress by automobile manufacturers.*

* Barbat, S., Li, X., Reagan, S., & Prasad. (2007, June 18-21). *Vehicle compatibility assessment using test data of full frontal vehicle-to-vehicle and vehicle-to-full width deformable barrier impacts* (Paper number 07-0348). 20th International Technical Conference on the Enhanced Safety of Vehicles, Lyon, France. www-esv.nhtsa.dot.gov/Proceedings/20/07-0348-O.pdf

Benito Cia, L., Mospak, C., & Kaulich, C. (2020, June 10-11). *MPDB Pre- and postprocessing in Animator4 and Generator4*. LS-DYNA Conference 2020. 16th International LS-DYNA Users Conference, Detroit, MI.

* Benmimoun, M., Pütz, A., Zlocki, A., & Eckstein, L. (2013). *Wirkungsanalyse von Abstandsregelung und Abstandswarnung* [Impact analysis of distance control and distance warning]*, ATZ-Automobiltechnische Zeitschrift, 115* (4), 336-342.

* Brewer, J., Patel, S., Summers, S., Prasad, A., Mohan, P. (2011, June 13-16). *Accuracy of AHOF400 with a moment-measuring load cell barrier* (Paper No. 11-0335). 22nd Enhanced Safety of Vehicles, Washington, DC.

Center for Collision Safety and Analysis. (n.d.). *Vehicle modeling* [Web page].

Davies, A. (2018, September 11). *A shape-shifting van concept prepares Mercedes for the future: It's a cargo van! It's a passenger van! It's the Vision Urbanetic, and it's part of Mercedes' bid for the future of transportation* [Web page]. Wired.com. www.wired.com/story/mercedes-vision-urbanetic-concept-van

* Delannoy, P., Faure, J., Coulombier, D., Zeitouni, R., Martin, T. (2004, November 30-December 2). *New barrier test and assessment protocol to control compatibility* (SAE Technical Paper 2004-01-1171). SAE 2004 World Congress & Exhibition, Dearborn, MI.

Ellway, J. (2019, June). *Compatibility assessment,* Version 1.1 Report No. TB 027). European New Car Assessment Programme (Euro NCAP). https://cdn.euroncap.com/media/53017/tb-027-compatiblity-assessment-v11.pdf

* Enhanced Vehicle-to-Vehicle Crash Compatibility Technical Working Group. (2009, April 16). *Report on voluntary industry effort to further enhance front-to-front vehicle crash compatibility*. Insurance Institute for Highway Safety, Alliance of Automobile Manufacturers, & Association of International Automobile Manufacturers. https://downloads.regulations.gov/NHTSA-2003-14623-0100/attachment_2.pdf

European New Car Assessment Programme. (2019, October). *MPDB* [mobile progressive deformable barrier] *frontal impact testing protocol, Version 1.1.1* [Implementation January 1, 2020]. https://cdn.euroncap.com/media/55858/euro-ncap-mpdb-testing-protocol-v111.pdf

Federal Highway Administration. (2016). *Next generation simulation (NGSIM) vehicle trajectories and supporting data.* [Dataset]. http://doi.org/10.21949/1504477

FHWA. (2022). *CARMA Products* [Web page and portal]. https://highways.dot.gov/research/research-programs/operations/CARMA/design-and-architecture

* Hobbs, C. A. (1998. May 29–June 1). *The influence of car structures and padding on side impact injuries.* 12th International Technical Conference on Experimental Safety Vehicles, Göteborg, Sweden.

* Insurance Institute for Highway Safety, Alliance of Automobile Manufacturers, & Association of International Automobile Manufacturers. (2006, May 16). *Enhancing vehicle-to-vehicle crash compatibility: Commitment for continued progress by leading automakers*. [Correspondence]. [Docket submission, Document ID NHTSA-2003-14623-0035-0001 in Regulations.gov] https://downloads.regulations.gov/NHTSA-2003-14623-0035-0001/attachment_1.pdf and www.regulations.gov/document/NHTSA-2003-14623-0035-0001

IIHS. (2014, May). *Side impact crashworthiness evaluation: guidelines for rating injury measures, Version III.*

Janovicz, D., & Fischer, B. (2011, December 12). New Car Assessment Program Side Impact MDB Testing of a 2012 Toyota Camry LE 4-Dr Sedan; NHTSA No.: YC5101 (Report No. SINCAP-MGA-2012-026, a.k.a. NHTSA test 7517). National Highway Traffic Safety Administration. https://nrd-static.nhtsa.dot.gov/reports/vehdb/v00000/-v07500/v07517R001.pdf

* Jenness, J., Lerner, N., Mazor, S., Osberg, J., & Tefft, B. (2008, March). *Use of advanced in-vehicle technology by young and older early adopters: Survey results on adaptive cruise control systems* (Report No. DOT HS 810 917). National Highway Traffic Safety Administration. (2008). https://citeseerx.ist.psu.edu/viewdoc/download?doi=-10.1.1.173.3775&rep=rep1&type=pdf

* Liers, H., & Unger, T. (2019, September 11-13). *Prediction of the expected crash scenario of future Level 2 and Level 3 cars on German motorways.* International Research Council on the Biomechanics of Injury Conference, Florence, Italy.

* Mohan, P. (2007, May 15). *NHTSA compatibility crash test update: Vehicle crash test program on compatibility in front-to-front impacts* [PowerPoint]. 2007 SAE Government/Industry Meeting, Washington, DC.

* Mohan, P., Marzougui, D., & Kan, C.-D. (2007, April 16-19). *Modified approach to accurately measure height of force (HOF)* (Paper Number 2007-01-1182). SAE World Congress, Detroit, MI. Also published in *Vehicle Aggressivity & Compatibility in Automotive Crashes* (Paper No. 2007-SP-2136). SAE 2007 Transactions Journal of Passenger Cars: Mechanical Systems-V116-6.

* Mohan, P., & Smith, D. L. (2007, June 18-21.) *Finite element analysis of compatibility metrics in frontal collisions* (Paper Number 07-0188). 20th International Technical Conference on the Enhanced Safety of Vehicles, Lyon, France.

* National Highway Traffic Safety Administration. (1990, April 25). *Laboratory test procedure for Regulation Part 581 - Bumper standard* (Report No. TP-581-01. www.nhtsa.gov/sites/nhtsa.gov/files/tp-581-01.pdf

NHTSA. (2015, December 16). *New Car Assessment Program request for comment*. [Docket submission, Document ID NHTSA-2015-0119 in Regulations.gov]. https://www.regulations.gov/document/NHTSA-2015-0119-0001

* NHTSA. (2017, September). *Automated Driving Systems 2.0 - A vision for safety* (Report No. DOT HS 812 442). www.nhtsa.gov/sites/nhtsa.gov/files/documents/13069a-ads2.0_-090617_v9a_tag.pdf

Nuro. (2018). *Delivering safety: Nuro's approach*. https://dokumen.tips/documents/delivering-safety-nuroas-approach-it-never-gets-distracted-in-the-us-more-than.html

* Östling, M., Jeppsson, H., & Lubbe, N.. (2019, September 11-13). *Predicting crash configurations in passenger car to passenger car crashes to guide the development of future passenger car safety* (Paper No. IRC-19-92). International Research Council on the Biomechanics of Injury Conference, Florence, Italy. www.ircobi.org/wordpress/downloads/irc19/pdf-files/92.pdf

* Patel, S., Prasad, A., & Mohan, P. (2009, June 15-18). *NHTSA's Recent test program on vehicle compatibility* (Paper No.). Proceedings of the 21st International Technical Conference on the Enhanced Safety of Vehicles, Stuttgart, Germany.

* Patel, S., Smith, D. L., Prasad, A., & Mohan, P. (2007, June 18-21). *NHTSA's recent vehicle crash test program on compatibility in front-to-front impacts* (Paper Number 07-0231). 20th International Technical Conference on the Enhanced Safety of Vehicles, Lyon, France.

* Pereira, M., Beggiato, M., & Petzoldt, T. (2015). Use of adaptive cruise control functions on motorways and urban roads: Changes over time in an on-road study. *Applied Ergonomics, 50*:105 -112.

* Powell, N. J., Preuss, M., & Lund. (1999, October 25-27). *Factors contributing to front-side compatibility – a comparison of crash test results.* 43rd Stapp Conference, Warrendale, PA.

Reichert, R., & Kan, S. (2017, May 9-11). *Development of a 2015 mid-size sedan vehicle model*. 11th European LS-DYNA Conference 2017, Salzburg, Austria. www.dynalook.com/-conferences/11th-european-ls-dyna-conference/crash-model-building/development-of-a-2015-mid-size-sedan-vehicle-model

Reichert, R., Kan, C.-D., & Park, C.-K. (2022, September). *Crash simulation of FMVSS No. 214 safety performance* (Report No. DOT HS 813 276). National Highway Traffic Safety Administration. https://rosap.ntl.bts.gov/view/dot/63424

Reichert, R., Marzougui, D., & Kan, C.-D. (2020, June). *Crash simulations between non-occupied automated driving systems and roadside hardware* (Report No. DOT HS 812 871). National Highway Traffic Safety Administration. https://rosap.ntl.bts.gov/view/dot/54288/dot_54288_DS1.pdf

Sawers, P. (2017, July 4). *Einride debuts prototype T-pod, an autonomous electric truck that can also be controlled remotely* [Web page]. VentureBeat. https://venturebeat.com/transportation/swedens-einride-debuts-prototype-t-pod-an-autonomous-electric-truck-that-can-also-be-controlled-remotely/

Sawers, P. (2019, June 13). *Volvo's Vera autonomous trucks will transport DFDS goods on public roads* [Web page]. VentureBeat. https://venturebeat.com/ai/volvos-vera-autonomous-trucks-will-transport-dfds-goods-on-public-roads/

* Side Airbag Out-of-Position Injury Technical Working Group. (2003, July). *Recommended procedures for evaluating occupant injury risk from deploying side airbags.* Alliance of Automobile Manufacturers, Association of International Automobile Manufacturers, Automotive Occupant Restraints Council, & Insurance Institute for Highway Safety. www.iihs.org/media/020f855e-79e2-4f5c-b560-3ccc991bdfb2/0tCvYA/Ratings/-Protocols/current/twg_final_procedures.pdf

* Subramaniam, K., Verma, M., Nagappala, R., Tedesco, R., & Carlin, L. (2007, June 18-21). *Evaluation of stiffness matching concepts for vehicle safety improvement* (Paper Number 07-00112). 20th International Technical Conference on the Enhanced Safety of Vehicles, Lyon, France.

* Teoh, E. R., & Nolan, J. M. (2012). *Is passenger vehicle incompatibility still a problem? Traffic Injury Prevention, 13*:585-591.

Transportation Research Center Inc. (2016a, June 20). New Car Assessment Program (NCAP) side impact MDB test: Nissan Motor Co., LTD., 2016 Nissan Rogue S AWD (TRC Test No. 160426; a.k.a. NHTSA test 9786). National Highway Traffic Safety Administration. https://nrd-static.nhtsa.dot.gov/reports/vehdb/v00000/v09700/v09786R001.pdf

Transportation Research Center Inc. (2016b, July 30). New Car Assessment Program (NCAP) side impact pole test: Nissan Motor Co., LTD., 2016 Nissan Rogue S AWD (TRC Test No. 160329; a.k.a. NHTSA test 9780 . National Highway Traffic Safety Administration. https://nrd-static.nhtsa.dot.gov/reports/vehdb/v00000/v09700/v09780R001.pdf

* Trübswetter, N. M. (2015). *Akzeptanzkriterien und Nutzungsbarrieren älterer Autofahrer im Umgang mit Fahrerassistenzsystemen* [Acceptance criteria and barriers to use for older drivers when dealing with driver assistance systems] [Dissertation]. Technische Universität München.

Walsh, V. (2015, February 19). Moving barrier to vehicle crash test in support of NHTSA's frontal oblique offset program research moving deformable barrier into left front of a 2014 Toyota Camry 90.1kph, 15 degree angle, 35% overlap (Report No. R&D-CAL-14-004, NHTSA No. R2014414, a.k.a. NHTSA test# 8790). National Highway Traffic Safety Administration. https://nrd-static.nhtsa.dot.gov/reports/vehdb/v00000/-v08700/v08790R002.pdf

Walsh, V., & Dutton, E. (March 31, 2014, March 31). *New Car Assessment Program (NCAP) frontal barrier impact test* (Report No. NCAP-CAL-14-009). National Highway Traffic Safety Administration. https://nrd-static.nhtsa.dot.gov/reports/vehdb/v00000/v08500-/v08545R001.pdf

Wyoming Department of Transportation. (2018, Oct. 31). *WYDOT moves forward with new safety communication technology for vehicles* [Web page]. https://www.dot.state.wy.us/news/wydot-moves-forward-with-new-safety-communication-technology-for-vehic

This page intentionally left blank.

Appendix A: ODV Model Variation Details

Table A-1. Small ODV Structural Changes Design 1 Versus Baseline Model

Small UADS (Baseline; 804 kg)					Small UADS (Design 1; 812 kg)			
Part Image	Part ID	Yield Stength [N/mm^2]	Thickness [mm]		Part Image	Part ID	Yield Stength [N/mm^2]	Thicknes s [mm]
	2000161	270	1.1			2000161	n/a	3.0
	2000178	270	0.9			2000178	1000	0.9
	2000181	270	1.2			2000181	1000	1.2
	2000182	270	1.2			2000182	1000	1.2
	2000215	270	0.7			2000215	1000	0.7
	2000219	270	0.7			2000219	1000	0.7
	2000220	270	3.8			2000220	1000	3.8
	2000221	380	1.9			2000221	1000	3.0
	2000222	380	1.9			2000222	1000	3.0
	2000223	270	4.2			2000223	1000	4.2
	2000232	800	2.3			2000232	800	3.0
	2000233	270	0.9			2000233	1000	3.0
	2000234	270	0.9			2000234	1000	3.0
	2000235	270	2.4			2000235	1000	2.4
	2000237	270	1.4			2000237	1000	1.4
	2000238	380	1.3			2000238	1000	3.0
	2000239	270	0.8			2000239	1000	0.8
	2000242	380	1.3			2000242	1000	3.0
	2000244	180	0.9			2000244	n/a	3.0
	2000245	180	0.9			2000245	n/a	3.0
	2000248	270	1.5			2000248	1000	1.5
	2000257	270	1.6			2000257	1000	1.6
	2000263	380	1.7			2000263	1000	3.0
	2000264	350	1.8			2000264	n/a	3.0
	2000266	350	1.9			2000266	n/a	3.0
	2000268	380	1.7			2000268	1000	3.0

Table A-2. Small ODV Structural Changes Design 2 Versus Baseline Model

Small UADS (Baseline; 804 kg)					Small UADS (Design 2; 834 kg)			
Part Image	Part ID	Yield Stength [N/mm^2]	Thickness [mm]		Part Image	Part ID	Yield Stength [N/mm^2]	Thicknes s [mm]
	2000161	270	1.1			2000161	n/a	5.0
	2000178	270	0.9			2000178	1000	0.9
	2000181	270	1.2			2000181	1000	1.2
	2000182	270	1.2			2000182	1000	1.2
	2000215	270	0.7			2000215	1000	0.7
	2000219	270	0.7			2000219	1000	0.7
	2000220	270	3.8			2000220	1000	3.8
	2000221	380	1.9			2000221	1000	5.0
	2000222	380	1.9			2000222	1000	5.0
	2000223	270	4.2			2000223	1000	4.2
	2000232	800	2.3			2000232	800	5.0
	2000233	270	0.9			2000233	1000	5.0
	2000234	270	0.9			2000234	1000	5.0
	2000235	270	2.4			2000235	1000	2.4
	2000237	270	1.4			2000237	1000	1.4
	2000238	380	1.3			2000238	1000	5.0
	2000239	270	0.8			2000239	1000	0.8
	2000242	380	1.3			2000242	1000	5.0
	2000244	180	0.9			2000244	n/a	5.0
	2000245	180	0.9			2000245	n/a	5.0
	2000248	270	1.5			2000248	1000	1.5
	2000257	270	1.6			2000257	1000	1.6
	2000263	380	1.7			2000263	1000	5.0
	2000264	350	1.8			2000264	n/a	5.0
	2000266	350	1.9			2000266	n/a	5.0
	2000268	380	1.7			2000268	1000	5.0
	2000268	380	1.7			2000268	1000	3.0

Table A-3. Mid-size ODV Structural Changes Design 1 Versus Baseline Model

Mid-size UADS (Baseline; 1467 kg)				Mid-size UADS (Design 1; 1513 kg)		
Part Image	**Part ID**	**Thickness [mm]**		**Part Image**	**Part ID**	**Thickness [mm]**
	2100166	1.9			2100166	8.0
	2100167	1.9			2100167	8.0
	2100174	2.3			2100174	8.0
	2100180	1.3			2100180	8.0
	2100184	1.3			2100184	8.0
	2100201	1.7			2100201	8.0
	2100206	1.7			2100206	8.0

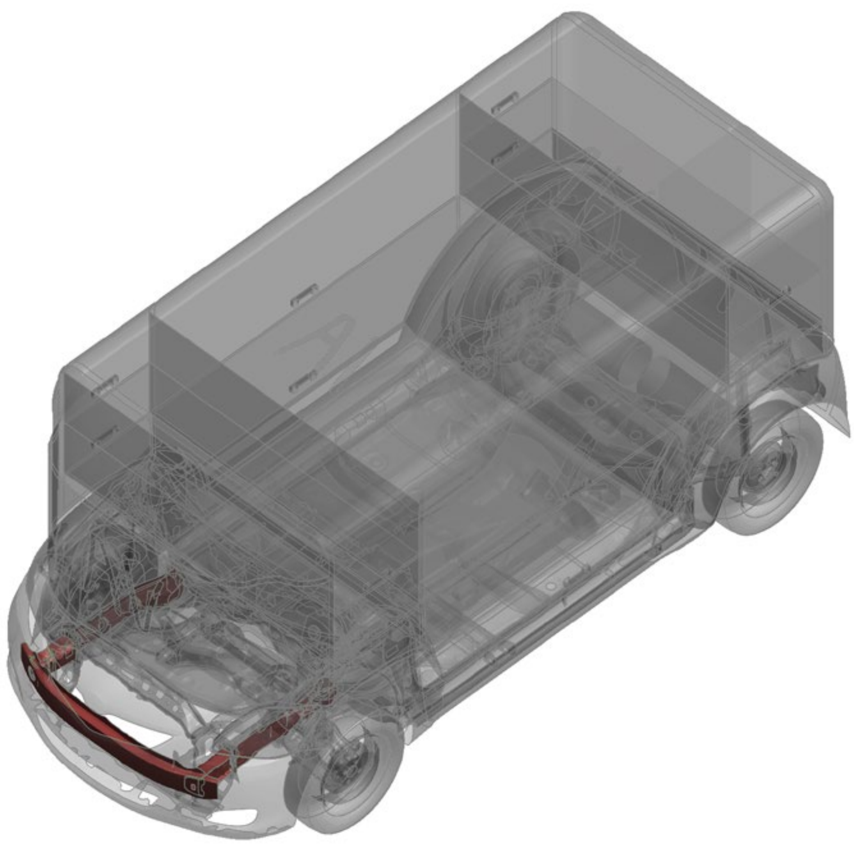

Table A-4. Large ODV Structural Changes Design 1 Versus Baseline Model

Large UADS (Baseline; 4000 kg)					Large UADS (Design 1; 3810 kg)			
Part Image	Part ID	Yield Stength [N/mm^2]	Thickness [mm]		Part Image	Part ID	Yield Stength [N/mm^2]	Thicknes s [mm]
	1000120	140	1.6			1000120	140	0.5
	1000145	240	1.1			1000145	240	0.5
	1000182	140	1.5			1000182	140	0.5
	1000188	240	1.1			1000188	240	0.7
	1000199	370	1.2			1000199	370	0.5
	1000231	370	3.0			1000231	370	0.7
	1000232	300	3.8			1000232	300	0.5
	1000241	675	4.0			1000241	370	0.7
	1000266	370	3.0			1000266	370	0.7
	1000281	370	3.0			1000281	370	0.7
	1000282	420	4.0			1000282	420	0.8
	1000283	370	1.6			1000283	370	0.5
	1000284	370	2.5			1000284	370	0.7
	1000285	370	3.5			1000285	370	0.7
	1000286	370	2.5			1000286	370	0.5
	1000287	370	3.5			1000287	370	0.7
	1000288	370	3.0			1000288	370	0.7
	1000289	370	1.6			1000289	370	0.5

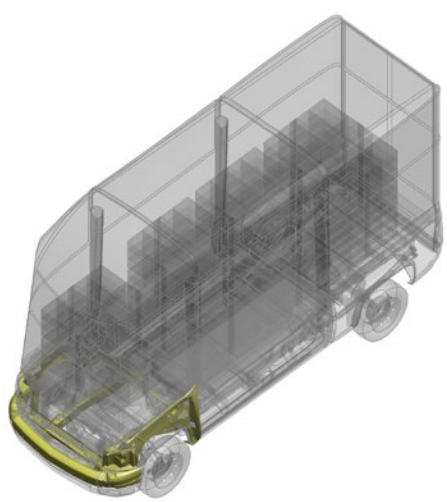

Table A-5. Large ODV Structural Changes Design 1 Versus Baseline Model

Large UADS (Baseline; 4000 kg)					Large UADS (Design 2; 4021 kg)			
Part Image	Part ID	Yield Stength [N/mm^2]	Thickness [mm]		Part Image	Part ID	Yield Stength [N/mm^2]	Thicknes s [mm]
	1000282	420	4.0			1000282	675	4.0
	1000289	370	1.6			1000289	675	4.6
	1000496	60	3.0			1000496	675	4.0

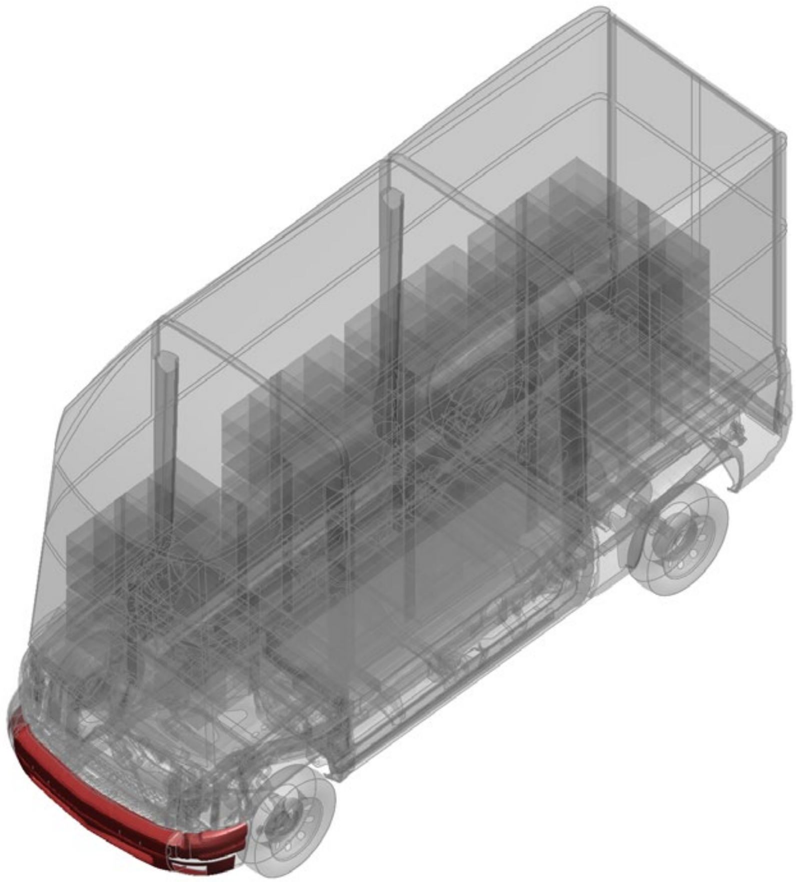

Table A-6. Tractor ODV Structural Changes Design 1 Versus Baseline Model

Tractor UADS (Baseline; 3400 kg)					Tractor UADS (Design 1; 2400 kg)			
Part Image	Part ID	Yield Stength [N/mm^2]	Thickness [mm]		Part Image	Part ID	Yield Stength [N/mm^2]	Thicknes s [mm]
	1000238	370	3.7			1000238	240	3.7
	1000241	370	3.0			1000241	240	2.5
	1000249	300	3.2			1000249	240	3.2
	1000263	370	3.7			1000263	240	3.7
	1000266	370	3.0			1000266	240	2.5
	1000272	300	3.2			1000272	240	3.2
	1000282	420	1.7			1000282	240	1.7

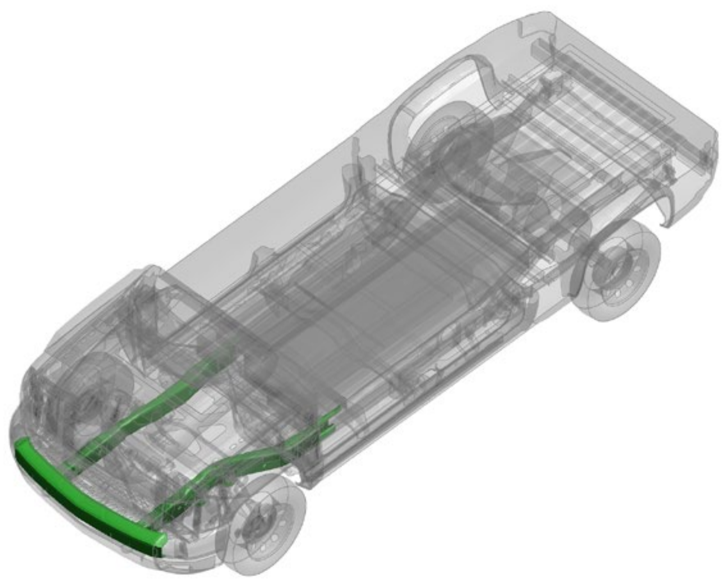

Table A-7. Tractor ODV Structural Changes Design 2 Versus Baseline Model

Tractor UADS (Baseline; 3400 kg)					Tractor UADS (Design 2; 3407 kg)			
Part Image	Part ID	Yield Stength [N/mm^2]	Thickness [mm]		Part Image	Part ID	Yield Stength [N/mm^2]	Thicknes s [mm]
	1000238	370	3.7			1000238	500	3.7
	1000241	370	3.0			1000241	675	3.5
	1000250	370	2.8			1000250	675	2.8
	1000263	370	3.7			1000263	500	3.7
	1000266	370	3.0			1000266	675	3.5
	1000276	370	2.8			1000276	675	2.8
	1000282	420	1.7			1000282	1300	1.7

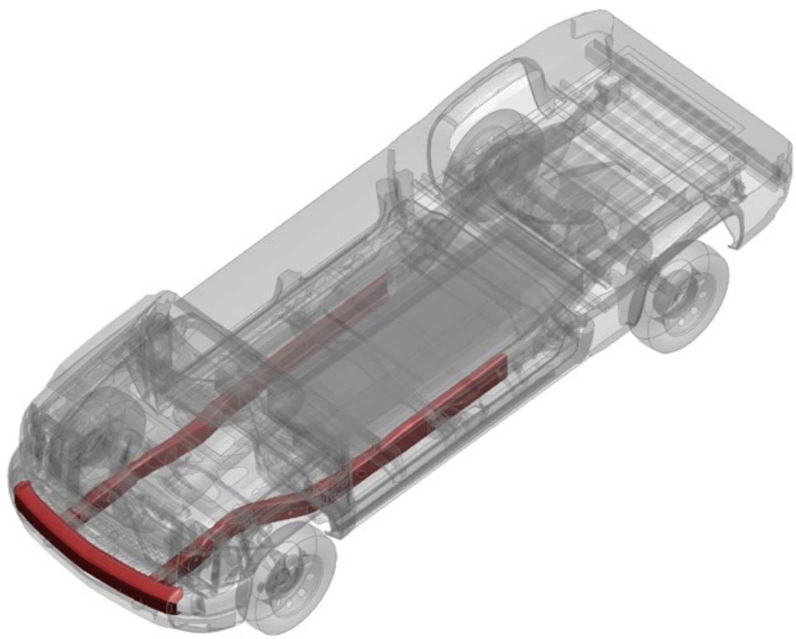

DOT HS 813 332
March 2024

U.S. Department
of Transportation

National Highway
Traffic Safety
Administration

NHTSA

15659-022624-v2